Energy flow and forces in multi-layer dielectric structures

A Thesis Submitted to the
College of Graduate Studies and Research
in Partial Fulfillment of the Requirements
for the degree of Master of Science
in the Department of Physics and Engineering Physics
University of Saskatchewan
Saskatoon

By
Winston Frias

Permission to Use

In presenting this thesis in partial fulfilment of the requirements for a Postgraduate degree from the University of Saskatchewan, I agree that the Libraries of this University may make it freely available for inspection. I further agree that permission for copying of this thesis in any manner, in whole or in part, for scholarly purposes may be granted by the professor or professors who supervised my thesis work or, in their absence, by the Head of the Department or the Dean of the College in which my thesis work was done. It is understood that any copying or publication or use of this thesis or parts thereof for financial gain shall not be allowed without my written permission. It is also understood that due recognition shall be given to me and to the University of Saskatchewan in any scholarly use which may be made of any material in my thesis.

Requests for permission to copy or to make other use of material in this thesis in whole or part should be addressed to:

Head of the Department of Physics and Engineering Physics
Rm 163
116 Science Place
University of Saskatchewan
Saskatoon, Saskatchewan
Canada
S7N 5E2

Abstract

This thesis is devoted to studies of two selected problems which are of great interest for newly emerging fields of metamaterials and plasmonics. We study the energy flow and momentum balance for various dielectric structures of interest, in particular, for multi-layer structures that involve tunneling barriers. The propagation of electromagnetic waves in layered media is analyzed and different definitions of energy transport velocities are compared. It is argued that the energy flow velocity is the most universal concept that describes energy flow. It always remains sub-luminal contrary to the group delay velocity which may become superluminal for some situations. For the wave packet in an infinite medium the energy flow velocity is equivalent to the group velocity. However also for the structures of a finite width (compared to the length of the wave packet), nonlocal effects due to reflections from boundaries become important and the actual energy flow velocity is different from the group velocity. Energy flow velocity is also applicable to the case when the energy is transported by evanescent wave as in surface wave resonant structures. The energy flow velocity is calculated for some resonant configurations. It is shown that such multi-layer configurations delay the light velocity by orders of magnitude which might be of interest for slow/stopped light applications.

The second problem concerns with the analysis of radiation pressure on the dielectric structures. The forces on dielectric bodies of different configurations are calculated from the Lorentz and the Helmholtz expressions. For finite size dielectric structures in vacuum, both expressions give the identical results for the total force, however the local force densities are different. This difference is interpreted as a result of the partial averaging of the internal forces present in the Helmholtz force expression. Partial compensation of the internal forces occurs as a result of the different size of the control volume inherently assumed in both averaging procedures: the sampling size of the Lorentz force is chosen to smooth out the charge distribution of the microscopic charges, while the Helmholtz force has a macroscopic sampling size of the order of the object dimensions. It is shown that the average of the microscopic

Lorentz force results in the macroscopic Lorentz force expression with charge and current density defined by macroscopic polarization and magnetization vectors.

Acknowledgements

I want to thank my supervisor Andrei Smolyakov and my co-supervisor Akira Hirose for supporting me and helping me understand the problem in hand. The discussions and talks with them form the basis of the present report. I also want to thank all the people in the Department and in the Plasma Lab for creating an atmosphere of friendship and support throughout all my time in Saskatoon. And last but not least I want to thank my family and friends for the support that they have given me in all this process, without you none of this would have been possible.

A mis papás y mi hermanita, a mi Lili y mis amigos de aquí y de allá, gracias por todo, sin ustedes a mi lado nada de esto hubiera sido posible.

Contents

List of Figures

Chapter 1

Introduction

1.1 Background and Motivation

New areas in optics and nanotechnology, such as plasmonics, and more generally, metamaterials, have recently emerged and are attracting a great deal of attention. A number of new physical phenomena and applications anticipated and studied in these fields are largely based on the ability to manipulate evanescent waves [1–3]. New technologies such as more efficient antireflection coatings, "superlenses", ultrasensitive detectors and invisibility cloaks have been developed using new findings from the field of plasmonics and negative-index materials. A crucial phenomenon that occurs in metamaterials and in materials with negative permittivity of $\varepsilon < 0$ (and, or, negative permeability, $\mu < 0$) is the amplification of evanescent waves [1], a feature responsible, among other things, for the extraordinary (resonant) transmission of electromagnetic waves in layered media with alternating layers of positive and negative permittivity materials. This unusual behavior is also the basis for superlensing, which opens the way for super-resolution at subdiffraction scales [1] . Tunneling in general, remains a subject of controversy in modern physics. Much of the controversy is related to the fact that the most accepted definitions for the tunneling time seem to imply a superluminal propagation velocity for the tunneling though the sufficiently thick barrier, an effect known as *Hartman's Effect* [4–6]. Such phenomena occur in electromagnetic and quantum mechanical systems [7–9]. The controversial question of the tunneling velocity [5–7, 10] is also important in nanooptics and plasmonics, namely for the problem of slow and fast light. In recent years, there has been renewed interest in the question of how fast the energy (information)

propagates in material media. Slow and fast light phenomena have been investigated and various applications have been proposed. Related questions of the pulse propagation in metamaterials as well as in tunneling systems have also been actively studied. In our work, we endeavor to investigate the problem of tunneling and tunneling velocity for several configurations that involve surface wave resonances and thus exhibit phenomena of resonant amplification of evanescent waves. The configurations that involve surface wave resonances are building blocks of many plasmonics devices and applications.

In this thesis we also study the momentum balance and forces in materials. The question of the force exerted on a dielectric body is an old problem of electrodynamics. It is related to the issue of the momentum of light in media, usually referred to as the Abraham-Minkowski controversy [11–16]. Recently, the problem of the force acting on dielectrics has attracted new interest due to advances in nanotechnology and potential applications of these forces such as in nano-motors and for separation of nano-particles. The related issues of forces and momentum in metamaterials is also of great fundamental interest. In this thesis we investigate the structure of microscopic forces in the materials. Starting from the microscopic Maxwell equations and the microscopic Lorentz force, we derive a macroscopic expression for the macroscopic force and compare this force with other expressions in the literature such as Helmholtz force. Our studies lay framework for futures studies of forces in metamaterials.

This thesis is organized as follows: in chapter 1 , the general properties of electromagnetic waves, surface modes and energy transport are introduced. Chapter 2, introduces the problem of tunneling and various definitions of tunneling time as introduced in quantum mechanics and electromagnetic theory. In Chapter 3, the tunneling of electromagnetic waves through different structures is analyzed and the velocities from different definitions are calculated and compared. In Chapter 4, the microscopic Maxwell equations and the microscopic Lorentz force are introduced. These expressions are averaged and macroscopic expressions for the force on dielectric media are derived. The obtained expression for the Lorentz force is compared

with other force definitions existing in literature. In Chapter 5, the forces on different structures are calculated and compared. Chapter 6 summarizes the results of the thesis.

1.2 Maxwell's Equations

The classical electromagnetic field can be described using Maxwell's equation (In SI units) [17]

$$\nabla \times \mathbf{E} + \frac{\partial \mathbf{B}}{\partial t} = 0, \tag{1.1}$$

$$\nabla \times \mathbf{H} - \frac{\partial \mathbf{D}}{\partial t} = \mathbf{J}, \tag{1.2}$$

$$\nabla \cdot \mathbf{D} = \rho, \tag{1.3}$$

$$\nabla \cdot \mathbf{B} = 0. \tag{1.4}$$

$\mathbf{E}$ and $\mathbf{B}$ are the electric and magnetic fields, $\mathbf{D}$ and $\mathbf{H}$ are the electric displacement and magnetic induction. The latter are introduced to include the effects of the field on matter, ρ and $\mathbf{J}$ are the free charge (Coulomb per cubic meter) and current densities (Ampere per square meter).

These equations relate the macroscopic electric and magnetic fields to the free charge and current densities in matter. Another important set of relations necessary to fully define the fields are the material relations, which define effects of the polarization and magnetization in matter

$$\mathbf{D} = \varepsilon_0 \mathbf{E} + \mathbf{P} = \varepsilon \mathbf{E}, \tag{1.5}$$

$$\mathbf{B} = \mu_0 \mathbf{H} + \mathbf{M} = \mu \mathbf{H}, \tag{1.6}$$

where the parameters ε and μ are the electric permittivity and magnetic permeability of the media respectively. These parameters are in general tensors, but in isotropic linear media they are scalar quantities [18]. The parameters ε_0 and μ_0 are the electric permittivity and magnetic permeability of vacuum respectively. The vectors $\mathbf{P}$ and $\mathbf{M}$ are the electric and magnetic polarization of the medium.

A very important role is played by the boundary conditions for the fields, which are consequence of the general equations (1.1)-(1.4) [17]

$$\mathbf{n} \cdot (\mathbf{B}_2 - \mathbf{B}_1) = 0, \tag{1.7}$$

$$\mathbf{n} \cdot (\mathbf{D}_2 - \mathbf{D}_1) = \sigma, \tag{1.8}$$

$$\mathbf{n} \times (\mathbf{E}_2 - \mathbf{E}_1) = 0, \tag{1.9}$$

$$\mathbf{n} \times (\mathbf{H}_2 - \mathbf{H}_1) = \mathbf{J}_s, \tag{1.10}$$

where $\mathbf{n}$ is the normal vector to the surface separating the media, σ and $\mathbf{J_s}$ are the surface charge density and the surface current density. The equations (1.1)-(1.4) along with the conditions (1.7)-(1.10) are the basis for studying all classic electromagnetic phenomena including the properties of electromagnetic metamaterials. The response of different media to electromagnetic radiations is dependent, among other factors, on the frequency of the radiation. In general for dispersive materials ε and μ are function of frequency, $\varepsilon = \varepsilon(\omega)$ and $\mu = \mu(\omega)$.

1.3 Energy Conservation

Energy conservations is an important concept in the study of electromagnetic interactions of radiation with matter. Using Maxwell's equations (1.1)-(1.4) and the vector theorem $\nabla \cdot (\mathbf{A} \times \mathbf{B}) = \mathbf{B} \cdot \nabla \times \mathbf{A} - \mathbf{A} \cdot \nabla \times \mathbf{B}$, the following holds [17, 18]

$$\nabla \cdot (\mathbf{E} \times \mathbf{H}) = \mathbf{H} \cdot \nabla \times \mathbf{E} - \mathbf{E} \cdot \nabla \times \mathbf{H} = -\mathbf{H} \cdot \frac{\partial \mathbf{B}}{\partial t} - \mathbf{E} \cdot \frac{\partial \mathbf{D}}{\partial t} - \mathbf{J} \cdot \mathbf{E}. \tag{1.11}$$

From this last equation it is possible to define the vector $\mathbf{S} = \mathbf{E} \times \mathbf{H}$, called Poynting vector [17]

$$\mathbf{S} = \mathbf{E} \times \mathbf{H}. \tag{1.12}$$

For a medium without dispersion, such that ε and μ are real positive constants, it is possible to write [18]

$$U = \frac{1}{2} \left[\mathbf{E} \cdot \mathbf{D} + \mathbf{B} \cdot \mathbf{H} \right], \tag{1.13}$$

such that equation (1.11) becomes

$$\frac{\partial U}{\partial t} + \nabla \cdot \mathbf{S} = -\mathbf{J} \cdot \mathbf{E}, \tag{1.14}$$

where U is the electromagnetic energy density, $\mathbf{S}$ is the energy flux and $\mathbf{J} \cdot \mathbf{E}$ is the energy loss.

In the case of a medium with dispersion, the result in equation (1.13) is not true. In the present work only medium with purely real ε and μ will be considered. In this case, it is possible to neglect the term $\mathbf{J} \cdot \mathbf{E}$ since the losses are defined by the imaginary parts of ε and μ [19].

To derive the expression for the electromagnetic energy density consider an electric and magnetic fields with carrier frequency ω_0:

$$\mathbf{E} = \mathbf{E}_0(t)e^{-i\omega_0 t}, \qquad \mathbf{H} = \mathbf{H}_0(t)e^{-i\omega_0 t}. \tag{1.15}$$

To obtain the time averaged value of the electromagnetic energy density in a dispersive medium, first it is necessary to write the fields in equation (1.11) as

$$\mathbf{E} = \frac{\mathbf{E} + \mathbf{E}^*}{2}, \qquad \dot{\mathbf{D}} = \frac{\dot{\mathbf{D}} + \dot{\mathbf{D}}^*}{2}, \tag{1.16}$$

$$\mathbf{H} = \frac{\mathbf{H} + \mathbf{H}^*}{2}, \qquad \dot{\mathbf{B}} = \frac{\dot{\mathbf{B}} + \dot{\mathbf{B}}^*}{2}. \tag{1.17}$$

When the time average is performed, the members with factors $\sim \exp(\pm 2i\omega t)$ disappear. Following Landau [19], consider now $\partial \mathbf{D}/\partial \mathbf{t} = \hat{f}\mathbf{E}$ where $\hat{f} = \partial/\partial t\hat{\varepsilon}$ is defined for a field with constant amplitude as:

$$\hat{f}\mathbf{E} = f(\omega)\mathbf{E}, \qquad f(\omega) = -i\omega\varepsilon(\omega). \tag{1.18}$$

Supposing now that the amplitude is not constant but a slowly varying function of time and using its Fourier expansion $E_0 = E_j e^{-i\alpha t}$ with the factor E_j constant

$$\mathbf{E} = \mathbf{E}_j e^{-i(\omega_0+\alpha)t}, \tag{1.19}$$

and taking into account that $\alpha << \omega_0$ (due to the E_0 being a slowly changing function of t), we have

$$\hat{f}\mathbf{E}_j e^{-i(\omega+\alpha)t} = f(\omega_0 + \alpha)\mathbf{E}_j e^{-i(\omega+\alpha)t}, \tag{1.20}$$

but

$$\frac{f(\omega_0+\alpha)-f(\omega_0)}{\alpha} \approx \frac{\partial f}{\partial \omega_0},$$

$$f(\omega_0+\alpha)\mathbf{E}_j e^{-i(\omega+\alpha)t} = \left[f(\omega_0)+\alpha\frac{\partial f}{\partial \omega_0}\right]\mathbf{E}_j e^{-i(\omega+\alpha)t}$$

$$f(\omega_0+\alpha)\mathbf{E}_j e^{-i(\omega_0+\alpha)t} = -i\omega_0\varepsilon\mathbf{E}_j e^{-i(\omega_0+\alpha)t} + \frac{\partial(\omega_0\varepsilon(\omega_0))}{\partial\omega_0}(-i\alpha\mathbf{E}_j e^{-i\alpha t})e^{-i\omega_0 t}$$

$$f(\omega_0+\alpha)\mathbf{E}_j e^{-i(\omega_0+\alpha)t} = -i\omega_0\varepsilon\mathbf{E}_j e^{-i(\omega_0+\alpha)t} + \frac{\partial(\omega_0\varepsilon(\omega_0))}{\partial\omega_0}\frac{d\mathbf{E}_0}{dt}e^{-i\alpha t})e^{-i\omega_0 t}. \quad (1.21)$$

Putting equation (1.21) into the product in equation (1.11), we obtain :

$$\left\langle \mathbf{E}\cdot\frac{\partial\mathbf{D}}{\partial t}\right\rangle = \frac{1}{4}\frac{\partial\omega\varepsilon}{\partial\omega}\frac{d\mathbf{E}\cdot\mathbf{E}^*}{dt}, \quad (1.22)$$

and analogously for $\mathbf{H}$:

$$\left\langle \mathbf{H}\cdot\frac{\partial\mathbf{B}}{\partial t}\right\rangle = \frac{1}{4}\frac{\partial\omega\mu}{\partial\omega}\frac{d\mathbf{H}\cdot\mathbf{H}^*}{dt}. \quad (1.23)$$

Using equations (1.12), (1.22)-(1.23), the values for the average energy flux and the average electromagnetic energy density are [19]:

$$\langle\mathbf{S}\rangle = \frac{1}{2}\,\Re(\mathbf{E}\times\mathbf{H}^*), \quad (1.24)$$

$$\langle U\rangle = \frac{1}{4}\,\mathbf{E}\cdot\mathbf{E}^*\frac{\partial\omega\varepsilon}{\partial\omega} + \frac{1}{4}\,\mathbf{H}\cdot\mathbf{H}^*\frac{\partial\omega\mu}{\partial\omega}. \quad (1.25)$$

1.4 Wave equation

Using Maxwell's equations (1.1)-(1.4), and the material relations (1.5)-(1.6), we can obtain the following set of equations for the magnetic and electric fields [17, 18]

$$\varepsilon\nabla\times\varepsilon^{-1}\nabla\times\mathbf{H} + \varepsilon\mu\frac{\partial^2\mathbf{H}}{\partial t^2} = 0, \quad (1.26)$$

$$\mu\nabla\times\mu^{-1}\nabla\times\mathbf{E}+\varepsilon\mu\frac{\partial^2\mathbf{E}}{\partial t^2}=0. \tag{1.27}$$

Or assuming a harmonic time variation for the fields ($\sim e^{-i\omega t}$)

$$\varepsilon\nabla\times\varepsilon^{-1}\nabla\times\mathbf{H}-\omega^2\varepsilon\mu\mathbf{H}=0, \tag{1.28}$$

$$\mu\nabla\times\mu^{-1}\nabla\times\mathbf{E}-\omega^2\varepsilon\mu\mathbf{E}=0. \tag{1.29}$$

For homogeneous media, equations (1.28)-(1.29) reduce to Helmholtz equations [17–19]:

$$\nabla^2\mathbf{H}+\omega^2\varepsilon\mu\mathbf{H}=0, \tag{1.30}$$

$$\nabla^2\mathbf{E}+\omega^2\varepsilon\mu\mathbf{E}=0. \tag{1.31}$$

We will deal mainly with solutions to the Helmholtz equation with different inhomogeneous profiles for the electric permittivity ε. A general solution for this equation, representing plane waves is given by

$$\mathbf{E}(\mathbf{r},\omega)=\mathbf{E}(\omega)e^{i\mathbf{k}\cdot\mathbf{r}}. \tag{1.32}$$

In general, $\mathbf{k}$ is a complex number, having a real and an imaginary part for lossy materials, and a purely imaginary part for evanescent modes; this fact will be very important in the following discussion [18].

For the propagation of electromagnetic waves in layered media two important polarizations can be distinguished: Transverse Electric (TE) polarization, or S-polarization, in which the electric field is perpendicular to the plane of incidence, and Transverse Magnetic (TM), or P-polarization, in which the electric field is in the plane of incidence [17].

For TE-waves taking the electric field $\mathbf{E}=(E_x,0,0)$ linearly polarized in x, and harmonic time dependance $\mathbf{E}(\mathbf{r},t)=\mathbf{E}(\mathbf{r})e^{-i\omega t}$, the wave equation reduces to [18]

$$\left(\frac{\partial^2}{\partial y^2} + \mu\frac{\partial}{\partial z}\frac{1}{\mu}\frac{\partial}{\partial z} + \frac{\omega^2}{c^2}\varepsilon\mu\right) E_x = 0. \tag{1.33}$$

Similarly, for TM-waves taking the magnetic field $\mathbf{H}=(H_x, 0, 0)$ linearly polarized in x, and harmonic time dependance $\mathbf{H}(\mathbf{r}, t) = \mathbf{H}(\mathbf{r})e^{-i\omega t}$, the wave equation reduces to [18]

$$\left(\frac{\partial^2}{\partial y^2} + \varepsilon\frac{\partial}{\partial z}\frac{1}{\varepsilon}\frac{\partial}{\partial z} + \frac{\omega^2}{c^2}\varepsilon\mu\right) H_x = 0. \tag{1.34}$$

Further, these equations can be reduced assuming that $\frac{\partial}{\partial y} \rightarrow ik_y$, where k_y now is a parameter that includes the angle of incidence of the incoming radiation. The new equations are

$$\left(\mu\frac{\partial}{\partial z}\frac{1}{\mu}\frac{\partial}{\partial z} + k_z^2\right) E_x = 0, \tag{1.35}$$

$$\left(\varepsilon\frac{\partial}{\partial z}\frac{1}{\varepsilon}\frac{\partial}{\partial z} + k_z^2\right) H_x = 0, \tag{1.36}$$

$$k_z^2 = \frac{\omega^2}{c^2}\varepsilon\mu - \frac{\omega^2}{c^2}\sin^2(\theta_i). \tag{1.37}$$

These equations are symmetrical and the difference between polarizations is clear in the different boundary conditions for each polarization. These boundary conditions are

$$E, \frac{1}{\mu}\frac{\partial E}{\partial z} \rightarrow \text{continuous}, \tag{1.38}$$

for TE-waves, and

$$H, \frac{1}{\varepsilon}\frac{\partial H}{\partial z} \rightarrow \text{continuous}, \tag{1.39}$$

for TM-waves.

1.5 Interference of Evanescent Waves and Energy Transport

In media with a negative value of k_z^2 the wave now has an exponential dependence of the form $e^{\mp\kappa z}$; the wave becomes evanescent.

In general, it will be supposed that the electric permittivity of the layers in the system will be given by

$$\varepsilon(z,\omega) = 1 - \frac{\omega_{pe}^2(z)}{\omega^2}, \tag{1.40}$$

where

$$\omega_{pe}^2(z) = \left(\frac{e^2 n(z)}{\varepsilon_0 m}\right)^{1/2} \tag{1.41}$$

is the plasma electron frequency [19].

As can be seen from (1.37) and (1.40), if the frequency of the incoming electromagnetic wave is such that $\omega^2 < \omega_{pe}^2$, $\varepsilon < 0$ the wave will become evanescent in that region. Another aspect of importance is the incident angle. As seen from (1.37) there will be angles such that $k_z^2 < 0$, even when not necessarily $\omega^2 < \omega_{pe}^2$ (this is basically the phenomenon of full internal reflection). For that layer the wave will also become evanescent. In general, the wave equation can be solved analytically given that the electric permittivity is given as a step function [1], and having dependence only on the frequency for each layer, in such a way that the solutions can be matched using the boundary conditions for the electromagnetic field.

Evanescent waves are by nature non propagating [7, 17, 18], the wave just decays exponentially within the region. Often it has been said that because evanescent waves are non propagating they do not carry energy with them, but it is exactly the interference of these waves within a region what causes the phenomenon of extraordinary transmission [1], so the question is how exactly is energy transport performed by these waves. Considering a region of evanescence such that the $H_x(z)$ is given by

$$H_x(z) = C\ \exp(-\kappa z) + D\ \exp(\kappa z), \tag{1.42}$$

with κ a real number but C and D possibly complex, being the amplitudes of the two interfering waves in the region. By Maxwell's equations, the electric field associated

with these waves is given by [17]

$$E_y(z) = -i\frac{1}{\omega\varepsilon}\frac{\partial H_x}{\partial z}, \tag{1.43}$$

or

$$E_y(z) = i\frac{\kappa}{\omega\varepsilon}\left(C\,\exp(-\kappa z) - D\,\exp(\kappa z)\right). \tag{1.44}$$

For the Poynting flux we have

$$S_z = \frac{1}{2}\Re(E_y H_x^*) \sim (CD^* - C^*D) \sim \Im(CD^*). \tag{1.45}$$

As can be seen from (1.45) the z-component of the Poynting flux becomes finite when the product CD^* has an imaginary part other than zero; in other words, there has to be a finite phase shift between the amplitudes C and D. Therefore, a finite energy flux occurs as a result of the superposition of two evanescent modes with a finite phase shift [1]; this is called interference of evanescent waves [1].

This last result is very important because apart from giving an explanation on how energy is transported by evanescent waves, it also implies that both reflected and transmitted waves are the result of the interference of the evanescent waves in the barrier region and that they are coupled in such a way that it is not possible to say that the reflected wave is the result of the backwards going evanescent wave and the transmitted the result of the forward going evanescent wave. The reflected and transmitted waves are the result of energy "leaking" from the system through two different channels (reflection and transmission respectively) [1].

Chapter 2

Tunneling and Tunneling Times

The group velocity has been widely used as a measure for the velocity of energy transport. However, in a number of situations, it becomes ill-defined. Examples are wave propagation in absorbing media and in tunneling structures, in which the wave vector becomes complex or purely imaginary. The group velocity, $\partial\omega/\partial\mathbf{k}$, is a local quantity and is defined for wavepackets in an infinite medium. As such it does not depend on the geometry of the medium, e.g. on the boundary conditions. In fact, the energy flux through the medium, and, consequently the energy flow velocity, is in general a non-local quantity. It is not simply a local property of the dielectric medium (via the local function $\omega = \omega(\mathbf{k})$) but depends on the overall geometry of the system, in particular, on the boundary conditions as can be seen from the simple example of a standing wave in a transparent medium with well defined $\varepsilon(\omega) > 0$ and $\partial\omega/\partial\mathbf{k} \neq 0$, which does not transport energy.

In other cases, such as evanescent waves tunneling the group velocity is not well defined at all. In the latter case, a commonly used measure of the velocity of propagation is based on the group delay. The group delay, which is interpreted as the time the transmitted packet reaches its peak at the exit of the media, is used to define a velocity $v_{gd} = \partial\omega/\partial\kappa$, where $\kappa = L\varphi_t$ and φ_t is the phase of the transmission coefficient.

In quantum mechanics the question of how long does it take for a particle or a wavepacket to tunnel through a potential barrier has been a subject of many discussions and debate [5–7, 10]. In 1962, Hartman, working for Texas Instruments, obtained the time delay in tunneling in a metal-insulator-metal structure. He applied the stationary phase approximation analysis developed by Wigner and Bohm and

found that this time (called group delay or phase time) is shorter than the time it would take light to transverse a distance equal to the width of the structure he analyzed, he also found that this time saturates with distance [4] leading to the conclusion that the group delay velocity becomes superluminal for a thick barrier. In 1960, Smith, analyzing the scattering process for tunneling proposed a dwell time, that was defined by him as a scattering lifetime [20]. Since then more different definitions of time for tunneling have been proposed, some leading to complex times and imaginary or even infinite velocities for tunneling phenomena [5–7, 10]. Good reviews of this field can be found in literature [5, 10, 21]. In this chapter we will discuss the definitions of group delay, dwell time, and energy velocity, and discuss relations between these measures and the Hartman effect.

2.1 Quantum Tunneling

In quantum mechanics, when a particle of energy E, is incident on a potential barrier $V(x)$, such that $E < V(x)$, there is a finite (although generally small) probability that the particle will go across the barrier and end up on the other side of it, whereas in a classical picture, the particle will always be reflected by the barrier [21]. The probability of the particle being transmitted or reflected by the barrier is measured by the transmission coefficient $T = |T|e^{i\phi_t}$ and the reflection coefficient $R = |R|e^{i\phi_r}$. The particle is described by the wavefunction $\psi(x,t)$ that is solution to the time dependent Schrodinger equation [21]

$$\frac{\hbar^2}{2m}\frac{\partial^2\psi}{\partial x^2} - V(x)\psi = -i\hbar\frac{\partial\psi}{\partial t}. \tag{2.1}$$

For stationary states, we can separate spatial and time components of the wave function as [21]

$$\psi(x,t) = \psi_E(x)\exp(-iEt/\hbar), \tag{2.2}$$

where $\psi_E(x)$ is the spatial part of ψ and E is the energy of the particle.

The spatial part of the wave function is solution to the time-independent Schrodinger

equation [21]

$$-\frac{\hbar^2}{2m}\frac{\partial^2\psi_E}{\partial x^2} + (V - E)\psi_E = 0. \tag{2.3}$$

In free space, this equation has solution in the form of traveling waves.

For the region to the left of the barrier we have [7, 21]

$$\psi_I = e^{ikx} + Re^{-ikx}, \quad k^2 = \frac{2mE}{\hbar^2}, \tag{2.4}$$

for the region to the right of the barrier

$$\psi_{III} = Te^{ikx}, \tag{2.5}$$

and inside the barrier the solutions are exponentially decaying waves [7, 21]:

$$\psi_{II} = C\,e^{-\kappa x} + D\,e^{\kappa x}, \quad \kappa^2 = \frac{2m(V - E)}{\hbar^2}. \tag{2.6}$$

2.2 Group Delay

If we analyze a wave packet, sharply peaked around an energy value E_0, it is possible to construct a solution of the form [7, 21]

$$\psi(x, t) = \int_E f(E - E_0)\psi_E(x)e^{-iEt/\hbar}dE. \tag{2.7}$$

This packet propagates with a group velocity $\hbar^{-1}\partial E/\partial k = \hbar k/m$ [21], when it collides with the barrier, it is replaced by a reflected wave packet and a transmitted wavepacket, represented respectively by [7, 21]

$$\psi_(x, t) = \int_E f(E - E_0)|R| \exp[i\phi_r(E) + ikx - iEt/\hbar]\, dE \tag{2.8}$$

and

$$\psi_(x, t) = \int_E f(E - E_0)|T| \exp[i\phi_t(E) + ikx - iEt/\hbar]\, dE. \tag{2.9}$$

Assuming that the functions $f(E-E_0)T$ and $f(E-E_0)R$ are slowly varying functions of E and that the phase changes rapidly with E, using the stationary phase method [4, 7, 21], these integrals can be estimated setting the rate of change of the phase to

zero, which for a barrier of width L yields for the transmitted packet

$$\begin{aligned} \frac{d}{dE}\left(\phi_t + kL - \frac{Et}{\hbar}\right) &= 0, \\ \frac{d}{dE}\left(\phi_t + kL\right) &= \frac{t}{\hbar}, \end{aligned} \tag{2.10}$$

and for the reflected packet

$$\begin{aligned} \frac{d}{dE}\left(\phi_r - \frac{Et}{\hbar}\right) &= 0, \\ \frac{d}{dE}\left(\phi_r\right) &= \frac{t}{\hbar}. \end{aligned} \tag{2.11}$$

These last equations suggest that the peaks of the reflected and transmitted packets appear at the positions $x = L$ (for the transmitted packet) and $x = 0$ (for the reflected packet) with a delay defined by [4, 7, 21]

$$\begin{aligned} \tau_{gt} &= \hbar \frac{d}{dE}\left(\phi_t + kL\right), \\ \tau_{gr} &= \hbar \frac{d\phi_r}{dE}. \end{aligned} \tag{2.12}$$

It can be shown that for symmetric barriers, the delay in transmission and in reflection are identical [22], and that will be the case considered here. In the most general case of an asymmetric barrier, the bi-directional delay is defined as [21, 22]

$$\tau_g = |R|^2 \tau_{gr} + |T|^2 \tau_{gt}. \tag{2.13}$$

2.3 Dwell Time

The concept of dwell time was first introduced by Smith in 1960 in the context of potential scattering [20]. Smith defined the dwell time as the time spent by a particle in the potential region. For tunneling, this dwell time was defined by Büttiker and Landauer as [9, 23]

$$\tau_d = \frac{\int_0^L |\psi(x)|^2 \, dx}{j_{in}}, \tag{2.14}$$

where $j_{in} = \hbar k/m$ is the incoming (incident) flux and $\int_0^L |\psi(x)|^2 \, dx$ is the probability of finding the particle in the barrier region.

Quoting Hauge *et al.* [10]: "The dwell time is the average time spent by particles in the interval x_1, x_2, where no attempt is made to distinguish between scattering channels (reflection or transmission)". That is, the dwell time is the time spent on the barrier region averaged over all incoming particles and does not pretend to be an expression regarding the transversal time due to the fact that it does not distinguish between reflection and transmission and that it is a property of the wavefunction [7, 10]. As it will be shown latter, the dwell time and the group delay are closely related and can be proven to be equivalent in some situations [8, 22, 24].

It is worth noticing that in the definition of the dwell time, the term j_{in} refers only to the flux of incident particles. Looking at the fact that the conservation of probability also yields a continuity equation in the form [21]

$$\frac{\partial|\psi|^2}{\partial t} + \nabla \cdot \mathbf{j} = 0, \tag{2.15}$$

where j is the probability flux, defined as

$$\mathbf{j} = \frac{\hbar^2}{2im}\left(\psi^*\nabla\psi - \psi\nabla\psi^*\right). \tag{2.16}$$

It would also be possible to define a dwell time of the form

$$\tau_d = \frac{\int |\psi|^2 dV}{j_{barrier}}, \tag{2.17}$$

where $j_{barrier}$ is the probability current inside of the barrier region. An analogous to equation (2.17) will be used later to define the energy velocity.

2.4 The Hartman Effect

In 1962, Thomas Hartman analyzed the passage of a one-dimensional Gaussian wave packet through a rectangular potential barrier and compared the transmission time with the time required for the incident packet to transverse a distance equal to the barrier thickness in vacuum, such a time he called the "proper time" [4]. In general he found that for thick barriers, the form of the transmitted packet is basically the same as the incident packet, but that it is shifted with respect to the packet in

vacuum, with the greatest contributions coming from the components having energy just greater than the height of the barrier. He also found that the transversal time was less than the proper time and becomes independent of the barrier thickness as the barrier width increases. Such independence of the transit time on the thickness of the barrier for thick barriers is called now the Hartman Effect [4].

To illustrate this, let us take a look at a wavepacket of energy E, passing a barrier of height V_0.

The wave function has the following form [7]:

$$\psi_I = \exp(ikz) + R\exp(-ikz) \qquad z < 0,$$

$$\psi_{II} = C\exp(-\kappa z) + D\exp(\kappa z) \qquad 0 < z < L,$$

$$\psi_{III} = T\exp(ikz) \qquad z > L, \tag{2.18}$$

with

$$k = \sqrt{2mE}/\hbar \qquad \kappa = \sqrt{2m(E - V_0)}/\hbar.$$

The transmission coefficient is [7]

$$T = \frac{e^{-ikL}}{\cosh\kappa L + i\Delta\sinh\kappa L}, \tag{2.19}$$

with $\Delta = (\kappa/k - k/\kappa)/2$. The phase of the transmission coefficient $\phi_0 = \phi_t + kL$ is given by [7]

$$\phi_0 = -\arctan(\Delta\tanh\kappa L), \tag{2.20}$$

and the group delay is [7]

$$\tau_g = \frac{mL}{\hbar k}\frac{\cos^2\phi_0}{2}\left[\left(\frac{k}{\kappa} - \frac{\kappa}{k}\right)^2\frac{\tanh\kappa L}{\kappa L} - \left(\frac{k^2}{\kappa^2} - 1\right)\mathrm{sech}^2\kappa L\right]. \tag{2.21}$$

Assuming for the purpose of illustration that $E = V_0/2$, this expression reduces to [7]

$$\tau_g = \frac{2\tanh\kappa L}{\kappa v} \qquad v = \hbar k/m, \tag{2.22}$$

and in the limit of thick barriers $\kappa L \to \infty$ [7]

$$\tau_g = \frac{2}{\kappa v}. \tag{2.23}$$

As can be seen from the last equation the delay is independent of the thickness of the barrier. In general this delay is less than the proper time, implicating that the particle inside the barrier travels with a group velocity given by L/τ_g, which leads some authors to conclude that the tunneling has a superluminal velocity [5, 6]. In most experiments, this delay is what is measured with the conclusion that tunneling is superluminal.

2.5 Relation between the Group Delay and Dwell Time

Even though the dwell time and the group delay are defined in completely different contexts, they very much related and that relationship is one of the basis for a possible explanation of the Hartman effect and the apparent superluminality of tunneling.

The dwell time is defined as [20]

$$\tau_d = \frac{\int_0^L |\psi(z)|^2 \, dx}{j_{in}}. \tag{2.24}$$

Writing $|\psi(z)|^2$ as $\psi^*\psi$ and replacing for ψ^* and $\partial\psi/\partial E$ in the dwell time using Schrodinger's equation, we have [22]

$$\psi = \frac{\hbar^2}{2m}\left(-\frac{\partial^3\psi}{\partial E \partial x^2} - k^2\frac{\partial\psi}{\partial E}\right), \quad k^2 = \frac{2m}{\hbar^2}(E-V), \tag{2.25}$$

$$\psi^*\psi = \frac{\hbar^2}{2m}\frac{\partial}{\partial z}\left(\frac{\partial\psi}{\partial E}\frac{\partial\psi^*}{\partial z} - \psi^*\frac{\partial^2\psi}{\partial E\partial z}\right). \tag{2.26}$$

Integrating this last expression in the barrier region and assuming that to the left there is the incident and reflected fields and to the right only the transmitted field [22]

$$\frac{2m}{\hbar^2}\int_0^L |\psi(z)|^2 \, dx = \left(\frac{\partial\psi}{\partial E}\frac{\partial\psi^*}{\partial z} - \psi^*\frac{\partial^2\psi}{\partial E\partial z}\right)_{z=L} - \left(\frac{\partial\psi}{\partial E}\frac{\partial\psi^*}{\partial z} - \psi^*\frac{\partial^2\psi}{\partial E\partial z}\right)_{z=0}, \tag{2.27}$$

which yields [22]

$$-2ik\left[|T|\frac{d|T|}{dk} + |R|\frac{d|R|}{dk} + i\left(|T|^2\frac{d\phi_0}{dk} + |R|^2\frac{d\phi_r}{dk} + \frac{Im(R)}{k}\right)\right]\frac{\partial k}{\partial E}. \tag{2.28}$$

Identifying the term

$$|T|^2\frac{d\phi_0}{dk} + |R|^2\frac{d\phi_r}{dk}$$

as the bidirectional group delay τ_g in (2.13), we obtain [22]

$$\tau_g = \frac{\int_0^L |\psi(z)|^2\, dx}{j_{in}} - \frac{\Im(R)}{k}\hbar\frac{\partial k}{\partial E}, \tag{2.29}$$

where $|T|^2+|R|^2 = 1$. For symmetric barriers $\tau_g = \tau_{gt} = \tau_{gr}$. This result, obtained by Winful [7], is in agreement with the one obtained by Hauge *et.al* [10] using a careful Fourier analysis of the transmission problem. The last term is the interference term, which results from the overlapping of incident and reflected waves in front of the barrier. As it is seen, at resonant values (or when $\Im(R) = 0$), the interference term is zero and the dwell time and group delay are equal. In such a way we can write [7, 10]

$$\tau_g = \tau_d + \tau_{interference}. \tag{2.30}$$

2.6 Electromagnetic Analog of Tunneling

In general, tunneling is a wave property, it has been observed for matter, sound and electromagnetic waves. In quantum mechanics, the equation used to describe steady state wave functions is Schrodinger's equation

$$\nabla^2\psi + \left[\frac{2m}{\hbar^2}(E-V)\right]\psi = 0. \tag{2.31}$$

In electromagnetism, the analog is Helmholtz equation for the electric or magnetic fields

$$\nabla^2\mathbf{E} + \left(\frac{\omega}{c}n\right)^2\mathbf{E} = 0, \tag{2.32}$$

where

$$n = \sqrt{\frac{\varepsilon\mu}{\varepsilon_0\mu_0}} \tag{2.33}$$

is the refractive index of the medium and $\varepsilon, \mu, \varepsilon_0, \mu_0$ are the electric permittivity and magnetic permeability of the medium and vacuum respectively.

Upon setting $n\omega/c = [2m/\hbar^2(E-V)]^{1/2}$ [5, 9], the two equations have the same form and the treatment is analogous. Here the role of the barrier is clearly played by

the refractive index n. Tunneling occurs in regions where $E < V$ and the wavepacket incident on a potential barrier decays, following the analogy, in regions where the refractive index is imaginary or more generally where $\frac{\omega^2}{c^2} n^2(\mathbf{r}, \omega) < 0$, the electromagnetic wave becomes evanescent. It is the coupling and interference of the evanescent waves in the region of imaginary n, what generates the tunneling [1].

In the electromagnetic case the definitions for dwell time and group delay are a little bit different, but their meaning is the same. In steady state, the derivative of the phase of the packet is taken with respect to the frequency ω, and the wavefunction is replaced by the electric and/or magnetic fields. Being that the cases, the integrated probability is replaced by the energy density of the fields and the flux by the Poynting vector [5, 7, 9, 24] resulting in the following definitions:

$$\psi(x,t) = \int_\omega f(\omega - \omega_0)|T| \exp[i\phi_t(\omega) + ikx - i\omega t]\, d\omega$$

$$\frac{d}{d\omega}\left(\phi_t + k_v L - \omega t\right) = 0,$$

$$\tau_g = \frac{d\phi_0}{d\omega} \qquad \phi_0 = \phi_t + k_v L, \tag{2.34}$$

$$\langle U \rangle = \frac{1}{4}\,\mathbf{E}\mathbf{E}^* \frac{\partial \omega\varepsilon}{\partial \omega} + \frac{1}{4}\,\mathbf{H}\mathbf{H}^* \frac{\partial \omega\mu}{\partial \omega}, \tag{2.35}$$

$$j_{inc} = \frac{1}{2}\Re\left(\mathbf{E_{inc}} \times \mathbf{H}^*{}_{inc}\right), \tag{2.36}$$

$$\tau_d = \frac{\frac{1}{4}\int_V \mathbf{E}\cdot\mathbf{E}^* \frac{\partial \omega\varepsilon}{\partial \omega} dV + \frac{1}{4}\int_V \mathbf{H}\cdot\mathbf{H}^* \frac{\partial \omega\mu}{\partial \omega} dV}{\frac{1}{2}\Re\int_A \mathbf{E_{inc}} \times \mathbf{H}^*{}_{inc} \cdot d\mathbf{S}}. \tag{2.37}$$

This last equation can be stated as [7]

$$\tau_d = \frac{\langle U \rangle}{P_{in}} \qquad \langle U \rangle = \langle U_e \rangle + \langle U_m \rangle, \tag{2.38}$$

where $\langle U \rangle$ is the time-averaged electromagnetic energy and P_{in} the time averaged incident power.

2.7 Energy Velocity

A very important concept in electromagnetism is the energy velocity, first introduced by Brillouin and Sommerfeld. The energy velocity is defined as [18, 25]

$$\mathbf{V_e} = \frac{\mathbf{S}}{U}. \tag{2.39}$$

For electromagnetic waves, the average value of the energy velocity is given by [18]

$$V_E = \frac{\frac{1}{2}\frac{1}{L}\Re\int_0^L \mathbf{E}\times\mathbf{H}^* dz}{\frac{1}{4}\frac{1}{L}\int_0^L \mathbf{E}\cdot\mathbf{E}^*\frac{\partial\omega\varepsilon}{\partial\omega}dz + \frac{1}{4}\frac{1}{L}\int_0^L \mathbf{H}\cdot\mathbf{H}^*\frac{\partial\omega\mu}{\partial\omega}dz}, \tag{2.40}$$

or for a wave in a barrier region by (see appendix B)

$$V_E = \frac{|T|^2 L}{\tau_d}. \tag{2.41}$$

If a time is associated with this energy velocity such that

$$V_E = \frac{L}{\tau_E}, \tag{2.42}$$

then

$$\tau_E = \frac{\tau_d}{|T|^2}. \tag{2.43}$$

This time τ_E, that will be called energy time, does not suffer from the saturation of the dwell time and group delays, and since with increasing width the transmission coefficient becomes smaller in general, the energy time grows as expected. This energy time resembles the time discussed by D'Aguanno [24], the difference being that D'Aguanno concludes that the group velocity is equal to the energy velocity at the resonances. In general the group velocity loses its meaning for evanescent waves, since for those waves the propagation vector is imaginary and so is the group velocity. In the case of a transparent infinite medium and no reflection, the energy velocity is equivalent to the group velocity. It is shown here that the energy velocity always remains subluminal.

Chapter 3

Tunneling of Electromagnetic waves in multi-layer structures

The very nature of the metamaterials is based on the resonance phenomena that are used to achieve simultaneous negative permittivity and negative permeability. It is thus of interest to study the energy transport in resonant structures. Our goal is to clarify the relations between different measures of the energy transport, in particular resonance conditions. We concentrate on two simple structures exhibiting two types of resonances: the surface mode resonance that occurs at the interface of materials with opposite signs of the dielectric permittivities (permeabilities) and the standing wave resonance that occur due to partial wave trapping between two barriers. Both types of structures involve tunneling barriers. A standard example of a single tunneling barrier is studied first to illustrate some main ideas. We note here that surface wave resonances are of interest for many problems in plasmonics and that wave resonances play an important role in determination of the bandgap structure of periodic systems such as photonic crystals which are often used in slow light systems.

There is a noticeable disconnect between different approaches in the study of slow light in various optical and electromagnetic structures and studies of pulse propagation in tunneling problems. The slow light phenomenon is mainly interpreted as an effect of very small group velocity $v_g \ll c$, resulting from large dispersion near the resonances (the nature of resonance vary for different systems). The concept of group velocity does not exist for evanescent waves in tunneling problems. In the latter, the concept of the group delay and dwell time are often used as a measure of

the propagation time. The interpretation of the group delay as the tunneling time leads to apparent paradoxes such as superluminality. It was noted [7] that the delay time is actually a storage time and thus should not be interpreted as the propagation time. Therefore saturation of the delay time for thick barriers has nothing to do with superluminal signal propagation. It is obvious that for a sufficiently thick barrier, the saturation time is independent of the barrier width as the field penetrates only into a narrow part of barrier ("skin"depth). There have been also discussions on whether smooth Gaussian wave packets, which are usually used to introduce and calculate the delay time, can be used for information transfer and therefore, whether the delay time is a relevant quantity for the information flow velocity.

As it was noted above, the group velocity is not defined in tunneling media, in which the wave vector becomes purely imaginary and the solution is a combination of the evanescent modes. For a transparent medium, which supports propagating waves, the concept of group velocity appears to be a valid measure of the energy flow velocity, and therefore information flow velocity, given that the information flow has to be associated with a finite energy flow. However, in a number of situations, the group velocity also becomes ill-defined or produces unphysical results. A simple example is wave propagation in a strongly dissipative medium where the group velocity may exceed the speed of light. The group velocity is not necessarily the measure of the energy velocity even for the case of non-dissipative medium. The group velocity, $\partial\omega/\partial\mathbf{k}$, is a local quantity and is defined for wavepackets in an infinite medium. It does not take into account the wave reflection, and as such it does not depend on the geometry of the medium, e.g. on the boundary conditions. As a matter of fact, the energy flux through the medium, and, consequently the energy flow velocity, is in general a non-local quantity. It is not simply a local property of the dielectric medium (via the local function $\omega = \omega(\mathbf{k})$) but depends on the overall geometry of the system, in particular, on the boundary conditions. A simple illustration can be seen from the example of a standing wave in a transparent medium with well defined $\varepsilon(\omega) > 0$ and $\partial\omega/\partial\mathbf{k} \neq 0$, which nevertheless does not transport any energy.

Brillouin has introduced the energy velocity $\mathbf{v}_E = \mathbf{S}/U$ as the ratio of the Poynt-

ing vector to the electromagnetic energy density inside the medium. In this section we analyze the relations among the energy velocity $\mathbf{v}_E$, the standard group velocity $\partial\omega/\partial\mathbf{k}$, and the group delay velocity v_{gd}. The group delay velocity is introduced by using the group delay, which is interpreted as the time the transmitted packet reaches its peak at the exit of the media: $v_{gd} = \partial\omega/\partial\kappa$, where $\kappa = L\varphi_t$ and φ_t is the phase of the transmission coefficient. Our interest lies in resonant regimes, in particular those involving surface mode resonances.

3.1 Dispersive slab

In this section we consider wave propagation through the slab of dispersive material. Group delay velocity, group velocity and energy velocity are compared.

In the following y-polarized plane waves propagating in the z-direction, normally incident on a dispersive medium will be considered. The electromagnetic fields are defined as

$$\mathbf{E} = [0, E_y, 0]e^{i(kz-\omega t)}, \tag{3.1}$$

$$\mathbf{H} = [H_x, 0, 0]e^{i(kz-\omega t)}. \tag{3.2}$$

The dielectric constant $\varepsilon(\omega)$ will be of the form

$$\varepsilon(\omega) = 1 - \frac{\omega_p^2}{\omega^2}, \tag{3.3}$$

and the vector k is a function of ω defined as

$$k^2 = \frac{\omega^2}{c^2}\,\varepsilon(\omega). \tag{3.4}$$

For the case where $\varepsilon(\omega) < 0$, the wavevector becomes imaginary and the fields become evanescent.

The reflection and transmission coefficients for this structure are given by

$$T = \frac{e^{-ik_v L}}{g}, \tag{3.5}$$

$$R = i\frac{(k\varepsilon_0/k_v\varepsilon - k_v\varepsilon/k\varepsilon_0)\sin kd}{2g}, \tag{3.6}$$

$$g = \cos kd - i\left(k\varepsilon_0/k_v\varepsilon + k_v\varepsilon_0/k\varepsilon\right)\sin kd/2, \tag{3.7}$$

$$k_v = \frac{\omega}{c}, \tag{3.8}$$

and

$$k = \frac{\omega}{c}\sqrt{\varepsilon(\omega)}, \tag{3.9}$$

when $\varepsilon(\omega) > 0$, and by

$$T = \frac{e^{-ik_vL}}{g}, \tag{3.10}$$

$$R = -i\frac{(\kappa\varepsilon_0/k_v\varepsilon + k_v\varepsilon/\kappa\varepsilon_0)\sinh\kappa L}{2g}, \tag{3.11}$$

$$g = \cosh\kappa L + i\left(\kappa\varepsilon_0/k_v\varepsilon - k_v\varepsilon/\kappa\varepsilon_0\right)\sinh\kappa L/2, \tag{3.12}$$

$$k_v = \frac{\omega}{c} \tag{3.13}$$

and

$$\kappa = \frac{\omega}{c}\sqrt{|\varepsilon(\omega)|}, \tag{3.14}$$

when $\varepsilon(\omega) < 0$.

The phase of the transmission coefficient is given by

$$\phi_0 = \phi_t + k_vd = \arctan\left(\frac{k\varepsilon_0/k_v\varepsilon + k_v\varepsilon_0/k\varepsilon}{2}\tan kd\right), \tag{3.15}$$

when $\varepsilon(\omega) > 0$, and by

$$\phi_0 = \phi_t + k_vd = -\arctan\left(\frac{\kappa\varepsilon_0/k_v\varepsilon - k_v\varepsilon_0/\kappa\varepsilon_0}{2}\tanh\kappa d\right), \tag{3.16}$$

when $\varepsilon(\omega) < 0$. In Fig 3.1 the reflection and transmission responses of the slab as functions of $\varepsilon(\omega)$ are given.

The group delay velocity is given by

$$v_d = \frac{d}{\tau_{gt}} = d\left(\frac{\partial\phi_0}{\partial\omega}\right)^{-1}. \tag{3.17}$$

The averaged energy velocity in the direction of propagation (z-direction) is given by

$$v_E = \frac{\frac{1}{2}Z_0|H_0|^2|T|^2}{\int_0^d U\,dz}, \tag{3.18}$$

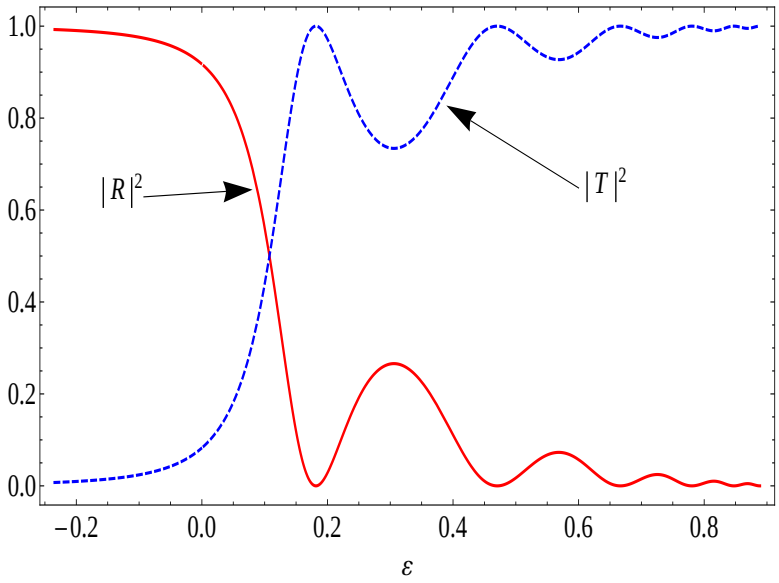

Figure 3.1: Reflection and transmission responses of the slab with ω_p=10 GHz and d=0.02 m

where U is given by

$$U = \frac{1}{4}\varepsilon_0 \frac{\partial(\omega\varepsilon)}{\partial\omega}|E_y|^2 + \frac{1}{4}\mu_0|H_x|^2. \tag{3.19}$$

The usual group velocity is given by the usual formula $v_g = \partial\omega/\partial k$ valid only for regions where $\varepsilon > 0$. The energy, group and group delay velocities are plotted in Fig 3.2. A close-up look of the region where $\varepsilon \to 0$ is given in Fig. 3.3.

Figure 3.2 illustrates the difference between group delay, group velocity and energy velocity. The group delay velocity is oscillating as a function of the dielectric constant. These oscillations correspond to the oscillations in the transmission coefficient as in Fig. 3.1. The energy velocity is different from the group velocity because of a finite thickness of the layer. The energy velocity becomes equivalent to group velocity in the limit of $\varepsilon- > 1$.

Figure 3.3 illustrate the region near $\varepsilon = 0$. Note that the group delay velocity becomes superluminal in the tunneling regime ($\varepsilon < 0$). It is worth noting here that while the group velocity approaches zero at $\varepsilon = 0$ the energy flow velocity is never zero. In tunneling, for the non resonant case it can be very small. It is interesting that energy velocity remains small for tunneling even in the resonant case as seen in

Sections 3.2 and 3.3.

This difference among the different velocities is valid even for propagating cases as can be seen from Fig. 3.4 and 3.5 where the different velocities are plotted as functions of frequency and barrier width for a nondispersive case with dielectric constant larger than 1. In these examples the difference between the group velocity and the energy velocity is clearly seen with the energy velocity being smaller than the group velocity. This can be seen from the expressions for the energy velocity in a non-dispersive slab. The group velocity as defined in (3.18) gives the result [3]

$$\begin{aligned} v_E &= \frac{c\,|T|^2}{|A|^2+|B|^2} \\ &= \frac{2\,c}{\varepsilon+1}, \end{aligned} \tag{3.20}$$

where A and B are the coefficients for the field inside the slab. As is clear from (3.20), the energy velocity is dependent on the dielectric constant of the slab and has a constant value. It is worth noticing that its value is always lower than the group velocity, which for non dispersive slabs is given by $v_g = c/\sqrt{\varepsilon}$, the only exception being of course in vacuum. The energy velocity remains always subluminal due to the fact that $\varepsilon < 1$ implies dispersion and therefore equation (3.20) is no longer valid. For $0 < \varepsilon < 1$, the group velocity will be superluminal.

The group delay velocity is oscillating along with the transmission coefficient of the slab. The group delay velocity becomes equal to the energy velocity in the regions where the transmission is resonant as can be seen from Figs. 3.4 and 3.5.

3.2 Double Layer Structure

Consider a two layer structure as shown in Fig. 3.6. The layers have a dielectric constants $\varepsilon_1 = \varepsilon_1(\omega)$ and $\varepsilon_2 = \varepsilon_2(\omega)$ and widths $L_1 = a_1$ and $L_2 = a_2 - a_1$ for a total width of $L = a_2$. The electromagnetic wave that will be considered is TM-polarized (p-polarized), with the electric field in the incidence plane (y, z) and the magnetic field in the x-direction. Denoting:

$$k_v^2 = k_0^2 - k_y^2, \qquad k_0 = \omega/c \quad k_y = k_0 \sin\theta_i, \tag{3.21}$$

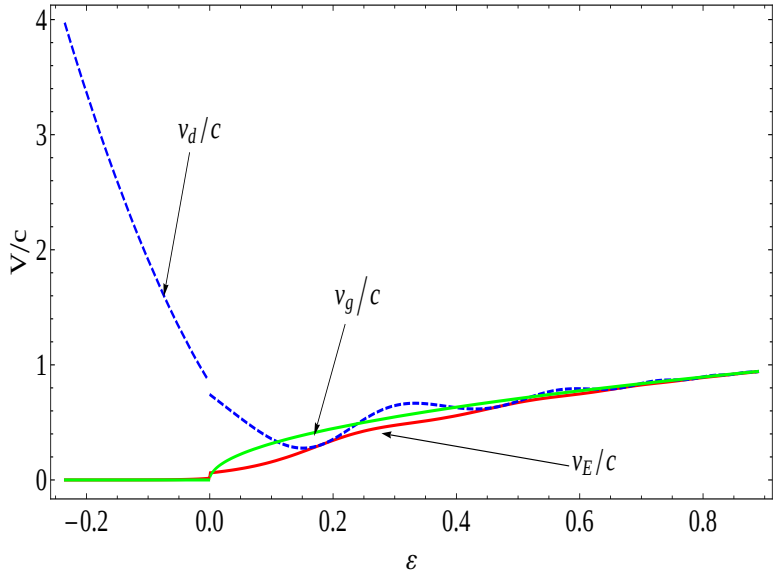

Figure 3.2: Energy, group delay and group velocities of the slab normalized to c with ω_p=10 GHz and d=0.02 m. As ε approaches unity, all velocities become equal. As ε goes to zero, group velocity goes to zero, energy velocity is small but finite. Delay velocity increases

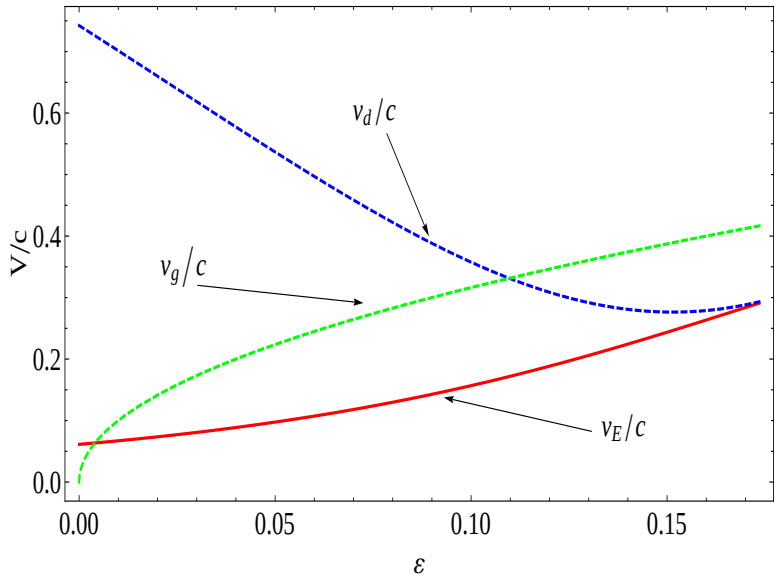

Figure 3.3: Energy, group delay and group velocities of the slab normalized to c with ω_p=10 GHz and d=0.02 m. As ε approaches zero group velocity goes to zero, energy velocity decreases but still finite, delay velocity increases.

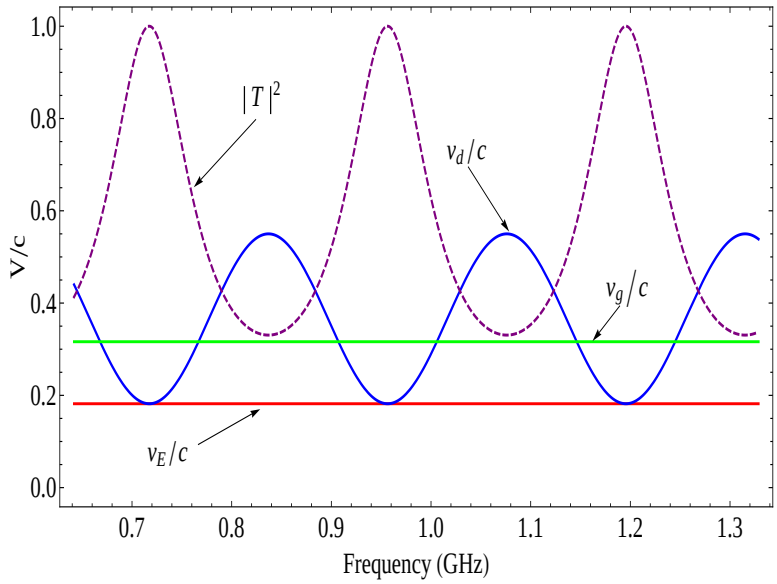

Figure 3.4: Energy, group delay and group velocities of the slab normalized to c. For this case, the width of the slab is 0.2 m $\varepsilon = 10$.

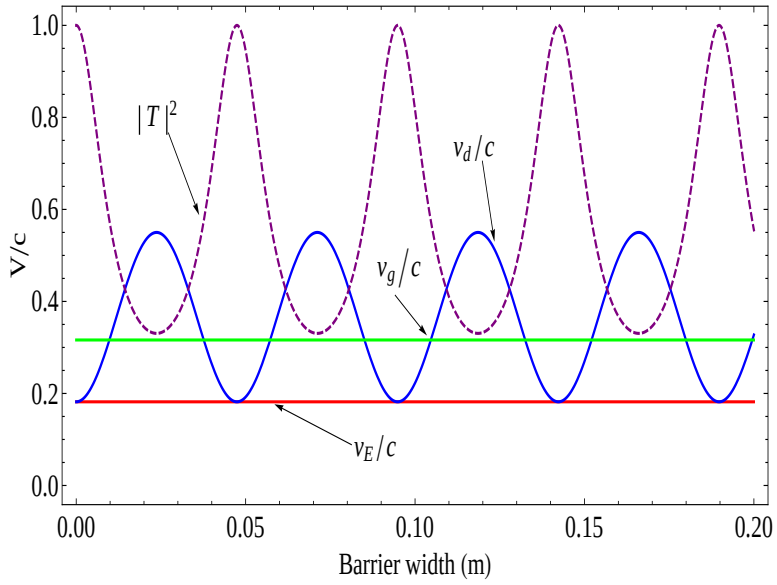

Figure 3.5: Energy, group delay and group velocities of the slab normalized to c as functions of the width of the slab. For this case, f=1 Ghz and $\varepsilon = 10$.

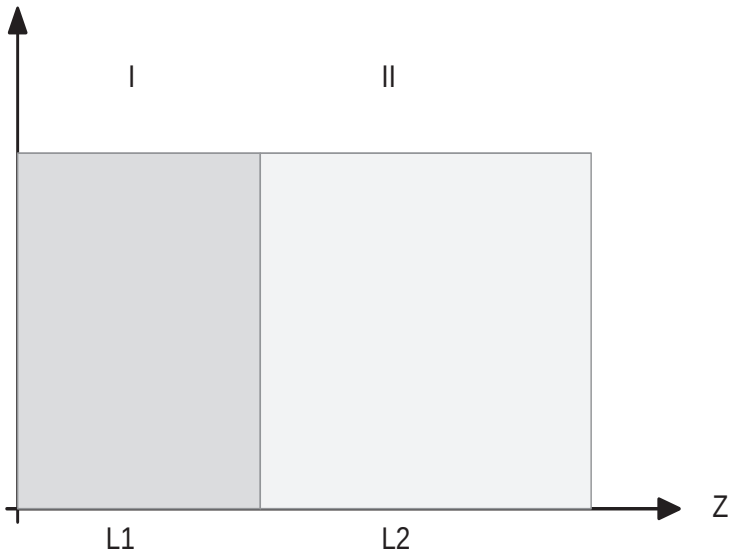

Figure 3.6: A two layered structure; the first layer is characterized by $0 < \varepsilon < 1$, the second by $\varepsilon < 0$

$$\kappa_1^2 = k_y^2 - \varepsilon_1(\omega)k_0^2, \tag{3.22}$$

$$\kappa_2^2 = k_y^2 - \varepsilon_2(\omega)k_0^2, \tag{3.23}$$

$$\eta_i = \varepsilon_i/\kappa_i, \tag{3.24}$$

the fields in the structure are given by

$$H(z) = e^{ik_v z} + R\, e^{-ik_v z} \qquad z < 0, \tag{3.25}$$

$$H(z) = A\, e^{-\kappa_1 z} + B\, e^{\kappa_1 z} \qquad 0 < z < a_1, \tag{3.26}$$

$$H(z) = C\, e^{-\kappa_2 (z-a_1)} + D\, e^{\kappa_2 (z-a_1)} \qquad a_1 < z < a_2, \tag{3.27}$$

$$H(z) = T\, e^{ik_v z} \qquad z > a_2. \tag{3.28}$$

Applying boundary conditions (continuity of H and $(dH/dz)/\varepsilon$ at the interfaces), the transmission coefficient is

$$T = \frac{e^{-ik_v L}}{g}, \tag{3.29}$$

$$g = \cosh\kappa_2 L_2 \cosh\kappa_1 L_1 + \Delta_1 \sinh\kappa_1 L_1 \sinh\kappa_2 L_2 + i\left[\Delta_2 \sinh\kappa_1 L_1 \cosh\kappa_2 L_2\right]. \tag{3.30}$$

The phase of the transmission coefficient is given by

$$\phi_0 = -\arctan\left[\frac{\Delta_2 \sinh\kappa_1 L_1 \cosh\kappa_2 L_2 + \Delta_3 \cosh\kappa_1 L_1 \sinh\kappa_2 L_2}{\cosh\kappa_2 L_2 \cosh\kappa_1 L_1 + \Delta_1 \sinh\kappa_1 L_1 \sinh\kappa_2 L_2}\right]. \tag{3.31}$$

Here Δ_1, Δ_2 and Δ_3 are defined as

$$\Delta_1 = \frac{1}{2}\left(\frac{\eta_1}{\eta_2} + \frac{\eta_2}{\eta_1}\right), \tag{3.32}$$

$$\Delta_2 = \frac{1}{2}\left(\frac{\eta_1}{\eta_0} - \frac{\eta_0}{\eta_1}\right), \tag{3.33}$$

$$\Delta_3 = \frac{1}{2}\left(\frac{\eta_2}{\eta_0} - \frac{\eta_0}{\eta_2}\right). \tag{3.34}$$

The resonant conditions of the structure are given by the conditions [1] (see appendix A)

$$\kappa_1 L_1 = \kappa_2 L_2, \tag{3.35}$$

$$\eta_1 + \eta_2 = 0. \tag{3.36}$$

This resonance corresponds to the excitation of surface modes in the structure. In Fig. 3.7 the resonance at the interface of the slabs can be seen.

The plots for the transmittance, the group delay, the dwell time and the energy velocity are given in Figs. 3.8-3.12. Normalized delays of less than unity suggest superluminality, but as can be seen from Figs. 3.12, the energy velocity stays subluminal. At the resonance, where the transmission coefficient is 1, the group delay velocity is equal to the energy velocity. The group delay velocity becomes superluminal away from the resonance.

3.3 Double Barrier Structure

Consider a region where two symmetrical barriers of width a are bounded by vacuum and separated by another vacuum region of width L as shown in Fig. 3.13.

As in the double layer case, a TM-polarized electromagnetic wave will be considered and the same notations will be used. The fields are given by

$$H(z) = e^{ik_v z} + R\, e^{-ik_v z} \qquad z < 0, \tag{3.37}$$

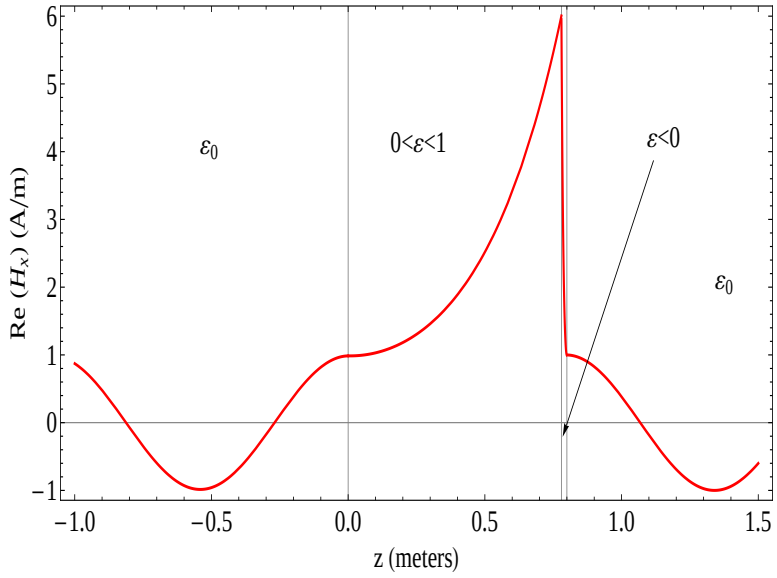

Figure 3.7: Magnetic field distribution for the double layer structure with $\omega = 6.28\times10^9$ rad s^{-1} (1GHz), $\omega_{p1} = 3.77\times10^{10}$ rad s^{-1} (6 GHz), $\omega_{p2} = 2\times10^9$ rad s^{-1} (0.32 GHz), $L_1 = 0.078m$, $L_2 = 0.02m$ the resonance occurs at $\theta \simeq 74°$. The surface resonance is in the interface of the two layers.

$$H(z) = A_0\, e^{-\kappa z} + B_0\, e^{\kappa z} \quad 0 < z < a, \tag{3.38}$$

$$H(z) = A_1\, e^{ik_v z} + B_1\, e^{-ik_v z} \quad a < z < L + a, \tag{3.39}$$

$$H(z) = A_2\, e^{-\kappa(z-L-a)} + B_2\, e^{\kappa(z-L-a)} \quad L + a < z < L + 2a. \tag{3.40}$$

Using boundary conditions at the interfaces (continuity of H and $(dH/dz)/\varepsilon$) the transmission coefficient is given by

$$T = \frac{e^{-2ik_v a}}{g}, \tag{3.41}$$

$$g = \cosh^2(\kappa a) + \frac{1}{4}\sinh^2(\kappa a)\left[\sigma^2\cos(k_v L) - \delta^2\right]$$
$$+i\sinh(\kappa a)\left[\delta\cosh(\kappa a) + \frac{1}{4}\sigma^2\sinh(\kappa a)\sin(2k_v L)\right]. \tag{3.42}$$

Here

$$\sigma = \frac{\eta_0}{\eta_1} + \frac{\eta_1}{\eta_0}, \tag{3.43}$$

$$\delta = \frac{\eta_1}{\eta_0} - \frac{\eta_0}{\eta_1}, \tag{3.44}$$

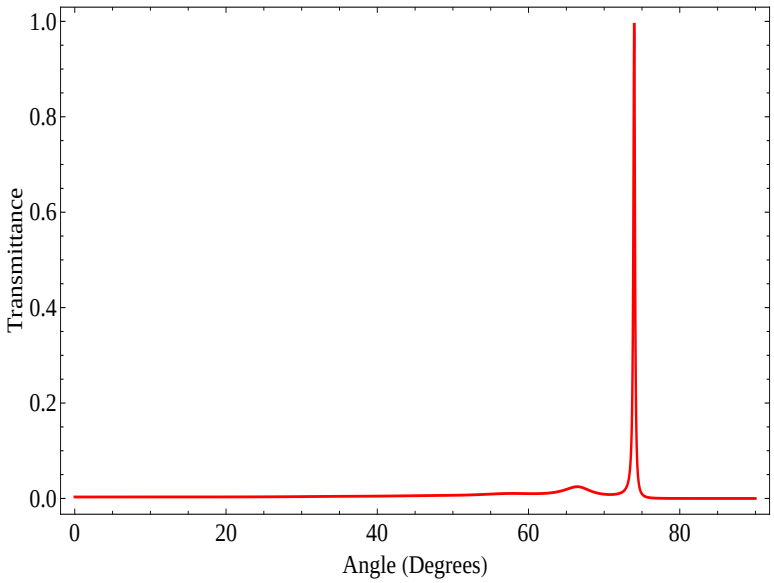

Figure 3.8: Transmissivity of the double layer structure with $\omega = 6.28 \times 10^9$ rad s^{-1} (1GHz), $\omega_{p1} = 3.77 \times 10^{10}$ rad s^{-1} (6 GHz), $\omega_{p2} = 2 \times 10^9$ rad s^{-1} (0.32 GHz), $L_1 = 0.078m$, $L_2 = 0.02m$ the resonance occurs at $\theta \simeq 74°$

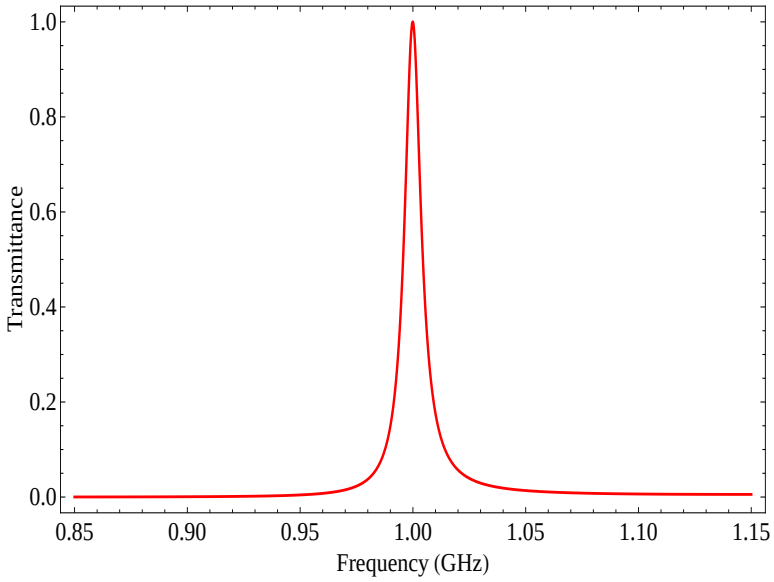

Figure 3.9: Transmissivity of the double layer structure with $\theta = 74°$, $\omega_{p1} = 3.77 \times 10^{10}$ rad s^{-1} (6 GHz), $\omega_{p2} = 2 \times 10^9$ rad s^{-1} (0.32 GHz), $L_1 = 0.078m$, $L_2 = 0.02m$

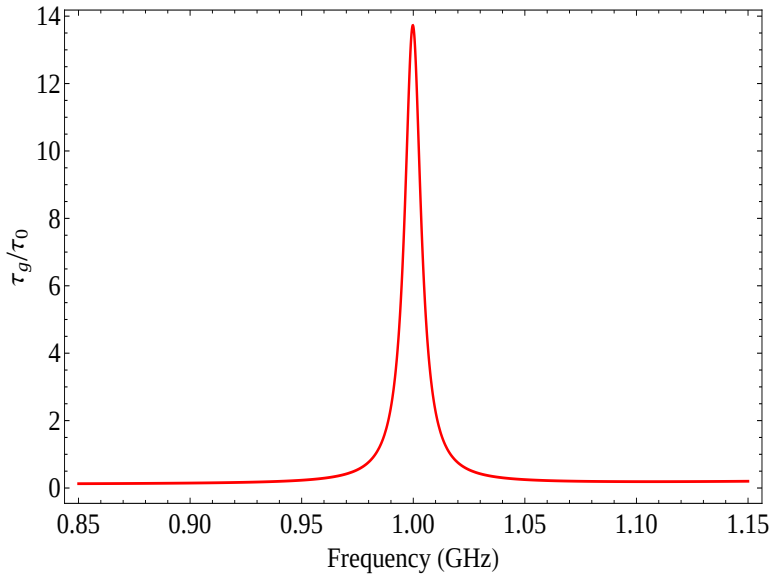

Figure 3.10: Group delay of the double layer structure normalized to the proper time with $\theta = 74°$, $\omega_{p1} = 3.77 \times 10^{10}$ rad s^{-1} (6 GHz), $\omega_{p2} = 2 \times 10^{9}$ rad s^{-1} (0.32 GHz), $L_1 = 0.078m$, $L_2 = 0.02m$

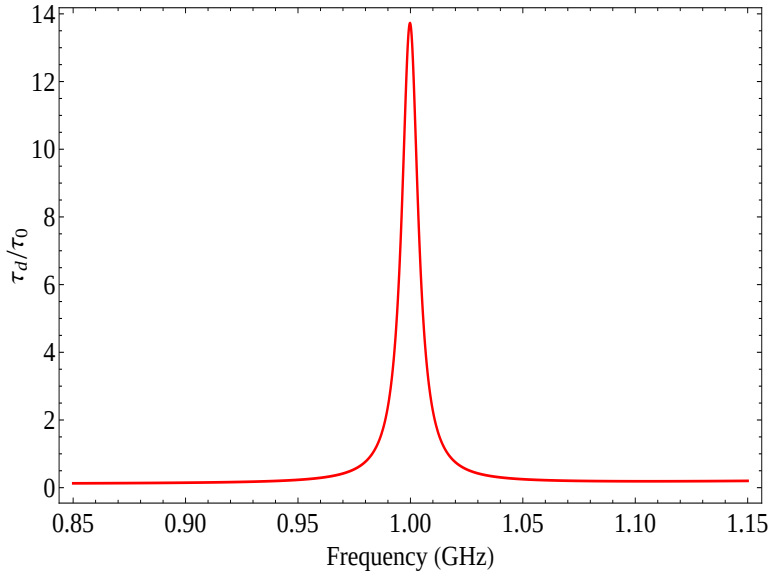

Figure 3.11: Dwell time of the double layer structure normalized to the proper time with $\theta = 74°$, $\omega_{p1} = 3.77 \times 10^{10}$ rad s^{-1} (6 GHz), $\omega_{p2} = 2 \times 10^{9}$ rad s^{-1} (0.32 GHz), $L_1 = 0.078m$, $L_2 = 0.02m$

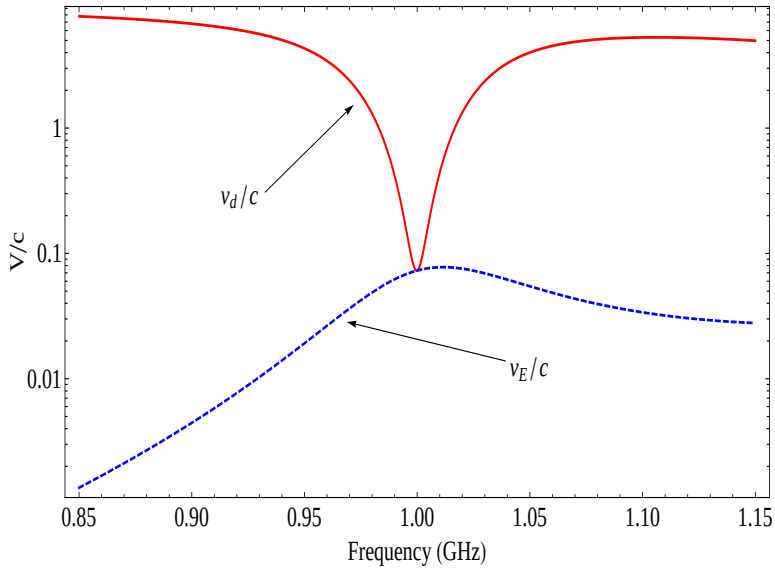

Figure 3.12: Energy velocity and group delay velocities of the double layer structure normalized to c with $\theta = 74°$, $\omega_{p1} = 3.77 \times 10^{10}$ rad s^{-1} (6 GHz), $\omega_{p2} = 2 \times 10^{9}$ rad s^{-1} (0.32 GHz), $L_1 = 0.078m$, $L_2 = 0.02m$

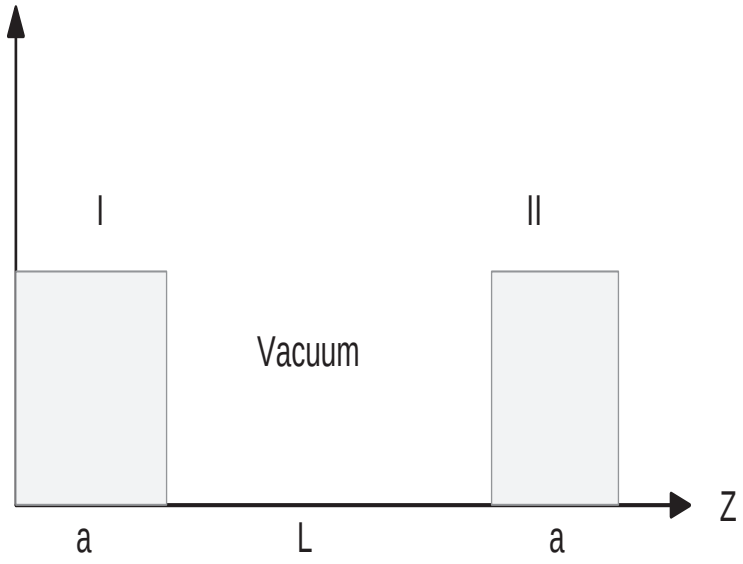

Figure 3.13: A double barrier structure; the two barrier regions are characterized by $\varepsilon < 0$ and separated by a vacuum region of width L.

$$\sigma^2 = \delta^2 + 4. \tag{3.45}$$

The resonant conditions for the double barrier structure are given by [21], [6]

$$\cot(k_v L) = -\frac{1}{2}\delta \tanh(\kappa a), \tag{3.46}$$

or by [1]

$$\tan(k_v L) = \frac{2\xi}{1-\xi^2} \qquad \xi = \frac{\eta_0}{\eta} = \frac{\kappa\varepsilon}{k_v \varepsilon_0}. \tag{3.47}$$

The phase of the transmission coefficient is given by

$$\phi_0 = k_v L - \arctan\left[\frac{\sinh(\kappa a)\left[\delta\cosh(\kappa a) + (1/4)\sigma^2 \sinh^2(\kappa a)\sin(2k_v L)\right]}{\cosh^2(\kappa a) + (1/4)\sinh^2(\kappa a)\left[\sigma^2\cos(2k_v L) - \delta^2\right]}\right]. \tag{3.48}$$

The resonant condition are the leaky eigenmode solutions to the finite depth well problem [1]. In Fig. 3.14 the resonances at the interface between the slabs and the inner vacuum region can be seen.

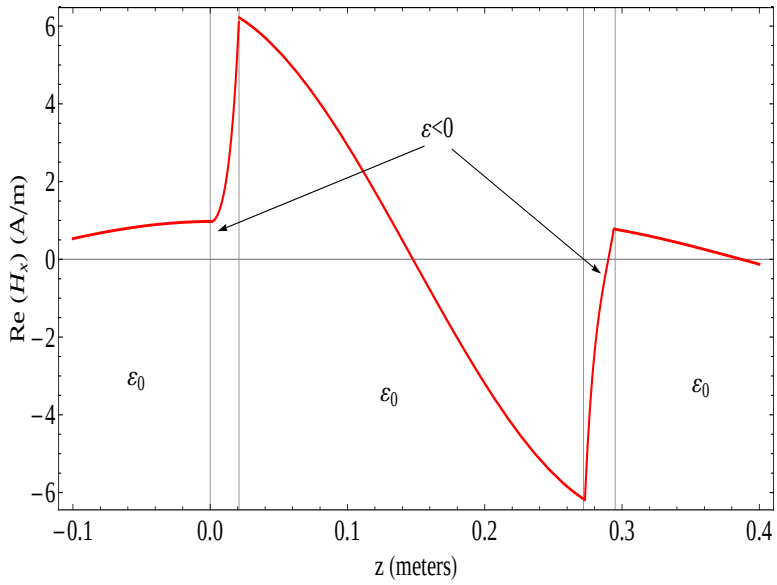

Figure 3.14: Magnetic field distribution for the double barrier structure with $\omega = 6.28 \times 10^9$ rad s^{-1} (1GHz), $\omega_p = 3.77 \times 10^{10}$ rad s^{-1} (6 GHz), $n_2 = 1$, $L = 0.25m$, $a = 0.021m$ the resonance occurs at $\theta = 62.3°$

The plots for the transmittance, the group delay, the dwell time and the energy velocity are given in Figs. 3.15-3.19. Normalized delays of less than unity suggest superluminality, but as can be seen from Fig. 3.19, the energy velocity stays subluminal.

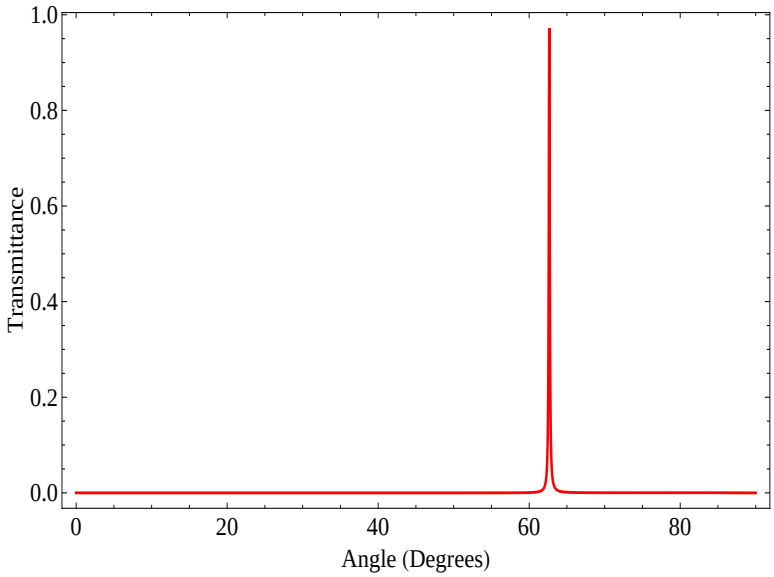

Figure 3.15: Transmissivity of the double barrier structure with $\omega = 6.28 \times 10^9$ rad s^{-1} (1GHz), $\omega_p = 3.77 \times 10^{10}$ rad s^{-1} (6 GHz), $n_2 = 1$, $L = 0.25m$, $a = 0.021m$ the resonance occurs at $\theta = 62.3°$

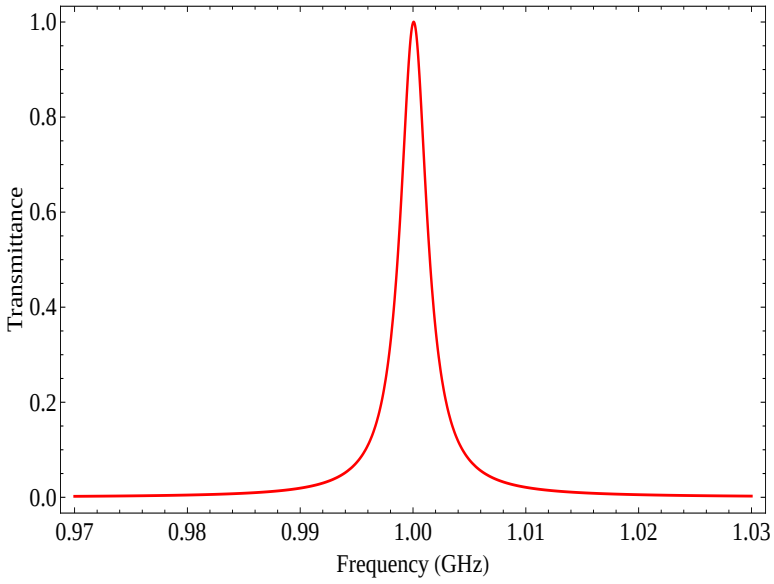

Figure 3.16: Transmissivity of the double barrier structure with $\theta = 62.3°$, $\omega_p = 3.77 \times 10^{10}$ rad s^{-1} (6 GHz), $n_2 = 1$, $L = 0.25m$, $a = 0.021m$

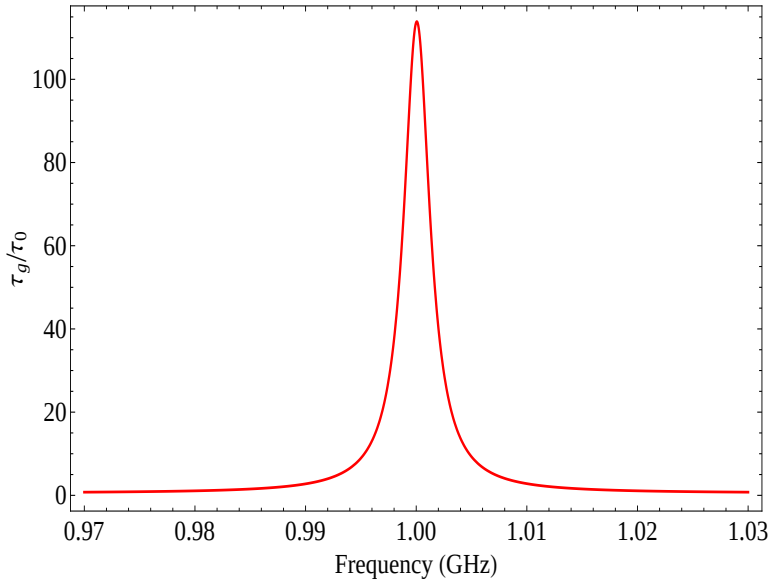

Figure 3.17: Group delay of the double barrier structure normalized to the proper time with $\theta = 62.3°$, $\omega_p = 3.77 \times 10^{10}$ rad s^{-1} (6 GHz), $n_2 = 1$, $L = 0.25m$, $a = 0.021m$

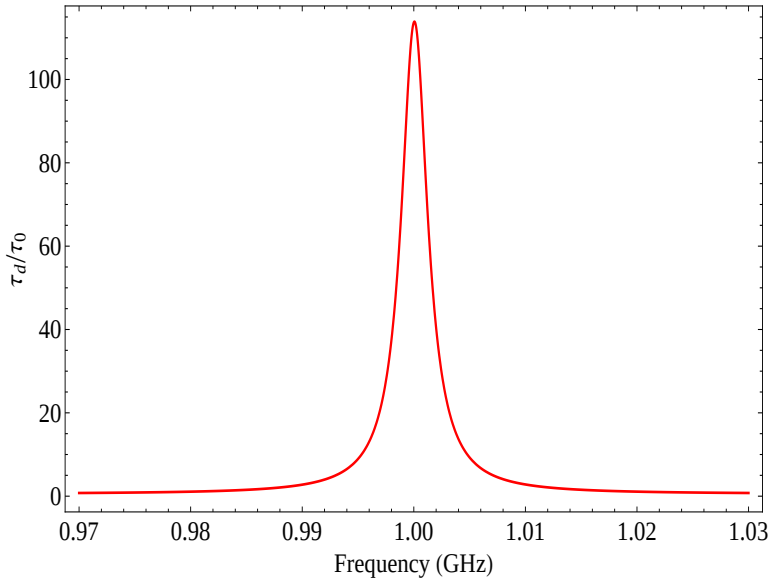

Figure 3.18: Dwell time of the double barrier structure normalized to the proper time with $\theta = 62.3°$, $\omega_p = 3.77 \times 10^{10}$ rad s^{-1} (6 GHz), $n_2 = 1$, $L = 0.25m$, $a = 0.021m$

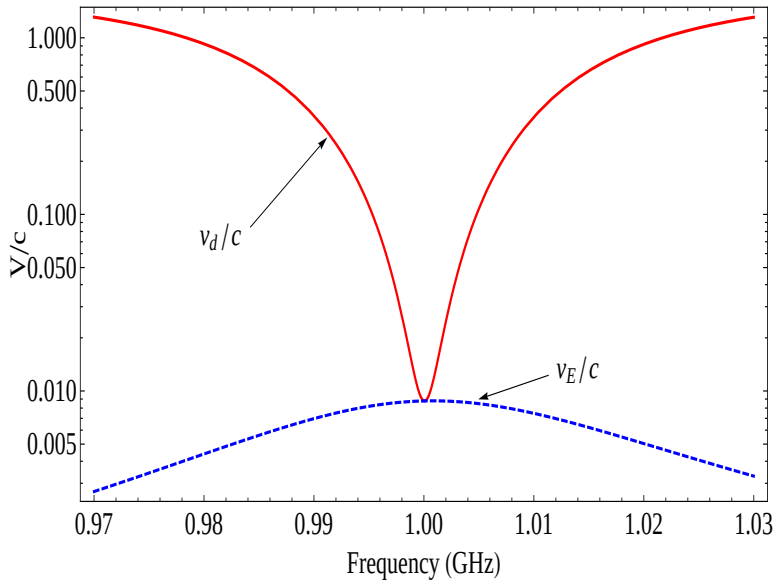

Figure 3.19: Energy velocity of the double barrier structure normalized to c with $\theta = 62.3°$, $\omega_p = 3.77 \times 10^{10}$ rad s^{-1} (6 GHz), $n_2 = 1$, $L = 0.25m$, $a = 0.021m$

3.4 Conclusions

A number of experiments have been performed to measure the tunneling time for different kinds of wave phenomena, ranging from laser radiation to acoustic waves. In the case of electromagnetic radiation, a good review can be found in [26] and [7]. It is worth mentioning that most if not all experiments, measure the group delay. In these experiments the following was confirmed [7]:

-The group delay is a measure of the time at which the transmitted gaussian pulse peaks at the exit.

-In reflection and transmission, the delays are the same for symmetric barriers.

-The group delay saturates with barrier length.

It has been noted , however, that the velocity of information transfer is not determined by the motion of the peak of the wave [7,21]. In order to have transmission of information by a wavepacket, it needs to have a point where it is non-analytical (e.g. sharp edge), requirement that is not satisfied for any gaussian packets.

Therefore the superluminal group delay velocity does not suggest superluminal information transport. The information flow requires energy transport, thus the energy flow velocity (which is always subluminal) has to be considered as an information flow velocity.

In this section, energy transport was analyzed for the cases of a finite width slab, tunneling of evanescent waves through multilayered structuresand dispersive media.

The group delay and the dwell time are shown to be equivalent and to represent the lifetime of the energy inside the barrier region and not to represent a transit time for the transmitted wave, therefore any conclusion that the tunneling process is superluminal based on these times is not correct. The tunneling process is explained based on the interference of evanescent waves inside the barrier region, interference that generates an energy transport responsible for both reflection and transmission of the wave, the velocity associated with this energy transport is shown to be always subluminal and not to saturate with distance via its dependence on the transmission coefficient. The resonance in the structures can be explained via amplification of evanescent waves in the case of the double barrier and via the leaky eigenmodes in the double barrier case [1]. The concept of group velocity as defined in literature loses its sense in the barrier region due to the fact that the wavevector inside this region is purely real, leading thus to a purely imaginary group velocity or a purely imaginary time, quantity that is not observable.

In general, the energy velocity $\mathbf{v}_E$ is a nonlocal quantity which is affected by the field distribution over the whole system, and in particular, by boundary conditions. It always remains subluminal. In resonant cases (and in absence of dissipation), the energy velocity $\mathbf{v}_E$ is equal to the group delay velocity $v_d = \partial\omega/\partial\kappa$.

It is argued therefore that the energy velocity $\mathbf{v}_E = \mathbf{S}/U$ is the most appropriate quantity describing the velocity of the energy flow, and hence, the velocity of the information flow. This conclusion is important for slow and fast light, where group velocity is usually sued, but the energy (information) velocity may be different as noted above.

Chapter 4

Microscopic and Macroscopic Forces in Dielectric Media

A body in an electromagnetic field experiences a force imparted by this field. This force is called radiation pressure. This radiation pressure is related to the reflection and absorbtion of light and gives rise to very important physical consequences.

Due to the fact that any medium is composed of atoms, the forces on a body due to the electromagnetic field are due to the action of the field on the individual charges and currents proper and on the charges and currents induced on the body by the electromagnetic field. In order to understand and study the nature of these forces it is necessary to study how the electromagnetic field gives rise to induced charges and currents on the body and how the field exerts a force onto them. The starting point is the microscopic Maxwell equations under the assumption that all microscopic effects are basically averages of the corresponding microscopical effects [17, 27, 28].

4.1 The Microscopic Maxwell Equations

The microscopic theory of electromagnetism was developed by Hendrik Lorentz at the end of the XIX century [29]. Although this is a purely classical theory, it accounts for most electrical properties of matter and it will be considered the theoretical backbone of all subsequent analysis on the radiation pressure of light on matter.

The starting point is the formulation of the microscopic Maxwell equations that are related to the microscopic properties of matter via the source terms (microscopic charge and current density). Based on this and carrying out an appropriate aver-

aging procedure, the macroscopic properties of matter can be obtained [28]. The microscopic Maxwell equations are

$$\begin{aligned} \nabla \cdot \mathbf{e} &= \frac{\varrho}{\varepsilon_0}, && (4.1)\\ \nabla \cdot \mathbf{b} &= 0 && (4.2)\\ \nabla \times \mathbf{e} &= -\frac{\partial \mathbf{b}}{\partial t}, && (4.3)\\ \nabla \times \mathbf{b} &= \mu_0 \mathbf{j} + \mu_0 \varepsilon_0 \frac{\partial \mathbf{e}}{\partial t}, && (4.4) \end{aligned}$$

where $\mathbf{e}$ and $\mathbf{b}$ are the microscopic electric and magnetic fields, ϱ and $\mathbf{j}$ are the microscopic charge and current densities respectively.

The microscopic Maxwell equations connect the fields via the source terms. It is clear from these equations that the origin of the fields are the electric charges [28] and that the distinction between electric, magnetic and electromagnetic fields lies only in the relative movement of these charges with respect to the observation point [27].

In addition to the microscopic Maxwell equations, the microscopic Lorentz theory is completed by the microscopic force density that acts upon all the charges and currents. This microscopic force density can be expressed as

$$\mathbf{f} = \varrho\, \mathbf{e} + \mathbf{j} \times \mathbf{b}. \qquad (4.5)$$

This tells us that there is a momentum associated with the electromagnetic field in such a way that the change of this momentum gives raise to the microscopic Lorentz force (i.e the moment the electromagnetic field loses is then given to the respective charge and current densities) [27, 30].

This can be seen considering Newton's second law of motion

$$\frac{d\mathbf{p}_{mech}}{dt} = \int_V (\varrho\, \mathbf{e} + \mathbf{j} \times \mathbf{b})\, dV. \qquad (4.6)$$

The task is now from (4.1)-(4.4) obtain the expressions for ϱ and $\mathbf{j}$ and plug them into (4.5).

Using the microscopic Lorentz equations (4.1)-(4.4), the charge and current den-

sities are

$$\begin{aligned} \varrho &= \varepsilon_0 \nabla \cdot \mathbf{e}, & (4.7) \\ \mathbf{j} &= \frac{1}{\mu_0}\left(\nabla \times \mathbf{b} - \mu_0 \varepsilon_0 \frac{\partial \mathbf{e}}{\partial t}\right). & (4.8) \end{aligned}$$

Plugging these last expressions into (4.5), the microscopic Lorentz force can be expressed as

$$\begin{aligned} \varrho\,\mathbf{e} + \mathbf{j} \times \mathbf{b} &= \varepsilon_0 (\nabla \cdot \mathbf{e})\mathbf{e} + \frac{1}{\mu_0}\left(\nabla \times \mathbf{b} - \mu_0 \varepsilon_0 \frac{\partial \mathbf{e}}{\partial t}\right) \times \mathbf{b} \\ &= \varepsilon_0 (\nabla \cdot \mathbf{e})\mathbf{e} + \frac{1}{\mu_0}(\nabla \times \mathbf{b}) \times \mathbf{b} - \varepsilon_0 \frac{\partial \mathbf{e}}{\partial t} \times \mathbf{b}. \qquad (4.9) \end{aligned}$$

This way, the microscopic Lorentz force density reduces to:

$$\mathbf{f} = -\nabla \cdot \left\{ \frac{1}{2}\left(\varepsilon_0 \mathbf{e} \cdot \mathbf{e} + \frac{1}{\mu_0}\mathbf{b} \cdot \mathbf{b}\right) \delta_{ij} - \varepsilon_0 \mathbf{e}\mathbf{e} - \frac{1}{\mu_0}\mathbf{b}\mathbf{b} \right\} - \frac{\partial}{\partial t}(\varepsilon_0\, \mathbf{e} \times \mathbf{b}). \qquad (4.10)$$

With this in mind, the conservation for the total system of particles and fields reads

$$\begin{aligned} \frac{d}{dt}(\mathbf{p}_{mech} + \mathbf{p}_{em}) &= \int_V \nabla \cdot \bar{\mathcal{T}}^{mic}\, dV \\ &= \oint_S \hat{\mathbf{n}} \cdot \bar{\mathcal{T}}^{mic}\, dS. \qquad (4.11) \end{aligned}$$

The quantity $\bar{\mathcal{T}}^{mic}$ in (4.11) is the microscopic Maxwell stress tensor defined as

$$\bar{\mathcal{T}}^{mic} = \frac{1}{2}\left(\varepsilon_0 \mathbf{e} \cdot \mathbf{e} + \frac{1}{\mu_0}\mathbf{b} \cdot \mathbf{b}\right) \delta_{ij} - \varepsilon_0 \mathbf{e}\mathbf{e} - \frac{1}{\mu_0}\mathbf{b}\mathbf{b}, \qquad (4.12)$$

and the quantity $\mathbf{p}_{em}$ is the microscopic electromagnetic momentum given by

$$\mathbf{p}_{em} = \int_V \varepsilon_0\, \mathbf{e} \times \mathbf{b}\; dV. \qquad (4.13)$$

If the region of integration is taken to be all space, and such that all the components of $\bar{\mathcal{T}}^{mic}$ go to zero fast enough such that the surface integral vanishes as the surface goes to infinity, (4.11) reduces to [27]

$$\frac{d}{dt}(\mathbf{p}_{mech} + \mathbf{p}_{em}) = 0. \qquad (4.14)$$

This last equation tells us that it is the total momentum of the system particles-fields that is conserved in all of space, rather than just the momentum of the particles.

This quantity $\hat{\mathbf{n}} \cdot \bar{\mathcal{T}}^{mic}$ in (4.11) can be regarded as the force per unit area across a surface S transmitted by the microscopic electromagnetic field. It can be argued that the total flow of momentum across a surface is not completely specified by the integral over the surface of $\hat{\mathbf{n}} \cdot \bar{\mathcal{T}}^{mic}$ since one can always add a quantity such that its integral over the surface vanishes [13, 27], but the expression obtained in (4.12) is a direct consequence of the Maxwell-Lorentz theory and therefore a self-consistent one [27, 31, 32].

4.2 Averaging of Microscopic Equations

As pointed before, in the Maxwell-Lorentz theory, matter is regarded as composed of point charges that produce microscopic electromagnetic fields. The macroscopic theory along with all macroscopic phenomena is then obtained by using a suitable averaging procedure of the corresponding microscopic quantities. This view was the original one exposed by Lorentz [29] and has been extended since by numerous authors [17, 28, 33].

4.2.1 Average Value of the Microscopic Quantities

A microscopic quantity $A(\mathbf{r})$ given as a function of position can be averaged using a suitable distribution function $w(\mathbf{s})$ such that $w(\mathbf{s})$ is a positive function and that is not equal to zero only in the vicinity of the point $\mathbf{s} = 0$. With this in mind, the average of the microscopic quantity $A(\mathbf{r})$ with respect to $w(\mathbf{s})$ is given by [33]

$$\langle A(\mathbf{r}) \rangle = \int_V A(\mathbf{r} - \mathbf{s})\, w(\mathbf{s})\, d^3 s, \tag{4.15}$$

$$\int_V w(\mathbf{s})\, d^3 s = 1. \tag{4.16}$$

It is assumed that $w(\mathbf{s})$ varies slowly enough such that it can be expanded by Taylor as

$$w(\mathbf{s} + \mathbf{d}) \approx w(\mathbf{s}) + (\mathbf{d} \cdot \nabla) w(\mathbf{s}) + \frac{1}{2} (\mathbf{d} \cdot \nabla)^2 w(\mathbf{s}). \tag{4.17}$$

It is seen from these definitions of the average that space and time differentiations are commutable, such that

$$\begin{aligned} \frac{\partial}{\partial x_j}\left\langle A(\mathbf{r},t)\right\rangle &= \int w(\mathbf{s})\frac{\partial A(\mathbf{r}-\mathbf{s},t)}{\partial x_j}\,d^3s \\ &= \left\langle \frac{\partial A(\mathbf{r},t)}{\partial x_j}\right\rangle \end{aligned} \tag{4.18}$$

and

$$\begin{aligned} \frac{\partial}{\partial t}\left\langle A(\mathbf{r},t)\right\rangle &= \int w(\mathbf{s})\frac{\partial A(\mathbf{r}-\mathbf{s},t)}{\partial t}\,d^3s \\ &= \left\langle \frac{\partial A(\mathbf{r},t)}{\partial t}\right\rangle. \end{aligned} \tag{4.19}$$

The macroscopic fields $\mathbf{E}$ and $\mathbf{B}$ are obtained from the averaging of the corresponding microscopic fields $\mathbf{e}$ and $\mathbf{b}$, such that [28]

$$\mathbf{E} \equiv \left\langle \mathbf{e}\right\rangle, \tag{4.20}$$

$$\mathbf{B} \equiv \left\langle \mathbf{b}\right\rangle. \tag{4.21}$$

It is the fact that the average of the microscopic field $\mathbf{b}$ gives $\mathbf{B}$ as expressed in (4.21) that justifies regarding $\mathbf{b}$ as the fundamental magnetic field instead of $\mathbf{H}$ [28].

In this fashion, the average of the microscopic Maxwell equations given in (4.1)-(4.4) are [17, 28]

$$\nabla\cdot\mathbf{E} = \frac{\langle\varrho\rangle}{\varepsilon_0}, \tag{4.22}$$

$$\nabla\cdot\mathbf{B} = 0, \tag{4.23}$$

$$\nabla\times\mathbf{E} = -\frac{\partial\mathbf{B}}{\partial t}, \tag{4.24}$$

$$\nabla\times\mathbf{B} = \mu_0\left\langle\mathbf{j}\right\rangle + \mu_0\varepsilon_0\frac{\partial\mathbf{E}}{\partial t}. \tag{4.25}$$

The task in hand is therefore to calculate $\langle\varrho\rangle$ and $\langle\mathbf{j}\rangle$ in (4.22) and (4.25) to obtain the corresponding expressions for the macroscopic quantities $\mathbf{D}$ and $\mathbf{H}$ respectively. It is these fields $\mathbf{D}$ and $\mathbf{H}$ that can be identified with the bulk properties of matter.

4.2.2 Spatial Average of the Charge Density

The microscopic charge density can be divided into the charges carried by the conduction electrons and the charges bounded to the molecules. As such the microscopic

charge density can be written as

$$\begin{aligned}\varrho(\mathbf{r}) &= \sum_j q_j\,\delta(\mathbf{r}-\mathbf{r}_j) = \sum_{j(e)} q_j\,\delta(\mathbf{r}-\mathbf{r}_j) + \sum_{j(mol)} q_j\,\delta(\mathbf{r}-\mathbf{r}_j) \\ &= \sum_{j(e)} q_j\,\delta(\mathbf{r}-\mathbf{r}_j) + \sum_l \sum_{j(l)} q_j\,\delta(\mathbf{r}-\mathbf{r}_j). \end{aligned} \tag{4.26}$$

Considering only the $l-th$ molecule, from the definition of average and (4.26) we have

$$\begin{aligned}\langle\varrho_l\rangle &= \int w(\mathbf{r})\varrho(\mathbf{r}-\mathbf{s})\,d^3s = \int w(\mathbf{s}) \sum_{j(l)} q_j\,\delta(\mathbf{r}-\mathbf{s}-\mathbf{r}_j)\,d^3s \\ &= \sum_{j(l)} q_j\,w(\mathbf{r}-\mathbf{r}_j) = \sum_{j(l)} q_j\,w(\mathbf{r}-\mathbf{r}_l+\mathbf{r}_l-\mathbf{r}_j) \\ &= \sum_{j(l)} q_j\,w(\mathbf{r}-\mathbf{r}_l-\mathbf{r}_{jl}), \end{aligned} \tag{4.27}$$

where $\mathbf{r}_{jl} = \mathbf{r}_j - \mathbf{r}_l$. The quantity $\mathbf{r}_{jl}$ is the distance between the charge in the molecule and its center of mass and is therefore of the order of the size of the molecule. Making a Taylor expansion around $\mathbf{r}-\mathbf{r}_l$ using (4.17)

$$\begin{aligned}\langle\varrho_l\rangle &\approx \sum_{j(l)} q_j \left[w(\mathbf{r}-\mathbf{r}_l) - (\mathbf{r}_{jl}\cdot\nabla)w(\mathbf{r}-\mathbf{r}_l) + \frac{1}{2}(\mathbf{r}_{jl}\cdot\nabla)^2 w(\mathbf{r}-\mathbf{r}_l)\right] \\ &= q_l w(\mathbf{r}-\mathbf{r}_l) - \mathbf{p}_l\cdot\nabla w(\mathbf{r}-\mathbf{r}_l) + \mathbf{q}_l\cdot\nabla\cdot\nabla w(\mathbf{r}-\mathbf{r}_l) \\ &= \int w(\mathbf{s}) q_l \delta(\mathbf{r}-\mathbf{s}-\mathbf{r}_l)d^3s - \nabla\cdot\int w(\mathbf{s})\mathbf{p_l}\delta(\mathbf{r}-\mathbf{s}-\mathbf{r}_l)d^3s \\ &\quad + \nabla\cdot\nabla\cdot\int w(\mathbf{s})\mathbf{q_l}\delta(\mathbf{r}-\mathbf{s}-\mathbf{r}_l)d^3s, \end{aligned} \tag{4.28}$$

where

$$\begin{aligned}\mathbf{p}_l &= \sum_{j(l)} q_j\mathbf{r}_{jl} \rightarrow \text{dipole moment l-th molecule}, \\ \mathbf{q}_l &= \frac{1}{2}\sum_{j(l)} q_j\mathbf{r}_{jl}\mathbf{r}_{jl} \rightarrow \text{quadrupole moment l-th molecule}. \end{aligned}$$

The total average of the microscopic charge density is then obtained combining (4.26) and (4.28)

$$\begin{aligned}\rho &= \left\langle \sum_{j(e)} q_j\,\delta(\mathbf{r}-\mathbf{r}_j)\right\rangle + \left\langle \sum_{l} \varrho_l(\mathbf{r})\right\rangle \\ &= \left\langle \sum_{j(e)} q_j\,\delta(\mathbf{r}-\mathbf{r}_j)\right\rangle + \left\langle \sum_{l} q_l\delta(\mathbf{r}-\mathbf{r}_l)\right\rangle \\ &\quad -\nabla\cdot\left\langle \sum_{l} \mathbf{p}_l\,\delta(\mathbf{r}-\mathbf{r}_l)\right\rangle + \nabla\cdot\nabla\cdot\left\langle \sum_{l} \mathbf{q}_l\,\delta(\mathbf{r}-\mathbf{r}_l)\right\rangle . \qquad (4.29)\end{aligned}$$

Defining the quantities ρ_f as the net free charge, $\mathbf{P}$ as the macroscopic polarization and $\mathcal{Q}$ as the quadrupole moment density tensor, such that

$$\rho_f = \left\langle \sum_{j(e)} q_j\,\delta(\mathbf{r}-\mathbf{r}_j)\right\rangle + \left\langle \sum_{l} q_l\,\delta(\mathbf{r}-\mathbf{r}_l)\right\rangle , \qquad (4.30)$$

$$\mathbf{P} = \left\langle \sum_{l} \mathbf{p}_l\,\delta(\mathbf{r}-\mathbf{r}_l)\right\rangle , \qquad (4.31)$$

$$\mathcal{Q} = \left\langle \sum_{l} \mathbf{q}_l\,\delta(\mathbf{r}-\mathbf{r}_l)\right\rangle , \qquad (4.32)$$

the final expression for the averaged charge density is then given by

$$\rho = \rho_f - \nabla\cdot(\mathbf{P}-\nabla\cdot\mathcal{Q}). \qquad (4.33)$$

4.2.3 Spatial Average of the Current Density

Similar to the charge density, the microscopic current density can be divided between the current charged by the conduction electrons and the current generated by the movement of the charges bounded to the molecules. As such the microscopic current density can be written as

$$\begin{aligned}\mathbf{j}(\mathbf{r}) &= \sum_{j} q_j\,\mathbf{v}_j\delta(\mathbf{r}-\mathbf{r}_j) \\ &= \sum_{j(e)} q_j\,\mathbf{v}_j\delta(\mathbf{r}-\mathbf{r}_j) + \sum_{j(mol)} q_j\,\mathbf{v}_j\delta(\mathbf{r}-\mathbf{r}_j) \\ &= \sum_{j(e)} q_j\,\mathbf{v}_j\delta(\mathbf{r}-\mathbf{r}_j) + \sum_{l}\sum_{j(l)} q_j\,\mathbf{v}_j\delta(\mathbf{r}-\mathbf{r}_j). \qquad (4.34)\end{aligned}$$

The average value for the $l-th$ molecule is thus given by

$$\begin{aligned}
\langle \mathbf{j}_l \rangle &= \int w(\mathbf{s}) \mathbf{j}_l(\mathbf{r}-\mathbf{s})\, d^3s \\
&= \int w(\mathbf{s}) \sum_{j(l)} q_j \mathbf{v}_j(\mathbf{r}-\mathbf{s}) \delta(\mathbf{r}-\mathbf{s}-\mathbf{r}_j)\, d^3s \\
&= \sum_{j(l)} q_j w(\mathbf{r}-\mathbf{r}_j) \mathbf{v}_j(\mathbf{r}-\mathbf{r}+\mathbf{r}_j) \\
&= \sum_{j(l)} q_j w(\mathbf{r}-\mathbf{r}_l-\mathbf{r}_{jl}) \mathbf{v}_j(\mathbf{r}_l+\mathbf{r}_{jl}). \qquad (4.35)
\end{aligned}$$

As before, expanding the function w by Taylor around the point $\mathbf{r}-\mathbf{r}_l$

$$\begin{aligned}
\langle \mathbf{j}_l \rangle = q_l \mathbf{v}_l w(\mathbf{r}-\mathbf{r}_l) + \frac{d\mathbf{p}_l}{dt} w(\mathbf{r}-\mathbf{r}_l) - \mathbf{v}_l(\mathbf{p}_l \cdot \nabla) w(\mathbf{r}-\mathbf{r}_l) \\
+\mathbf{v}_l(\mathbf{q}_l \cdot \nabla \cdot \nabla) w(\mathbf{r}-\mathbf{r}_l) - \sum_{j(l)} q_j \mathbf{v}_{jl}(\mathbf{r}_{jl} \cdot \nabla) w(\mathbf{r}-\mathbf{r}_l).
\end{aligned}$$

Using the identities

$$\frac{d\mathbf{p}_l w}{dt} + \nabla \times (\mathbf{p}_l \times \mathbf{v}_l w) = w \frac{d\mathbf{p}_l}{dt} - \mathbf{v}_l(\mathbf{p}_l \cdot \nabla) w,$$

$$\begin{aligned}
\nabla \times (\mathbf{m}_l w) - \frac{d\mathbf{q}_l \cdot \nabla w}{dt} - \nabla \times \nabla \cdot (\mathbf{q}_l \times \mathbf{v}_l w) = \\
\mathbf{v}_l(\mathbf{q}_l \cdot \nabla \cdot \nabla) w - \sum_{j(l)} q_j \mathbf{v}_{jl}(\mathbf{r}_{jl} \cdot \nabla) w,
\end{aligned}$$

where $\mathbf{m}_l$ is the magnetic moment of the molecule, defined as

$$\mathbf{m}_l = \frac{1}{2} \sum_{j(l)} q_j \mathbf{r}_{jl} \times \mathbf{v}_{jl},$$

and plugging these last equations into the Taylor expansion for $\mathbf{j}_l$, the average current density is then given by

$$\begin{aligned}
\langle \mathbf{j}_l \rangle &= q_l \mathbf{v}_l w(\mathbf{r}-\mathbf{r}_l) + \frac{d}{dt}(\mathbf{p}_l w(\mathbf{r}-\mathbf{r}_l) - \mathbf{q}_l \cdot \nabla w(\mathbf{r}-\mathbf{r}_l)) + \nabla \times \mathbf{m}_l w(\mathbf{r}-\mathbf{r}_l) \\
&\quad + \nabla \times (\mathbf{p}_l \times \mathbf{v}_l w(\mathbf{r}-\mathbf{r}_l)) - \nabla \times \nabla \cdot (\mathbf{q}_l \times \mathbf{v}_l w(\mathbf{r}-\mathbf{r}_l)) \\
&= \langle q_l \mathbf{v}_l \delta(\mathbf{r}-\mathbf{r}_l) \rangle + \frac{d}{dt} \left[\langle \mathbf{p}_l \delta(\mathbf{r}-\mathbf{r}_l \rangle - \nabla \cdot \langle \mathbf{q}_l \delta(\mathbf{r}-\mathbf{r}_l) \rangle \right] \\
&\quad + \nabla \times \langle \mathbf{m}_l \delta(\mathbf{r}-\mathbf{r}_l) \rangle \\
&\quad + \nabla \times [\langle \mathbf{p}_l \times \mathbf{v}_l \delta(\mathbf{r}-\mathbf{r}_l) \rangle - \nabla \cdot \langle \mathbf{q}_l \times \mathbf{v}_l \delta(\mathbf{r}-\mathbf{r}_l) \rangle]. \qquad (4.36)
\end{aligned}$$

As with the charge density, the average microscopic current density is then given by

$$\mathbf{J} = \left\langle \sum_{j(e)} q_j \mathbf{v}_j \delta(\mathbf{r} - \mathbf{r}_j) \right\rangle + \left\langle \sum_l \mathbf{j}_l \right\rangle$$

$$= \mathbf{J}_f + \frac{d}{dt}\left(\mathbf{P} - \nabla \cdot \mathcal{Q}\right) + \nabla \times \mathbf{M}$$

$$+\nabla \times \left[\left\langle \sum_l \mathbf{p}_l \times \mathbf{v}_l \delta(\mathbf{r} - \mathbf{r}_l) \right\rangle - \nabla \cdot \left\langle \sum_l \mathbf{q}_l \times \mathbf{v}_l \delta(\mathbf{r} - \mathbf{r}_l) \right\rangle \right], \tag{4.37}$$

where $\mathbf{J}_f$ is the net free current density

$$\mathbf{J}_f = \left\langle \sum_{j(e)} q_j \mathbf{v}_j \, \delta(\mathbf{r} - \mathbf{r}_j) \right\rangle + \left\langle \sum_l q_l \mathbf{v}_l \, \delta(\mathbf{r} - \mathbf{r}_l) \right\rangle.$$

4.2.4 Spatial Average of the Lorentz Force

Similarly to the procedure used to obtain the average charge density and current density, the macroscopic Lorentz force can be obtained by averaging equation (4.5)

$$\langle \mathbf{f} \rangle = \mathbf{f}_L = \int w(\mathbf{s}) [\varrho(\mathbf{r} - \mathbf{s}) \mathbf{e}(\mathbf{r} - \mathbf{s}) + \mathbf{j}(\mathbf{r} - \mathbf{s}) \times \mathbf{b}(\mathbf{r} - \mathbf{s})] \, d^3 s. \tag{4.38}$$

Defining $\mathbf{e}' \equiv \mathbf{E} - \mathbf{e}$ and $\mathbf{b}' \equiv \mathbf{B} - \mathbf{b}$ as the difference between the macroscopic and microscopic fields, such that $\mathbf{E}(\mathbf{r} - \mathbf{s}) \approx \mathbf{E}(\mathbf{r})$ and $\mathbf{B}(\mathbf{r} - \mathbf{s}) \approx \mathbf{B}(\mathbf{r})$ [27], where $\mathbf{s}$ varies over the size of $w(\mathbf{s})$, the macroscopic Lorentz force becomes then

$$\mathbf{f}_L = \langle \varrho \rangle \, \mathbf{E} + \langle \mathbf{j} \rangle \times \mathbf{B} - \langle \varrho \mathbf{e}' \rangle + \langle \mathbf{j} \times \mathbf{b}' \rangle \, .$$

The volume of integration can be made such that as it gets smaller, $\mathbf{e}'$ and $\mathbf{b}'$ become smaller such that the final expression for the macroscopic Lorentz force is given by

$$\mathbf{f}_L = \rho \mathbf{E} + \mathbf{J} \times \mathbf{B},$$

with ρ and $\mathbf{J}$ are given by (4.33) and (4.37).

4.3 The Macroscopic Lorentz Force

By putting the results from equations (4.33) and (4.37) into the system (4.22)-(4.25) Maxwell equations can be written as

$$\nabla \times \mathbf{E} = -\frac{\partial \mathbf{B}}{\partial t}, \tag{4.39}$$

$$\nabla \cdot \mathbf{D} = \rho_f, \tag{4.40}$$

$$\nabla \cdot \mathbf{B} = 0 \tag{4.41}$$

$$\nabla \times \mathbf{H} = \mathbf{J}_f + \frac{\partial \mathbf{D}}{\partial t}, \tag{4.42}$$

with $\mathbf{D}$ and $\mathbf{H}$ defined as

$$\mathbf{D} = \varepsilon_0 \mathbf{E} + \mathbf{P} - \nabla \cdot \mathcal{Q}, \tag{4.43}$$

$$\mathbf{H} = \frac{\mathbf{B}}{\mu_0} - \mathbf{M} + \left\langle \sum_l \mathbf{p}_l \times \mathbf{v}_l \delta(\mathbf{r} - \mathbf{r}_l) \right\rangle + \nabla \cdot \left\langle \sum_l \mathbf{q}_l \times \mathbf{v}_l \delta(\mathbf{r} - \mathbf{r}_l) \right\rangle . \tag{4.44}$$

It is understood that the fundamental fields are $\mathbf{E}$ and $\mathbf{B}$ and $\mathbf{D}$ and $\mathbf{H}$ are just shorthand notation for writing Maxwell equations in a more compact way [33]. They are in general an approximation that can be made as accurate as needed. In this spirit, it is customary to "truncate" the expansion for the macroscopic charge and current density to the dipole terms, and define the fields $\mathbf{D}$ and $\mathbf{H}$ as

$$\mathbf{D} = \varepsilon_0 \mathbf{E} + \mathbf{P}, \tag{4.45}$$

$$\mathbf{H} = \frac{\mathbf{B}}{\mu_0} - \mathbf{M}, \tag{4.46}$$

such that [17, 27, 33]

$$\mathbf{D} = \varepsilon \mathbf{E}, \tag{4.47}$$

$$\mathbf{H} = \frac{\mathbf{B}}{\mu}. \tag{4.48}$$

Here the quantities μ and ε are defined as [28]

$$\varepsilon = \frac{\mathbf{D}}{\mathbf{E}}, \tag{4.49}$$

$$\mu = \frac{\mathbf{B}}{\mathbf{H}} \tag{4.50}$$

with this in mind , the final form used in this work for the equation of evolution of the momentum exchange between the particles and the fields is given by

$$\mathbf{f}_L = (\rho_f - \nabla \cdot \mathbf{P})\mathbf{E} + \left(\mathbf{J}_f + \frac{\partial \mathbf{P}}{\partial t} + \nabla \times \mathbf{M}\right) \times \mathbf{B}. \tag{4.51}$$

$\mathbf{f_L}$ is basically the *macroscopic* Lorentz force density acting on the *macroscopic* current and charges (in media without free charges and currents, the Lorentz force acts then only on the *bound* charges and currents). This form for the Lorentz force has been obtained by using the macroscopical Maxwell's equations by Yaghjian [30] and also discussed by other authors [13, 31, 34].

Using this result for the Lorentz force and the macroscopic Maxwell equations (4.22)-(4.25), an expression for the conservation of momentum can be constructed as

$$\mathbf{f}_L = -\nabla \cdot \bar{\mathcal{T}}^A - \frac{\partial \mathbf{g}^A}{\partial t}. \tag{4.52}$$

In this last expression, the quantities $\mathbf{g}^A$ and $\bar{\mathcal{T}}^A$ are the momentum of the electromagnetic field and Maxwell's stress tensor defined as (see appendix D)

$$\mathbf{g}^A = \varepsilon_0 \mathbf{E} \times \mathbf{B}, \tag{4.53}$$

$$\bar{\mathcal{T}}^A = \varepsilon_0 \frac{E^2}{2}\,\delta_{ij} + \frac{B^2}{2\mu_0}\,\delta_{ij} - \varepsilon_0 \mathbf{E}\mathbf{E} - \frac{\mathbf{B}\mathbf{B}}{\mu_0}. \tag{4.54}$$

It is important to notice that the Maxwell stress tensor and the momentum $\mathbf{g}^A$ have the same form in vacuum and in media. With this in mind, the Lorentz force acts as the exchange of momentum between the electromagnetic field and the particles that make up the medium; the momentum that the fields lose is transferred to the medium via the Lorentz force, which acts directly onto the polarization and magnetization of the medium, material effects whose sole cause is the action of the fields on the constitutive particles of the medium.

One important issue to consider is that some authors use for the electric part of the Lorentz force the expression $(\mathbf{P} \cdot \nabla)\mathbf{E}$ instead of the quantity $(-\nabla \cdot \mathbf{P})\mathbf{E}$ in (4.51) [13, 14, 32, 35–37].

$$\mathbf{f}_K = \mathbf{P} \cdot \nabla \mathbf{E} + \left(\frac{\partial \mathbf{P}}{\partial t} + \nabla \times \mathbf{M}\right) \times \mathbf{B}. \tag{4.55}$$

This form for the electric part of the Lorentz force is a generalization of the force on point dipoles first discussed by Kelvin. To compare these two expressions it is useful to use the following identity

$$\nabla \cdot (\mathbf{PE}) = (\nabla \cdot \mathbf{P})\mathbf{E} + (\mathbf{P} \cdot \nabla)\mathbf{E}.$$

As seen from this last equation, the two expressions for the electric force differ by the full derivative of a tensor $\nabla \cdot (\mathbf{PE})$

$$\mathbf{f}_K = \mathbf{f}_L + \nabla \cdot (\mathbf{PE}). \tag{4.56}$$

Applying Gauss theorem and choosing a surface if integration such that on this surface $\mathbf{P} = 0$ the two expressions yield the same result [32,36]. This last assumption is true in vacuum but in material media, the expression $\nabla \cdot (\mathbf{PE})$ is not exactly zero and the difference between the expressions becomes important. Nonetheless since the expression $(-\nabla \cdot \mathbf{P})\mathbf{E}$ was derived directly form the Maxwell equations without any particular assumptions on the nature of the medium, this will be the one that will be used throughout.

4.4 The Helmholtz Force

There has been another approach in formulating the force on the dielectric due to Helmholtz. One can start from the macroscopic Maxwell equations for a material in absence of free charges

$$\nabla \times \mathbf{E} = -\frac{\partial \mathbf{B}}{\partial t}, \tag{4.57}$$

$$\nabla \cdot \mathbf{D} = 0, \tag{4.58}$$

$$\nabla \cdot \mathbf{B} = 0, \tag{4.59}$$

$$\nabla \times \mathbf{H} = \frac{\partial \mathbf{D}}{\partial t}. \tag{4.60}$$

Now we try to construct a form similar to the conservation of momentum by cross multiplying the equation (4.57) by $\mathbf{E}$, and equation (4.60) by $\mathbf{H}$ and using the

constitutive relations for the fields $\mathbf{D}$ and $\mathbf{H}$, which after some simple algebra [38] one obtains:

$$\frac{\partial}{\partial t}(\mathbf{D}\times\mathbf{B})+\nabla\cdot\left(\frac{1}{2}\mathbf{D}\cdot\mathbf{E}\,\delta_{ij}+\frac{1}{2}\mathbf{H}\cdot\mathbf{B}\delta_{ik}\ -\mathbf{DE}-\mathbf{HB}\right)=\frac{1}{2}E^2\nabla\varepsilon+\frac{1}{2}H^2\nabla\mu. \quad (4.61)$$

In (4.61), the quantity

$$\mathbf{g}^M=\mathbf{D}\times\mathbf{B} \quad (4.62)$$

is interpreted as a momentum in the medium (Minkowski momentum), and the quantity

$$\bar{\mathcal{T}}^M=\frac{1}{2}\mathbf{D}\cdot\mathbf{E}\,\delta_{ij}+\frac{1}{2}\mathbf{H}\cdot\mathbf{B}\delta_{ik}\ -\mathbf{DE}-\mathbf{HB} \quad (4.63)$$

as the Minkowski stress-tensor. The quantity on the left in (4.61) is interpreted as the loss of momentum from the subsystems of the $\mathbf{D}$, and $\mathbf{H}$ fields. This momentum is transferred to the medium , therefore imparting the force on the medium. This force is opposite in sign to the left side of (4.61) [11, 19, 39],

$$\mathbf{f}_H=-\frac{1}{2}E^2\nabla\varepsilon-\frac{1}{2}H^2\nabla\mu. \quad (4.64)$$

This expression was derived also by Hirose in [40] for the case of non-magnetic media by taking into account the energy due to the non-uniform polarization [40]. These considerations are consistent with the Fresnel equation [41] and symmetry arguments [42].

This expression is valid for the case of real ε and μ. It can be readily generalized for a general dissipative case when ε is complex by defining

$$f_{Hi}=\frac{1}{2}D_j\frac{\partial}{\partial x_i}E_j-\frac{1}{2}E_j\frac{\partial}{\partial x_i}D_j. \quad (4.65)$$

Using

$$\mathbf{E} = \frac{1}{2}\left(\mathbf{E}+\mathbf{E}^*\right), \quad (4.66)$$

$$\mathbf{D} = \frac{1}{2}\left(\mathbf{D}+\mathbf{D}^*\right) \quad (4.67)$$

and plugging this into (4.65) we obtain

$$\left\langle f_z^H\right\rangle = \frac{1}{8}\left(D_x^*\frac{\partial}{\partial z}E_x+D_x\frac{\partial}{\partial z}E_x^*-E_x^*\frac{\partial}{\partial z}D_x-D_x\frac{\partial}{\partial z}E_x^*\right). \quad (4.68)$$

Assuming a complex dielectric constant of the form $\varepsilon = \varepsilon_r + i\,\varepsilon_i$ and the constitutive relations, (4.68) reduces to

$$\begin{aligned}\left\langle f_z^H \right\rangle &= \frac{1}{4}\Re\left\{\varepsilon\left(E_x\frac{\partial}{\partial z}E_x^* - E_x^*\frac{\partial}{\partial z}E_x\right)\right\} - \frac{1}{4}\left|E_x\right|^2\frac{\partial\varepsilon_r}{\partial z} \\ &= -\frac{1}{2}\,\varepsilon_i\,\Im\left(E_x\frac{\partial}{\partial z}E_x^*\right) - \frac{1}{4}\left|E_x\right|^2\frac{\partial\varepsilon_r}{\partial z}. \end{aligned} \tag{4.69}$$

From equation (4.69), it is clear that in general case of complex ε, the Helmholtz force has a surface part that depends on the real part of the dielectric constant and a volume part that depends on the imaginary part of the dielectric constant. This fact is one of the main differences between the Helmholtz and the Lorentz forces, with the Lorentz force being a purely volume force.

Finally we can see how the Lorentz, Kelvin and Helmholtz forces are related with one another for a non-magnetic medium

$$\mathbf{f}_K = \mathbf{f}_L + \nabla\cdot(\mathbf{PE})\,, \tag{4.70}$$

$$\mathbf{f}_H = \mathbf{f}_L + \nabla\cdot\left(\mathbf{PE} - \frac{1}{2}\,\mathbf{P}\cdot\mathbf{E}\,\delta_{ij}\right) - \frac{\partial}{\partial t}\left(\mathbf{P}\times\mathbf{B}\right). \tag{4.71}$$

With this previous result, it is worth noting here that different expressions for the local Lorentz, Kelvin and Helmholtz forces produce the same net force when integrated over whole body bounded by vacuum, which can be seen from the fact that they differ from each other by the divergence of a tensor that includes the polarization and magnetization, which vanish in vacuum and therefore do not contribute to the force upon integration (see appendix C).

Chapter 5

The Electromagnetic Force on Dielectric Slabs

In this chapter we calculate the electromagnetic force on dielectric slabs in various configurations. A non dispersive, non magnetic medium with real dielectric permittivity will be considered but we allow for dissipation in certain cases. We consider steady state forces for harmonic radiation; time averaged quantities are considered. We will use the Lorentz force given in the form (4.51) and compare it with the results produced by the Helmholtz force (4.69). A single dielectric slab, a semi-infinite slab and a quarter wavelength film layer are considered.

5.1 Force on a Single Dielectric Slab

Consider a dielectric slab of thickness d. The slab is characterized by a dielectric constant ε and bounded by vacuum on both sides. Taking the z-axis as normal to the slab and linearly polarized monochromatic light normally incident on the slab, the electromagnetic fields, $\mathbf{E}$ and $\mathbf{B}$ are given by

$$\mathbf{E} = [E_x, 0, 0]e^{-i\omega t}, \tag{5.1}$$

$$\mathbf{B} = [0, B_y, 0]e^{-i\omega t} \tag{5.2}$$

Under these conditions, the electric contribution of the Lorentz force $(-\nabla \cdot \mathbf{P})\mathbf{E}$ is zero and the only force is the one on the polarization current. The component in the z-direction for the force is given only by the second member in the right hand side

of (4.51) whose time average is given by

$$\langle \mathbf{f}_{Lz} \rangle = \frac{1}{2} \Re(\mathbf{J} \times \mathbf{B}^*), \tag{5.3}$$

for $\mathbf{J}$ given by (in the absence of free currents)

$$\mathbf{J} = \frac{\partial \mathbf{P}}{\partial t}, \tag{5.4}$$

where the polarization given by

$$\mathbf{P} \;=\; \varepsilon_0(\varepsilon - 1)\,\mathbf{E}. \tag{5.5}$$

The electric field is given by

$$\begin{aligned} E_x &= \left(e^{ik_v z} + R\, e^{-ik_v z}\right) E_0 \qquad z > 0, \\ E_x &= \left(A\, e^{ik_1 z} + B\, e^{-ik_1 z}\right) E_0 \qquad 0 < z < d, \\ E_x &= T\, e^{ik_v z} E_0 \qquad d < z, \end{aligned}$$

and the magnetic field by

$$\begin{aligned} B_y &= \frac{k_v}{\omega}\left(e^{ik_v z} - R\, e^{-ik_v z}\right) E_0 \qquad z > 0, \\ B_y &= \frac{k_1}{\omega}\left(A\, e^{ik_1 z} - B\, e^{-ik_1 z}\right) E_0 \qquad 0 < z < d, \\ B_y &= \frac{k_v}{\omega} T\, e^{ik_v z} E_0 \qquad d < z, \end{aligned}$$

with $k_v = \frac{\omega}{c}$, $k_1 = k_v n$, $n = \sqrt{\varepsilon}$. Using these expressions, (5.3) becomes

$$\begin{aligned} \langle f_L \rangle_z &= \frac{1}{2} \Re\left\{-i\omega\varepsilon_0(\varepsilon - 1) E_x B_y^*\right\} \\ &= \frac{\varepsilon_0 |E_0|^2}{2} \Re\left\{-ik_1(\varepsilon - 1)\left[|A|^2 - |B|^2 + 2i\Im(A^* B\, e^{-2ik_1 z})\right]\right\} \\ &= \varepsilon_0(\varepsilon - 1) k_1 |E_0|^2 \Im(A^* B\, e^{-2ik_1 z}). \end{aligned} \tag{5.6}$$

The Lorentz force is given then by the integral over the slab of (5.6).

$$\langle F_L \rangle_z \;=\; A\varepsilon_0(\varepsilon - 1) k_1 |E_0|^2 \int_0^d \Im(A^* B\, e^{-2ik_1 z})\, dz \tag{5.7}$$

with A being the cross sectional area of the slab.

Obtaining the coefficients in (5.7) from the matching conditions for the fields, we have

$$\Im\left\{A^* B\, e^{-2ik_1 z}\right\} = \frac{(\varepsilon-1)\sin(2k_1(d-z))}{4\varepsilon\cos(k_1 d)+(\varepsilon+1)\sin^2(k_1 d)} \tag{5.8}$$

and

$$\begin{aligned}\int_0^d \Im(A^* B\, e^{-2ik_1 z})\, dz &= \int_0^d \frac{(\varepsilon-1)\sin(2k_1(d-z))}{4\varepsilon\cos(k_1 d)+(\varepsilon+1)\sin^2(k_1 d)}\, dz \\ &= \frac{1}{k_1}\frac{(\varepsilon-1)\sin^2(k_1 d)}{4\varepsilon\cos(k_1 d)+(\varepsilon+1)\sin^2(k_1 d)}.\end{aligned} \tag{5.9}$$

Then the Lorentz force reduces to

$$\begin{aligned}\langle F_L\rangle_z &= \frac{A\varepsilon_0(\varepsilon-1)^2|E_0|^2\sin^2(k_1 d)}{4\varepsilon\cos(k_1 d)+(\varepsilon+1)\sin^2(k_1 d)} \\ &= A\varepsilon_0|E_0|^2\left\{\frac{(\varepsilon-1)^2\sin^2(k_1 d)}{4\varepsilon\cos(k_1 d)+(\varepsilon+1)\sin^2(k_1 d)}\right\} \\ &= A\varepsilon_0|E_0|^2|R|^2.\end{aligned} \tag{5.10}$$

It is obvious from (4.71) that the integral values for the Lorentz and Helmholtz forces will be equal when the integration is done over the whole slab length bounded by vacuum. Nevertheless, we perform direct calculations of the Helmholtz to emphasize the volume and surface contributions.

We evaluate now the Helmholtz force directly by integrating (4.69) for real epsilon

$$\begin{aligned}\langle \mathbf{f}_H\rangle &= -\frac{1}{4}|E_x|^2\,\nabla\varepsilon, \\ \langle \mathbf{F}_H\rangle_z &= -\frac{1}{4}A\int_0^d |E_x|^2\,\frac{\partial\varepsilon}{\partial z}\,dz \\ &= -\frac{1}{4}A\int_0^d |E_x|^2\,\varepsilon_0(\varepsilon-1)\,\{\delta(z)-\delta(z-d)\}\,dz \\ &= \frac{1}{4}\varepsilon_0 A(1-\varepsilon)\left[|1+R|^2-|T|^2\right]|E_0|^2 \\ &= \frac{1}{2}\varepsilon_0 A(1-\varepsilon)\left(|R|^2+\Re(R)\right)|E_0|^2.\end{aligned} \tag{5.11}$$

In this last equations, the terms $|R|^2$ and $\Re(R)$ are defined as

$$\begin{aligned}|R|^2 &= \frac{(\varepsilon-1)^2\sin^2(k_1 d)}{4\varepsilon\cos(k_1 d)+(\varepsilon+1)\sin^2(k_1 d)}, \\ \Re(R) &= \frac{(1-\varepsilon^2)\sin^2(k_1 d)}{4\varepsilon\cos(k_1 d)+(\varepsilon+1)\sin^2(k_1 d)}, \\ |R|^2+\Re(R) &= \frac{2\,(1-\varepsilon)\sin^2(k_1 d)}{4\varepsilon\cos(k_1 d)+(\varepsilon+1)\sin^2(k_1 d)}.\end{aligned} \tag{5.12}$$

By plugging the result from (5.12) into (5.11), the Helmholtz force reduces to

$$\begin{aligned}
\langle \mathbf{F}_H \rangle_z &= \frac{1}{2}\varepsilon_0 A|E_0|^2(1-\varepsilon)\left(|R|^2+\Re(R)\right) \\
&= \frac{1}{2}\varepsilon_0 A|E_0|^2(1-\varepsilon)\left\{\frac{2\,(1-\varepsilon)\sin^2(k_1 d)}{4\varepsilon\cos(k_1 d)+(\varepsilon+1)\sin^2(k_1 d)}\right\} \\
&= A\varepsilon_0|E_0|^2\left\{\frac{(\varepsilon-1)^2\sin^2(k_1 d)}{4\varepsilon\cos(k_1 d)+(\varepsilon+1)\sin^2(k_1 d)}\right\} \\
&= A\varepsilon_0|E_0|^2|R|^2. \qquad (5.13)
\end{aligned}$$

As can be seen from (5.10) and (5.13), the Lorentz and Helmholtz forces yield the same result. The general result 5.13 also follows from a simple balance of the exchange of the momentum between photons and dielectric slab. Consider the photon beam normally incident on the dielectric layer. The incident beam has a photon flux $N_i\,c$, where N_i is a photon density $N_i = w/(\hbar\omega)$, energy density $w = \varepsilon_0 E_0^2/2$, and momentum flux $S_i = N_i\hbar k$. The reflected beam will have a momentum $S_r = N_r\hbar k$, where $N_r = |R|^2\,N_i$. The transmitted beam with a flux N_t has a momentum flux $S_t = N_t\hbar k$ with $N_t = |T|^2\,N_i$. The total force per unit area applied to the dielectric is then $F = \hbar k\,(N_i + N_r - N_t) = \hbar k\,N_i\,(1+|R|^2-|T|^2)$, and obviously F is positive for any $|T|^2 < 1$ or since $|R|^2+|T|^2 = 1$, the force becomes $F = 2\hbar k\,N_i\,|R|^2 = \varepsilon_0 E_0^2|R|^2$. As the force is dependent on $|R|^2$, it will oscillate with it, the force being zero at the points where the reflectance is zero.

The plots of the force per unit area, normalized to $\varepsilon_0\,|E_0|^2$ are given in Fig. 5.1 as a function of width and in Fig. 5.2 as a function of the refraction index.

5.2 Force on a Semi-infinite Slab

In this section we want to consider the force on non-magnetic non dispersive semi-infinite slab. It is worth noting here that one cannot use the results of the previous section for a finite length slab by taking a limit of $d \to \infty$. In an ideal (non dissipative) medium there is always a standing wave and the force will oscillate indefinitely as shown in Figs. 5.1 and 5.2. In another words, the results of the previous sections are obtained assuming that in the slab there is a reflected wave

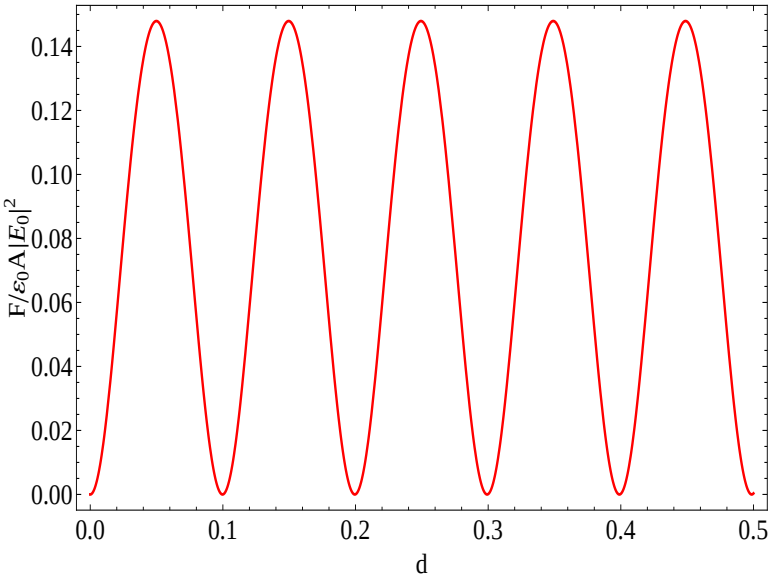

Figure 5.1: Force on a slab as function of width with $k_v = 21\ m^{-1}$ and $n = 1.5$ as calculated using (5.10) and (5.13)

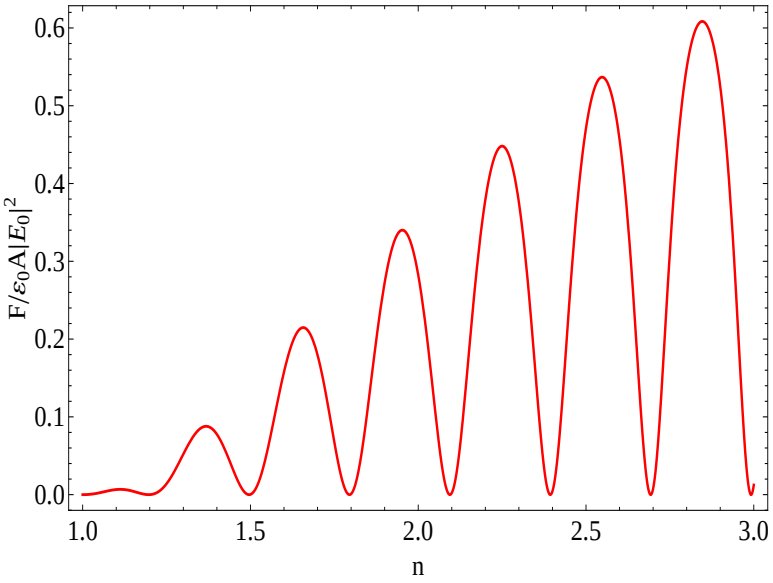

Figure 5.2: Force per unit area on a slab as function of n with $k_v = 21\ m^{-1}$ and $d = 0.5$ m as calculated using (5.10) and (5.13)

(though it would require an infinite time to return for an slab of infinite length). This problem can be corrected by assuming a finite length pulse with a length shorter than the length of the slab (so that there is no reflected wave). However this would be a non stationary problem which is beyond the scope of this thesis. We will employ a different approach; we will assume a weak dissipation inside the slab, so that the wave amplitude decreases as the wave propagates. This will eliminate the reflected wave inside the slab. Therefore the electric field inside the semi-infinite slab is given by

$$E_x = E_0\, T\, e^{ikz}$$

and the magnetic field is:

$$\begin{aligned} B_y &= \frac{1}{c}\sqrt{\varepsilon}\, E_0\, T\, e^{ikz}, \\ B_y^* &= \frac{1}{c}\sqrt{\varepsilon}^{\,*}\, E_0^*\, T^*\, e^{-ik^* z}. \end{aligned}$$

The final expression for the time averaged Lorentz force density is

$$\begin{aligned} \langle \mathbf{f}_{Lz} \rangle &= \frac{1}{2}\frac{\omega}{c}\varepsilon_0 \Re\left(-i\omega\sqrt{\varepsilon}^{\,*}(\varepsilon-1)|E_x|^2\right) \\ &= \frac{1}{2}\frac{\omega}{c}\varepsilon_0 |E_0|^2 |T_f|^2 \Re\left(-i\omega\sqrt{\varepsilon}^{\,*}(\varepsilon-1)\, e^{ikz}\, e^{-ik^* z}\right), \end{aligned} \tag{5.14}$$

where E_0 is the amplitude of the incident field and T_f is the Fresnel transmission coefficient for normal incidence which is given by

$$T_f = = \frac{2}{1+\sqrt{\varepsilon}}. \tag{5.15}$$

For a complex ε, we have the following

$$\begin{aligned} \varepsilon &= \varepsilon_r + i\,\varepsilon_i \\ &= \sqrt{\varepsilon_r^2+\varepsilon_i^2}\, e^{i\,\arctan(\varepsilon_i/\varepsilon_r)}, \qquad (5.16) \\ \sqrt{\varepsilon} &= (\varepsilon_r^2+\varepsilon_i^2)^{1/4}\, e^{i\,\arctan(\varepsilon_i/\varepsilon_r)/2}. \qquad (5.17) \end{aligned}$$

In what follows, we will use the following definitions: $n = \Re\sqrt{\varepsilon}$, $\kappa = \Im\sqrt{\varepsilon}$, $\varepsilon = (n+i\kappa)^2$.

Using these definitions, the time averaged Lorentz force is

$$\begin{aligned}\langle \mathbf{f}_{Lz} \rangle &= \frac{1}{2}\frac{\omega}{c}\varepsilon_0 \Re\left(-i\omega\sqrt{\varepsilon}^{\,*}(\varepsilon-1)|E_x|^2\right) \\ &= \frac{1}{2}\frac{\omega}{c}\varepsilon_0 |E_0|^2|T_f|^2 \Re\left(-i\omega\,(n-i\kappa)(n^2-\kappa^2+2in\kappa-1)\,e^{ikz}\,e^{-ik^*z}\right), \end{aligned} \tag{5.18}$$

with k given by

$$\begin{aligned} k &= k_r + i\,k_i \\ &= \frac{\omega}{c}\sqrt{\varepsilon} \\ &= \frac{\omega}{c}(n+i\,\kappa) \\ e^{ikz}\,e^{-ik^*z} &= e^{-2k_i z}. \end{aligned}$$

To obtain the total Lorentz force on the semi-infinite slab, the Lorentz force density has to be integrated over the whole volume

$$\begin{aligned}\langle F_{Lz} \rangle &= \int_V f_{Lz}\,dV \\ &= A\int_0^\infty f_{Lz}\,dz \\ &= A\,\frac{1}{2}\frac{\omega}{c}\varepsilon_0|E_0|^2|T_f|^2\Re\left(-i\omega\,(n-i\kappa)(n^2-\kappa^2+2in\kappa-1)\right)\int_0^\infty e^{-2k_i z}\,dz \\ &= A\,\frac{1}{2}\frac{\omega}{c}\varepsilon_0|E_0|^2|T_f|^2\frac{1}{2k_i}\kappa\,(n^2+\kappa^2+1) \\ &= \frac{1}{4}\,(n^2+\kappa^2+1)\varepsilon_0\,A\,|E_0|^2|T_f|^2. \end{aligned} \tag{5.19}$$

Finally, with $|T_f|^2$ is given by

$$|T_f|^2 = \frac{4}{(1+n)^2+\kappa^2}$$

and the final expression for the force on a semi-infinite slab is given by

$$\begin{aligned}\langle F_{Lz} \rangle &= \frac{1}{4}\,(n^2+\kappa^2+1)\varepsilon_0\,A\,|E_0|^2\,\frac{4}{(1+n)^2+\kappa^2} \\ &= \frac{n^2+\kappa^2+1}{(1+n)^2+\kappa^2}\,\varepsilon_0\,A\,|E_0|^2. \end{aligned} \tag{5.20}$$

This expression can be written as

$$\begin{aligned}\langle F_{Lz} \rangle &= \frac{1}{2}\varepsilon_0\,A\,|E_0|^2\left\{\frac{2(n^2+\kappa^2+1)}{(1+n)^2+\kappa^2}\right\} \\ &= \frac{1}{2}\varepsilon_0\,A\,(1+|R_f|^2)\,|E_0|^2, \end{aligned} \tag{5.21}$$

where R_f is the Fresnel reflection coefficient for the semi-infinite slab.

Now we evaluate the Helmholtz force to emphasize the surface and volume contributions to this force for a lossy medium. The surface component and a volume component can be calculated using equation (4.69). Plugging the fields into this equation we obtain for the local Helmholtz force density

$$\left\langle f_z^H \right\rangle = \frac{1}{2}\, k_r\, \varepsilon_i\, |T|^2\, |E_0|^2\, e^{-2k_i z} - \frac{1}{4}\, |T|^2\, |E_0|^2\, e^{-2k_i z}\, \frac{\partial \varepsilon_r}{\partial z}. \tag{5.22}$$

The integral over the whole volume of this last expression yields

$$\begin{aligned} \left\langle F_z^H \right\rangle &= \frac{A\varepsilon_0 |E_0|^2 (1+\kappa^2-n^2)}{(1+n)^2+\kappa^2} + 2n^2\, \frac{A\varepsilon_0 |E_0|^2}{(1+n)^2+\kappa^2} \\ &= \frac{n^2+\kappa^2+1}{(1+n)^2+\kappa^2}\, A\varepsilon_0 |E_0|^2 \\ &= \frac{1}{2}\, A\varepsilon_0 |E_0|^2 (1+|R|^2). \end{aligned} \tag{5.23}$$

The conclusion is then that the force given by (5.23) is equal to the expressions given by equation (5.21).

We can also obtain the same result by including a finite dissipation into the analysis for the finite length slab as said before. In the case of a lossy slab, the general result is given by (see appendix C)

$$\langle F \rangle = \frac{1}{2} \varepsilon_0\, A\, (1+|R|^2-|T|^2)\, |E_0|^2. \tag{5.24}$$

In the limit $k_i d \gg 1$, a lossy slab of a finite length is equivalent to a semi-infinite slab. Then $T = B = 0$ and for R and A we have:

$$R = \frac{1-\sqrt{\varepsilon}}{1+\sqrt{\varepsilon}}, \tag{5.25}$$

$$A = \frac{2}{1+\sqrt{\varepsilon}}. \tag{5.26}$$

It is important to note that these are the reflection and transmission coefficients for normal incidence on a semi-infinite slab. The force is then given by

$$\langle F \rangle = \frac{1}{2} \varepsilon_0\, A\, (1+|R|^2)\, |E_0|^2, \tag{5.27}$$

which is exactly the same as expression (5.21).

When $R = 1$, the force on the material is equivalent to that on a fully reflecting metal. For $n = 1 + i\delta$, when $\delta \to 0$, the force is also finite. In the latter case, there is no reflection. The force occurs due to the absorption of the transmitted wave. In a semi-infinite dielectric an infinitely small dissipation leads to the full absorption (over the infinitely large distance). The absorbed momentum creates the force equal to the half of that in the fully reflecting case $R = 1$. The force on the dielectric distributed over a large distance as given by equation (5.21), this distance increases as the dissipation decreases, $\delta \to 0$, though the total value of the force remains finite. The case with an infinitely small dissipation is therefore different from the case of no dissipation for the Helmholtz force which becomes negative and applied to the surface [40, 41] corresponding to the Minkowski momentum. In the medium, the momentum flux density is the sum of the transmitted wave momentum and the momentum of the medium. The transmitted wave momentum flux density is given by

$$\frac{4n^2)}{(n+1)^2}\,\varepsilon_0\,E_0^2, \tag{5.28}$$

therefore the medium should absorb a momentum given by

$$\frac{2(n^2+1)}{(n+1)^2}\,\varepsilon_0\,E_0^2 - \frac{4n^2)}{(n+1)^2}\,\varepsilon_0\,E_0^2$$

$$= \quad -\frac{2(n^2-1)}{(n+1)^2}\,\varepsilon_0\,E_0^2. \tag{5.29}$$

This last expression is the radiation pressure on a semi-infinite slab and it is clearly always negative, that is it pulls the medium. Hirose showed that this expression for the radiation pressure is consistent with both Fresnel's relations and Minkowski momentum [40, 41]. In Fig. 5.3, the force per unit area on a semi-infinite medium is shown. As can be seen from this plot, the force is always pulling and becomes stronger as the refraction coefficient of the medium increases till it reaches an asymptotic value of -2.

The plots of the force per unit area for the semi-infinite slab, normalized to $\varepsilon_0\,|E_0|^2$ are given in Fig. (5.4) as a function of n and in Fig. (5.5) as a function of κ. From these figures it is clear that in the case that the reflectance approaches zero the force

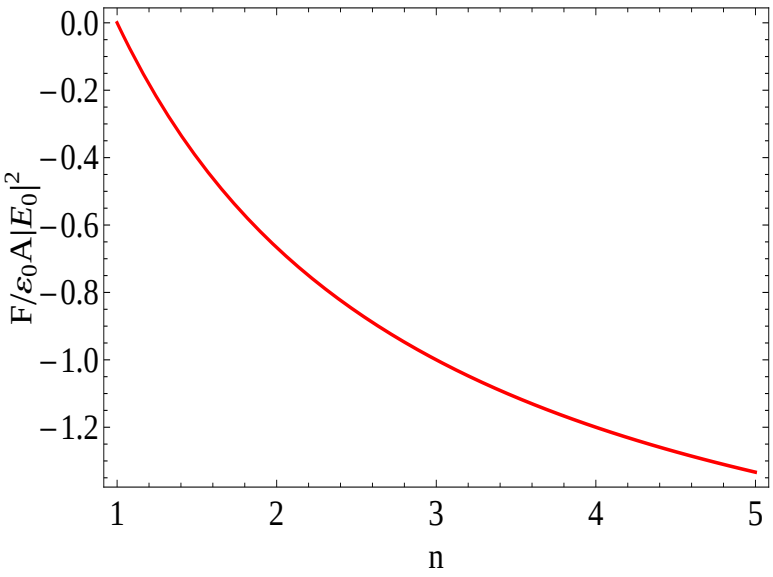

Figure 5.3: Force per unit area on a semi-infinite slab as given by (5.29)

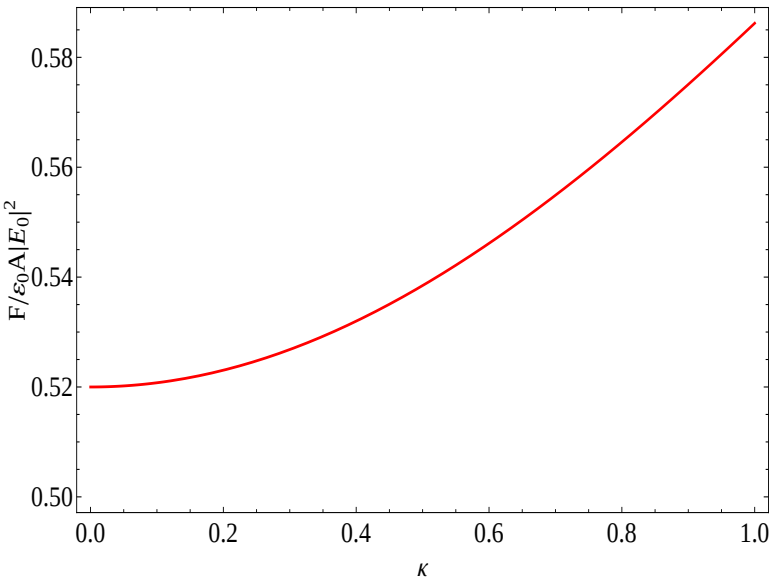

Figure 5.4: Force per unit area on a semi-infinite slab as function of κ with $k_v = 21\ m^{-1}$ and $n = 1.5$ as calculated using (5.21) and (5.23)

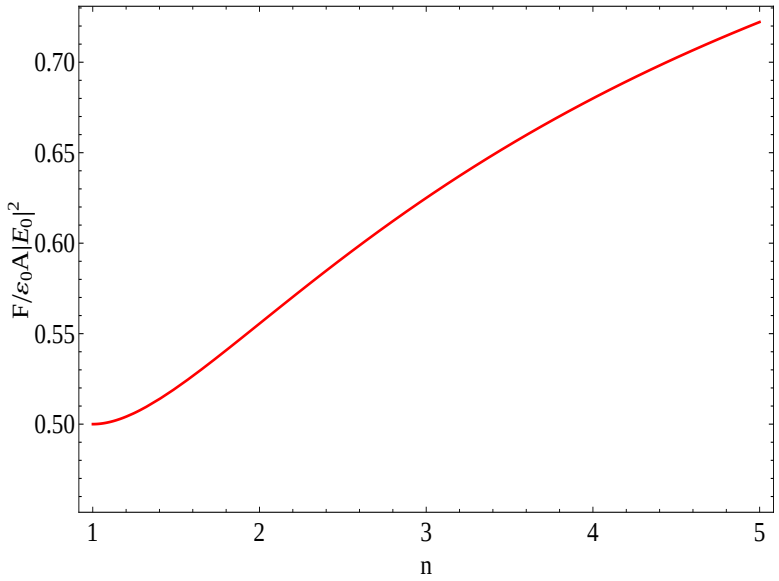

Figure 5.5: Force per unit area on a semi-infinite slab as function of n with $k_v = 21\ m^{-1}$ and $\kappa = 0$ as calculated using (5.21) and (5.23)

approaches the value 1/2. This result is also consistent with the total momentum balance argument, which should be modified for the case with dissipation. The incident beam has a photon flux $N_i\, c$, where N_i is a photon density $N_i = w/(\hbar\omega)$, energy density $w = \varepsilon_0 E_0^2/2$, and momentum flux $S_i = N_i \hbar k$. There is no reflected flux (for $n = 1$ and no transmitted flux because of the dissipation). The dissipation is infinitely small but for infinite slab it completely suppresses the reflected wave. The total force then applied to the dielectric is $F = \hbar k\, N_i = \varepsilon_0 E_0^2/2$. In this case, all momentum of the incoming radiation is absorbed by the slab. In the case of total reflection the force tends to 1, indicating the reversal of the momentum of the reflected wave.

5.3 Force on a Quarter-wavelength Coating

Finally, the electromagnetic force on a quarter-wavelength anti reflective coating will be calculated. This case differs from the two previous examples in the fact that the coating is bounded on both sides by two different media.

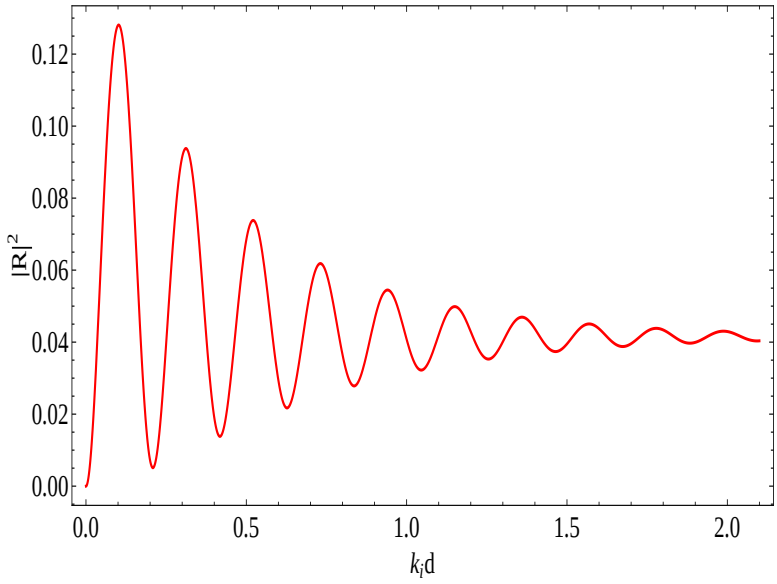

Figure 5.6: Reflectance of a lossy slab as function of $k_i d$ with $k_v = 21\ m^{-1}$, $n = 1$ and $\kappa = 0.1$

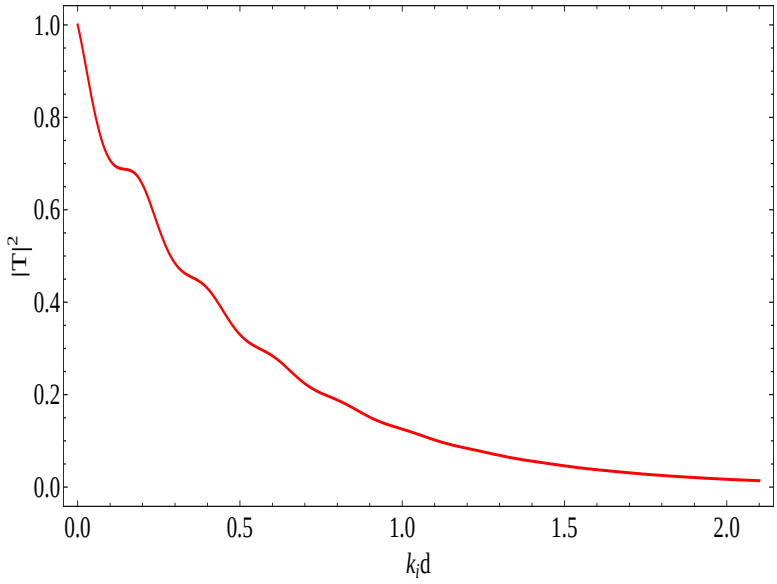

Figure 5.7: Transmittance of a lossy slab as function of $k_i d$ with $k_v = 21$ m^{-1}, $n = 1$ and $\kappa = 0.1$

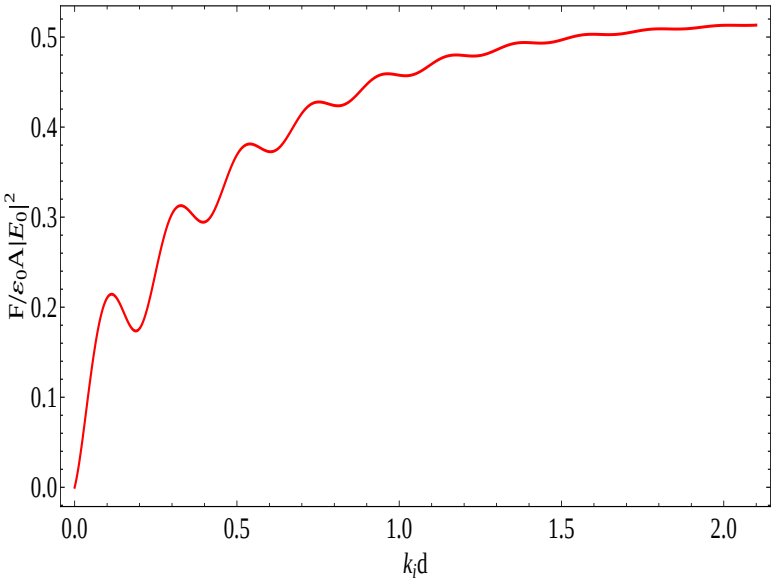

Figure 5.8: Force per unit area on a lossy slab as function of $k_i d$ with $k_v = 21$ m^{-1}, $n = 1$ and $\kappa = 0.1$ as calculated using (5.24)

For a quarter wavelength coating on a substrate, the electric field is given by

$$\begin{aligned} E_x &= \left(e^{ik_v z} + R\, e^{-ik_v z}\right) E_0 \qquad z > 0, \\ E_x &= \left(A\, e^{ik_1 z} + B\, e^{-ik_v z}\right) E_0 \qquad 0 < z < d, \\ E_x &= T\, e^{ik_2 z} E_0 \qquad d < z, \end{aligned}$$

and the magnetic field by

$$\begin{aligned} B_y &= \frac{k_v}{\omega}\left(e^{ik_v z} - R\, e^{-ik_v z}\right) E_0 \qquad z > 0, \\ B_y &= \frac{k_1}{\omega}\left(A\, e^{ik_1 z} - B\, e^{-ik_v z}\right) E_0 \qquad 0 < z < d, \\ B_y &= \frac{k_2}{\omega} T\, e^{ik_2 z} E_0 \qquad d < z. \end{aligned}$$

Using:

$$\begin{aligned} k_v &= \frac{\omega}{c}, \\ k_1 &= k_v n_1, \\ k_2 &= k_v n_2, \\ n_1 &= \sqrt{n_2}, \end{aligned}$$

the time average Lorentz force density is given by (5.3)

$$\begin{aligned}\langle \mathbf{f}_{Lz} \rangle &= \frac{1}{2}\Re\left\{-i\omega\varepsilon_0\frac{k_1^*}{\omega}(\varepsilon_1-1)\left(|A|^2-|B|^2+2\,i\Im\left\{A^*B\,e^{-2ik_1z}\right\}\right)|E_0|^2\right\} \\ &= \varepsilon_0(\varepsilon_1-1)\,k_1\,|E_0|^2\,\Im\left\{A^*B\,e^{-2ik_1z}\right\}. \end{aligned} \tag{5.30}$$

For the total force, this last expression has to be integrated over the whole coating, such that

$$\langle \mathbf{F}_{Lz} \rangle = \varepsilon_0(\varepsilon_1-1)\,k_1\,A\,|E_0|^2\,\Im\int_0^d A^*B\,e^{-2ik_1z}\,dz. \tag{5.31}$$

For this integral we have the following

$$\int_0^d e^{-2ik_1z}\,dz = \frac{\sin(2k_1d)}{2k_1} - i\frac{\sin^2(k_1d)}{k_1}, \tag{5.32}$$

with

$$\begin{aligned} d &= \frac{\lambda_0}{4n_1}, \\ k_1d &= \frac{\pi}{2}, \\ \int_0^d e^{-2ik_1z}\,dz &= -i\frac{1}{k_1}, \end{aligned}$$

and the force reduces to

$$\begin{aligned}\langle \mathbf{F}_{Lz} \rangle &= \varepsilon_0\,A\,(\varepsilon_1-1)\,|E_0|^2\,\Im\{-iA^*B\} \\ &= -\varepsilon_0\,A\,(\varepsilon_1-1)\,|E_0|^2\,\Re\{A^*B\}. \end{aligned} \tag{5.33}$$

For the coefficients A and B we have

$$\begin{aligned} A^* &= \frac{1}{2}\left(1+\frac{1}{\sqrt{n_2}}\right), \\ B &= \frac{1}{2}\left(1-\frac{1}{\sqrt{n_2}}\right), \\ A^*B &= \frac{1}{4}\left(\frac{n_2-1}{n_2}\right). \end{aligned} \tag{5.34}$$

For the factor (ε_1-1)

$$\begin{aligned}\varepsilon_1-1 &= \sqrt{\varepsilon_2}-1 \\ &= n_2-1. \end{aligned} \tag{5.35}$$

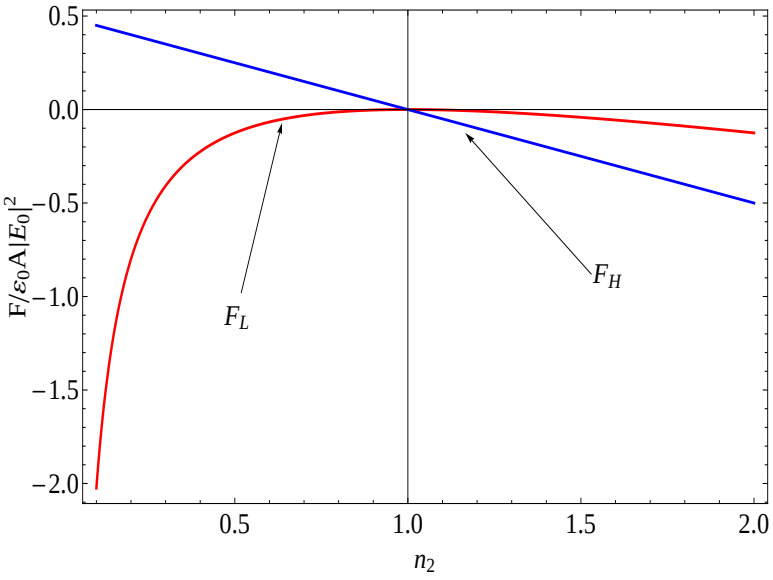

Figure 5.9: Force per unit area on a quarter-wavelength coating as function of the refractive index as calculated using (5.36) and (5.37)

Finally the Lorentz force on the quarter wavelength coating is

$$\langle \mathbf{F}_{Lz} \rangle = -\frac{1}{4}\,\varepsilon_0\,A\,\frac{(n_2-1)^2}{n_2}\,|E_0|^2. \tag{5.36}$$

The averaged Helmholtz force is given by

$$\begin{aligned}
\langle \mathbf{f}_H \rangle &= -\frac{1}{4}|E_x|^2\,\nabla\varepsilon, \\
\langle \mathbf{F}_H \rangle_z &= -\frac{1}{4}A\int_0^d |E_x|^2\,\frac{\partial\varepsilon}{\partial z}\,dz \\
&= -\frac{1}{4}A\int_0^d |E_x|^2\,\varepsilon_0(n_2-1)\,\{\delta(z)-\delta(z-d)\}\,dz \\
&= -\frac{1}{2}\varepsilon_0 A(n_2-1)\,|E_0|^2.
\end{aligned} \tag{5.37}$$

It is interesting to note that the Lorentz force expressions give a negative force for any value of n_2, while the Helmholtz force is negative for $n_2 > 1$ and positive for $n_2 < 1$. The expressions (5.36) and (5.37) are different. The difference can be seen more clearly from equation (4.71). From this equation it is clear that the integrated Helmholtz force has a contribution from the surface term which contributes on the right side at the boundary of the coating film and the substrate. Introduction of the

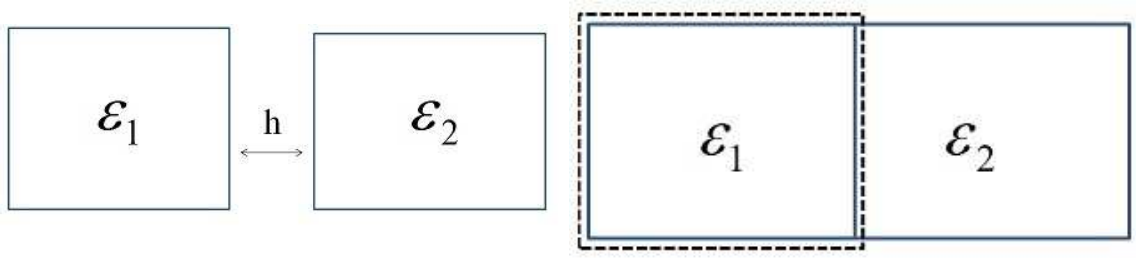

Figure 5.10: a) Two slabs with different permittivities, separated by an air gap of width h. The forces on each slab are illustrated in Figs. 5.11a and 5.11a b) Two slabs with different permittivities. The dashed line is the integration contour for the calculation of the force on the first slab. The force per unit area and the reflectance of the system are shown in Figs. 5.12 and 5.12b.

infinitely thin air gap at this boundary does not affect the value of the Lorentz force but affect the Helmholtz force, as the boundary term now ill be between the coating film and air in the gap.

Let us consider the case of two slabs with air gap in more details. There are two slabs of different dielectric constant, as in Fig. 5.10a both of the same length and separated by an air gap of length h. It is clear that the total force on the system of two slabs is proportional to $|R|^2$, and that as long as the width of the gap is not exactly zero, the integrated Lorentz and Helmholtz forces will be identical for each slab and the sum of this two forces will be equal to the total force on the system. This situation is illustrated in Figs. 5.11a-5.12.

Note that the total force on the first slab is oscillating as a function of the gap width, for the gap width approaching zero, the force becomes negative, see Fig. 5.11a. For the case when the width of the gap is zero as illustrated in Fig. 5.10b, we have a situation similar to the quarter wavelength case. In this situation the total Helmholtz and Lorentz forces on the two slab system are equal and proportional to $|R|^2$. To calculate the Helmholtz force on the left slab, a contour of integration that includes the interface is included. This way the force on the second slab is determined solely by the rightmost interface. The Helmholtz force on the left slab is

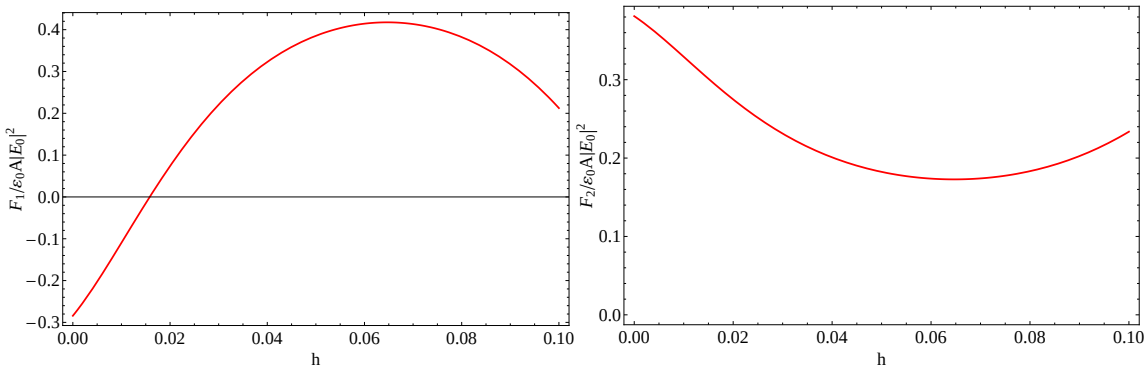

(a) F_1 **(b)** F_2

Figure 5.11: a) Force per unit area on left slab and b) force per unit area on right slab as a function of h for slabs of length 0.05 m. In this case $\varepsilon_1 = \sqrt{1.5}$, $\varepsilon_2 = \sqrt{2}$.

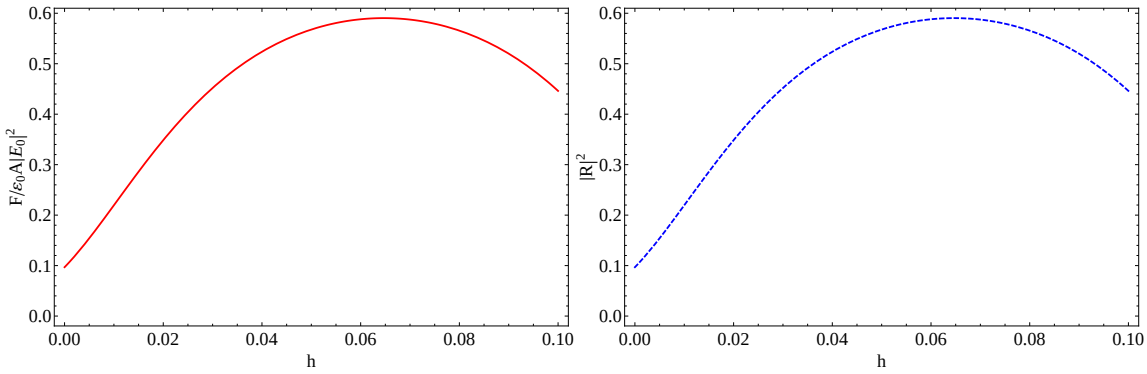

(a) F **(b)** $|R|^2$

Figure 5.12: a) Force per unit area on system of slabs and b) reflectance of systems of slabs slabs as a function of h for slabs of length 0.05 m. In this case $\varepsilon_1 = \sqrt{1.5}$, $\varepsilon_2 = \sqrt{2}$.

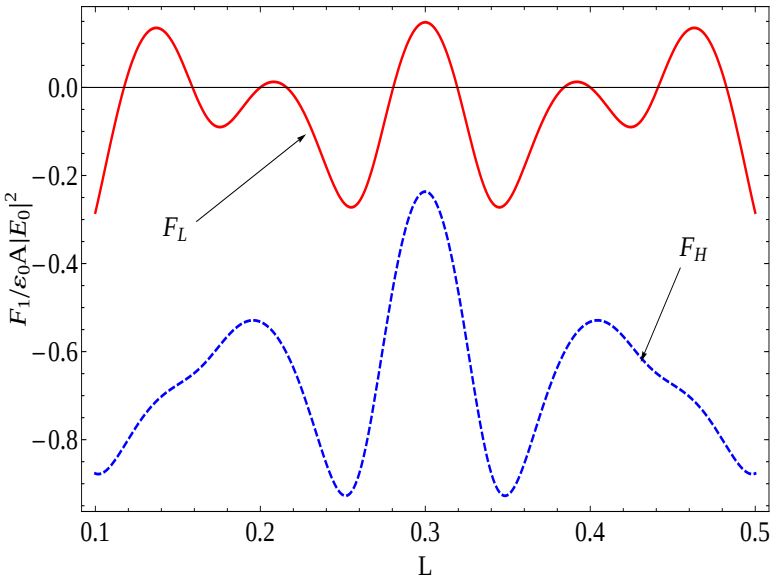

Figure 5.13: Force per unit area on slabs as a function of the length for h=0. In this case $\varepsilon_1 = \sqrt{1.5}$, $\varepsilon_2 = \sqrt{2}$

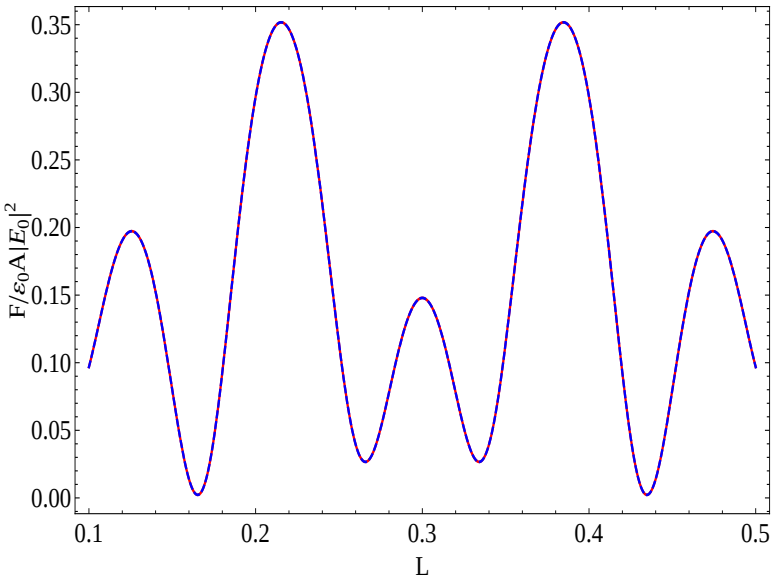

Figure 5.14: Force per unit area on slabs as a function of the length for h=0. In this case $\varepsilon_1 = \sqrt{1.5}$, $\varepsilon_2 = \sqrt{2}$

given, for the interface at $Z = L/2$ by

$$\langle F_{1Hz} \rangle = -\frac{1}{4} \left\{ (\varepsilon_1 - \varepsilon_0)|E(0)|^2 + (\varepsilon_2 - \varepsilon_1)|E(L/2)|^2 \right\}, \tag{5.38}$$

and for the second slab, the force is

$$\langle F_{2Hz} \rangle = -\frac{1}{4} (\varepsilon_0 - \varepsilon_2)|E(L)|^2. \tag{5.39}$$

The total force on the system is given by

$$\langle F_{Hz} \rangle = -\frac{1}{4} \left\{ (\varepsilon_1 - \varepsilon_0)|E(0)|^2 + (\varepsilon_2 - \varepsilon_1)|E(L/2)|^2 + (\varepsilon_0 - \varepsilon_2)|E(L)|^2 \right\}. \tag{5.40}$$

It is this last expression (5.40), that upon integration will be equal to the Lorentz force and proportional to $|R|^2$. The Lorentz and Helmholtz forces for the left slab and for the whole system are shown in Fig. 5.13.

From Figs. 5.11, 5.12 and 5.13, it is clear that the Lorentz force with the gap in between tend to the Lorentz force without the gap for $h \to 0$, which is not true for the Helmholtz force. This is due to the contribution of the surface force in the Helmholtz expression.

5.4 Summary Comments and Conclusions

This chapter presents the result of the calculations of the total force on the dielectric structures subject to the electromagnetic field. We have examined the Lorentz and Helmholtz forces for several different configurations and by direct calculations shown that the total force is the same for both expressions, however, locally, the force densities are different. The difference of the local force can be interpreted as a result of different length scales of the averaging operator. The Lorentz force describes the momentum exchange mechanism between the averaged electromagnetic field and the polarization charges and magnetization current. The transition to longer scale results in the Kelvin force (4.56). One can see from (4.56) that at the longer length scale the dipole moment appears and the net force on a system of charged particles is expressed through the dipole moment in the inhomogeneous electric field. It is possible to

interpret the Helmholtz force as a result of the averaging over the macroscopic length of the whole body (or rather macroscopic length scale of the body inhomogeneity); so that the net force is a result of the flux exchange through the boundary surface. The hierarchy of subgrid length scale involved in the averages means that at scales below the given subgrid, there exist internal forces due to interaction of charges within the averaging volume. These internal forces disappear upon averaging over the whole subgrid volume (except possibly the surface contributions). The local force density along with the internal forces distribution produce internal stresses that potentially can be measured. Upon averaging over the bulk, the internal forces and stresses are eliminated via Newton's Third Law and the resulting total force is unique for all representations: Lorentz force, Kelvin (or Einstein-Laub), and Helmholtz force.

The Lorentz and Helmholtz force expressions are closely related to the so called Abraham-Minkowski controversy regarding the light momentum in the medium that was much discussed in the literature. In this thesis we do not address the issue of the momentum, however we would like to make several comments related to recently published papers [32, 36, 43, 44].

The net force on a finite size dielectric body in vacuum is uniquely defined and is the same for different formulations (Lorentz force, Helmholtz force, Kelvin force). The perceived ambiguity of the forces on the semi-infinite body is related to the singularity due to uncertainty of the ratio of the size of the body to the length of the light pulse. This can be regularized in several ways. One approach is that if the length of the pulse is shorter than the size of the body, the problem should be considered non-stationary. Another approach is to introduce an infinitesimally small dissipation which removes the outgoing flux (out of the semi-infinite body) and leads to a unique solution (identical for Helmholtz and Lorentz forces formulation).

The differential conservation laws that involve different definitions of the wave momentum (e.g. Abraham momentum, Minkowski momentum, etc) are all correct and mathematically equivalent. The source terms is these expressions are responsible for the momentum exchange between different subsystems (e.g. electromagnetic field and individual charged particles). It is worth noting that the subgrid averaging may

result in further differentiation of the sub-system, e.g. the local microscopic vs the averaged field, collection of individual charges vs collection of dipoles etc. In the closed system, the momentum exchange term for one subsystem should appear with negative sign in the other subsystem. The physical model for the material is required to fully describe the redistribution of the momentum deposited in the medium. Note that most often only the electromagnetic field subsystem and corresponding force term are considered, while the other subsystem remains undetermined.

In general, the total momentum flux will consist of the electromagnetic and material parts. The appearance of the momentum exchange term (force) with opposite signs in different subsystems can be explicitly demonstrated in some models (e.g. plasma, see Appendix D) for the Lorentz force. This is consistent with the Abraham momentum as a true momentum of the electromagnetic field. The identification of the counterpart subsystem (with opposite sign of the exchange term) is however difficult for the Helmholtz force. This difficulty results from the fact that the Minkowski momentum is a pseudo-momentum related to the translation symmetry of the dielectric medium [36, 45, 46]. For a finite length dielectric, the translational symmetry is broken, the Minkowski pseudo-momentum is not conserved as a result of the pseudo-momentum generation at the boundaries of a homogeneous dielectric (Helmholtz force). Starting from the conservation of a true momentum for the counterpart subsystem , it is possible to formally construct the sub-system which will have the exchange terms in the form of the Helmholtz forces. These however will correspond to the conservation of the sum of the pseudo-momentum in the body and the true momentum of the electromagnetic field outside of the dielectric body [45]. Therefore the net force on the body can be calculated as well as from the pseudo-momentum balance [45]. This fact is a basis of the result that the net Lorentz force and net Helmholtz forces for the whole body are equal. This also provides explanations for a number of experiments which are consistent with the Minkowski momentum expression. It is argued in this thesis that the distribution of the internal forces (stresses) inside the dielectric medium should be consistent with Lorentz force expression. Such a distribution has to be determined for a given material model and

can be subject of further studies.

Chapter 6

Summary

This thesis analyzes two related problems of energy and momentum balance in multilayered dielectric structures, which are of interest for a number of applications in nanoplasmonics.

We considered electromagnetic systems and analyzed the relations among the standard group velocity $\partial\omega/\partial\mathbf{k}$, the group delay velocity $v_{gd} = \partial\omega/\partial\kappa$, and the energy velocity $\mathbf{v}_E = \mathbf{S}/U$, which is defined as the ratio of the Poynting vector to the electromagnetic energy density inside the medium. Energy transport is analyzed for the cases of a finite width slab, tunneling of evanescent waves through multilayered structures, and wave propagation in dispersive media. It is argued that the energy velocity $\mathbf{v}_E = \mathbf{S}/U$ is the most appropriate quantity describing the velocity of the energy flow, and hence, the velocity of the information flow. In general, the energy velocity $\mathbf{v}_E$ is a nonlocal quantity which is affected by the field distribution over the whole system, and in particular, by boundary conditions. It can be considerably different from the group velocity. It can be used for cases when the group velocity does not exist or produce nonphysical values (as in some case with dissipation). The energy flow velocity always remains subluminal. It is shown that the energy flow velocity is very low in resonant tunneling structures that may be used for designing of slow light devices.

The second part of thesis concerns with calculations of forces in multilayered structures. The expression for the Lorentz force is derived by averaging of the microscopic forces acting on individual charged particles. This force is identical to the Lorentz force acting on the polarization charges and magnetization current in the averaged electromagnetic field. The forces acting on dielectric structures are calcu-

lated by using the Lorentz force expression and the Helmholtz force expressions. It is noted that though after the integration over whole volume of the dielectric, the total force is identical in both approaches, the local force densities are very different. The Helmholtz force is characterized by the presence of significant surface contributions at the interface boundaries. The difference in local densities occurs due to presence of internal forces whose contributions average to zero for the whole body. The difference between the Helmholtz and Lorentz force can also be viewed as result of averaging over different volume samples, with Lorentz force being more local (or having smaller averaging sample size) while the Helmholtz force corresponds to the macroscopic averaging over the size of the object. The complete distribution of the internal forces depend on the material model and has to be determined taking into account material properties (e.g. Young modulus). The distribution of the internal stresses may be used to measure the local force densities. This can be a subject of future work.

References

[1] Fourkal E. Sternberg N.S. Smolyakov A.I., Krasheninnikov S.I. Resonant modes and tunneling in multi-layer metal-dielectric structures. *Progress In Electromagnetics Research*, 107:293, 2010.

[2] Zhang Z.M. Fu C.J. Energy transmission by photon tunneling in multilayer structures including negative index materials. *Transactions of the ASME*, 127:1046, 2005.

[3] Schriemer H. Cada M. Torrese G., Taylor J. Energy transport through structures with finite electromagnetic stop gaps. *Journal of Optics A: Pure and Applied Optics*, 8:973, 2006.

[4] Hartman T.E. Tunneling of a wave packet. *Journal of Applied Physics Reports*, 33:3427, 1962.

[5] Olkhovsky V.S. Recami E. Privitera G., Salesi G. Tunneling times: An elementary introduction. *Rivista del Nuovo Cimento*, 26 N.4:1, 2003.

[6] Zaichenko A.K. Olkhovsky V.S., Recami E. Resonant and non-resonant tunneling through a double barrier. *Europhysics Letters*, 70:712, 2005.

[7] Winful H.G. Tunneling time, the Hartman effect and superluminality: A proposed resolution to an old paradox. *Physics Reports*, 436:1, 2006.

[8] Winful H.G. Group delay, stored energy and the tunneling of evanescent electromagnetic waves. *Physical Review E*, 68:016615, 2003.

[9] Landauer R. Martin Th. Time delay of evanescent electromagnetic waves and the analogy to particle tunneling. *Physical Review A*, 45:2611–2618, 1992.

[10] Stovneng J.A. Hauge E.H. Tunneling times: a critical review. *Reviews of Modern Physics*, 61:917, 1989.

[11] Brevik I. Experiments in phenomenological electrodynamics and the electromagnetic energy-momentum tensor. *Physics Reports*, 3:133, 1979.

[12] Heckenberg N.R. Rubinztein-Dunlop H. Pfeifer R., Nieminen T.A. Colloquium: Momentum of an electromagnetic wave in dielectric media. *Reviews of Modern Physics*, 79:1197, 2007.

[13] Mansuripur M. Radiation pressure and the linear momentum of the electromagnetic field. *Optics Express*, 12:5375, 2004.

[14] Mansuripur M. Electromagnetic force and torque in ponderable media. *Optics Express*, 16:14821, 2008.

[15] Mansuripur M. Electromagnetic stress tensor in ponderable media. *Optics Express*, 16:5193, 2007.

[16] Kong J.A. Kemp B., Grzegorczyk T. Ab initio study of the radiation pressure on dielectric and magnetic media. *Optics Express*, 13:9280, 2005.

[17] Jackson J.D. *Classical Electrodynamics*. John Wiley and Sons, 1962.

[18] Yariv A. Yeh P. *Optical Waves in Crystals*. Wiley-Interscience, 1984.

[19] Landau L.D. Lifshiz E.M. *Electrodynamics of Continuous media (in Russian)*. Nauka, 1982.

[20] Smith F.T. Lifetime matrix in collision theory. *Physical Review*, 118:349, 1960.

[21] Razavy M. *Quantum Theory of Tunneling*. WorldScientific, 2003.

[22] Winful H.G. Delay time and the Hartman effect in quantum tunneling. *Physical Review Letters*, 91:260401, 2003.

[23] M. Büttiker and R. Landauer. Traversal time for tunneling. *Phys. Rev. Lett.*, 49:1739–1742, 1982.

[24] Sibilia C. Bloemer M.J. Bowden C.M. Haus J.W. Bertolotti M. D'Aguanno G., Scalora M. Group velocity, energy velocity and superluminal propagation in finite photonic band-gap structures. *Physical Review E*, 63:036610, 2001.

[25] Sommerfeld A. Brillouin L. *Wave Propagation and Group Velocity*. Academic Press, 1960.

[26] Ranfagni A. Mugnani D. Microwave experiments on tunneling time. In *Time in quantum mechanics, Volume 1 By Juan Gonzalo Muga, Rafael Sala Mayato, Iigo L. Egusquiza*, 2007.

[27] Oughstun K. *Electromagnetic and optical pulse propagation 1: Spectral Representations in Temporally Dispersive Media*. Springer, 2006.

[28] Van Vleck J.H. *The Theory of Electric and Magnetic Susceptibilities*. Oxford University Press, 1965.

[29] Lorentz H.A. *The Theory of Electrons*. Taubner, 1906.

[30] Yaghjian A.D. Internal energy, q-energy, Poynting's theorem, and the stress dyadic in dispersive material. *IEEE Trasactions on Antennas and Propagation*, 55:1495, 2007.

[31] Zakharian A.R. Mansuripur M. Maxwell's equations, the energy-momentum postulates, and the Lorentz law of force. *Physical Review E*, 79:026608–1, 2009.

[32] Mansuripur M. Resolution of the Abraham-Minkowski controversy. *Optics Communications*, 2010.

[33] Russakoff G. A derivation of the macroscopic Maxwell equations. *American Journal of Physics*, 38:1188, 1970.

[34] Stallinga Sj. Radiation force on a Fabry-Perot slab immersed in a dielectric. *Optics Express*, 14:1286, 2006.

[35] Gordon J.P. Radiation forces and momenta in dielectric media. *Physical Review A*, 8:14, 1973.

[36] Loudon R. Barnett S.M. The enigma of the optical momentum in a medium. *Philosophical Transactions of the Royal Society*, 368:927, 2010.

[37] Loudon R. Barnett S.M. On the electromagnetic force on a dielectric medium. *Journal of Physics B*, 39:S671, 2006.

[38] Tamm I.E. *Principles of Electricity (In Russian)*. Fizmatlit, 2003.

[39] Stratton J.A. *Electromagnetic Theory*. McGraw-Hill Book Company, 1941.

[40] Hirose Akira. Radiation pressure on a dielectric surface. *Canadian Journal of Physics*, 88:247, 2010.

[41] Reiner D. Hirose A. Fresnel's formulae and the Minkowski momentum. *Canadian Journal of Physics*, 87:407, 2010.

[42] Rainer Dick. The momentum of electromagnetic waves in dielectric materials. *Annalen der Physik*, 18:174, 2009.

[43] Zakharian A. Mansuripur M. Whence the Minkowski momentum? *Optics Communications*, 283:3557, 2010.

[44] Barnett S. Resolution of the Abraham-Minkowski dilemma. *Physical Review Letters*, 104:070401, 2010.

[45] Rudolf Peierls. *More Surprises in Theoretical Physics*. Princeton University Press, 1991.

[46] Nelson D.F. Momentum, pseudomomentum, and wave momentum: Toward resolving the Minkowski-Abraham controversy. *Physical Review A*, 44:3985, 1991.

[47] Maier S. *Plasmonics: Fundamentals and Applications*. Springer, 2007.

Appendix A

Surface waves

If we consider a structure with two layers characterized by electric permittivities $\varepsilon = \varepsilon_1(\omega)$ and $\varepsilon = \varepsilon_2(\omega)$, surrounded by two regions where $\varepsilon = 1$,. Considering the electric field in the plane of incidence (TM-polarization) $y - z$ and magnetic field in the direction parallel to the boundary $\mathbf{H} = (H_x, 0, 0)$, and assuming that $\varepsilon_1 > 0$ and $\varepsilon_2 < 0$, the solutions for the wave equation in regions $1 - 2$ are [1]

$$H_{1,2}(z) = H^+_{1,2}\, exp\,(-\kappa_{1,2} z) + H^-_{1,2}\, exp\,(\kappa_{1,2} z)\,, \tag{A.1}$$

with

$$\kappa^2_{1,2} = k^2_y - \varepsilon_{1,2} k^2_0 \quad k^2_0 = \omega^2/c^2, \tag{A.2}$$

where k_y is the component of the wavevector parallel to the interface between the layers. In the exterior regions, we can suppose outgoing waves of the form

$$H(z) = C_\pm\, exp(\mp i k_v z), \tag{A.3}$$

with

$$k_v = k^2_0 - k^2_y \quad k^2_0 = \omega^2/c^2. \tag{A.4}$$

Matching solutions and using the boundary conditions the following dispersion relation is obtained [1]

$$\eta_1 = \eta_2 = 2\eta_2 \frac{\eta_2 + i k_v}{\eta_2 - i k_v} \exp(-2\varphi_2) + 2\eta_1 \frac{\eta_1 + i k_v}{\eta_1 - i k_v} \exp(-2\varphi_1), \tag{A.5}$$

where $\varphi_{1,2} = 4\kappa_{1,2} a_{1,2}$ and $\eta_{1,2} = \varepsilon_{1,2}/\kappa_{1,2}$ and $2a_{1,2}$ the width of each layer.

Taking the limit of thick barriers,$\varphi_{1,2} >> 1$, the dispersion relation reduces to [1]

$$\eta_1 + \eta_2 \equiv \frac{\kappa_1}{\varepsilon_1} + \frac{\kappa_2}{\varepsilon_2} = 0, \tag{A.6}$$

or

$$k^2_0 = k^2_y \frac{\varepsilon_1 + \varepsilon_2}{\varepsilon_1 \varepsilon_2}. \tag{A.7}$$

This last equality is the standard dispersion relation of a localized surface wave. The conditions then for the existence of this mode are then $\kappa_{1,2} > 0$, $\varepsilon_1 \varepsilon_2 < 0$ and $\varepsilon_1 + \varepsilon_2$ [1].

It can be shown [1] that the conditions for resonant transmission in a two layered structure are the surface wave resonance $\eta_1 + \eta_2 = 0$ and $\varphi_1 = \varphi_2$, which means that

$$\kappa_1 a_1 = \kappa_2 a_2. \tag{A.8}$$

This is the matched amplification for evanescent waves. The two conditions (surface wave resonance relation and matched amplification) mean that the effective electric permittivity of the structure is zero at the resonance [1]

$$\bar{\varepsilon} \equiv \varepsilon_1 a_1 + \varepsilon_2 a_2 = 0. \tag{A.9}$$

As a comment, it can be shown that surface modes can be excited only by TM-polarized waves [47].

Appendix B

Energy velocity for evanescent TM-waves

For electromagnetic waves, the average value of the energy velocity is given by [18]

$$V_E = \frac{\frac{1}{2}\frac{1}{L}\Re\int_0^L \mathbf{E}\times\mathbf{H}^* dz}{\frac{1}{4}\frac{1}{L}\int_0^L \mathbf{E}\cdot\mathbf{E}^*\frac{\partial\omega\varepsilon}{\partial\omega}dz + \frac{1}{4}\frac{1}{L}\int_0^L \mathbf{H}\cdot\mathbf{H}^*\frac{\partial\omega\mu}{\partial\omega}dz}. \tag{B.1}$$

Evaluating this integral for the TM-modes where the electric field is given by

$$E_y(z) = -i\frac{1}{\omega\varepsilon}\frac{\partial H_x}{\partial z}. \tag{B.2}$$

For $\mu = \text{const}$ and using Helmholtz equation, the following holds

$$EE^* = \frac{1}{(\omega\varepsilon)^2}\frac{\partial H}{\partial z}\frac{\partial H^*}{\partial z}, \tag{B.3}$$

so that the integral that depends on the electric field can be written as

$$\int_0^L EE^*\frac{\partial\varepsilon\omega}{\partial\omega}dz = \int_0^L \frac{1}{(\omega\varepsilon)^2}\frac{\partial H}{\partial z}\frac{\partial H^*}{\partial z}\frac{\partial\varepsilon\omega}{\partial\omega}dz. \tag{B.4}$$

Integrating by parts and taking

$$\begin{aligned} a &= \frac{\partial H}{\partial z} \qquad da = \frac{\partial^2 H}{\partial z^2}dz, \\ db &= \frac{\partial H^*}{\partial z}dz \qquad b = H^*, \end{aligned} \tag{B.5}$$

the following is obtained

$$\int_0^L \frac{\partial H}{\partial z}\frac{\partial H^*}{\partial z} = H^*\frac{\partial H}{\partial z}\Big|_0^L - \int_0^L H^*\frac{\partial^2 H}{\partial z^2}dz, \tag{B.6}$$

and using (1.30) for the region, (the wave is evanescent here)

$$\frac{d^2H}{dz^2} - \kappa^2 H = 0, \tag{B.7}$$

the following holds

$$\int_0^L \frac{\partial H}{\partial z}\frac{\partial H^*}{\partial z} = H^*\frac{\partial H}{\partial z}\Big|_0^L + \int_0^L \kappa^2 HH^* dz \tag{B.8}$$

and

$$\int_0^L EE^*\frac{\partial\varepsilon\omega}{\partial\omega}dz = \int_0^L \frac{1}{(\omega\varepsilon)^2}\frac{\partial\varepsilon\omega}{\partial\omega}\kappa^2 HH^* dz + \frac{1}{(\omega\varepsilon)^2}\frac{\partial\varepsilon\omega}{\partial\omega}\ H^*\frac{\partial H}{\partial z}\Big|_0^L. \tag{B.9}$$

The denominator of (B.1) becomes

$$\frac{1}{4L}\int_0^L EE^*\frac{\partial\omega\varepsilon}{\partial\omega}dz+\frac{1}{4L}\int_0^L HH^*\frac{\partial\omega\mu}{\partial\omega}dz=$$

$$\frac{1}{4L}\int_0^L\frac{1}{(\omega\varepsilon)^2}\frac{\partial\varepsilon\omega}{\partial\omega}\kappa^2HH^*dz+\frac{1}{4L}\int_0^L\mu HH^*dz+\frac{1}{4L}\frac{1}{(\omega\varepsilon)^2}\frac{\partial\varepsilon\omega}{\partial\omega}\ H^*\frac{\partial H}{\partial z}\bigg|_0^L, \quad \text{(B.10)}$$

or

$$\frac{1}{4L}\int_0^L EE^*\frac{\partial\omega\varepsilon}{\partial\omega}dz+\frac{1}{4L}\int_0^L HH^*\frac{\partial\omega\mu}{\partial\omega}dz=$$

$$\frac{1}{4L}\int_0^L\left(\frac{1}{(\omega\varepsilon)^2}\frac{\partial\varepsilon\omega}{\partial\omega}\kappa^2+\mu\right)HH^*dz+\frac{1}{4L}\frac{1}{(\omega\varepsilon)^2}\frac{\partial\varepsilon\omega}{\partial\omega}\ H^*\frac{\partial H}{\partial z}\bigg|_0^L. \quad \text{(B.11)}$$

For the second term of the RHS of this last equation, we have that $\varepsilon|_0=\varepsilon|_L=\varepsilon_0$ and

$$\frac{1}{(\omega\varepsilon)^2}\frac{\partial\varepsilon\omega}{\partial\omega}=\frac{\varepsilon_0}{\omega^2\varepsilon_0^2}=\frac{1}{\omega^2\varepsilon_0}, \quad \text{(B.12)}$$

also

$$H^*|_0=1+R^* \qquad \frac{\partial H}{\partial z}\bigg|_0=ik_v(1-R), \quad \text{(B.13)}$$

$$H^*|_L=T^*e^{-ik_vL} \qquad \frac{\partial H}{\partial z}\bigg|_L=ik_vTe^{ik_vL}, \quad \text{(B.14)}$$

$$H^*\frac{\partial H}{\partial z}\bigg|_0^L=ik_v(|T|^2-1+|R|^2-R^*+R)=ik_v(R^*-R),$$

$$H^*\frac{\partial H}{\partial z}\bigg|_0^L=2k_v\Im(R). \quad \text{(B.15)}$$

Knowing that $k_v=\sqrt{k_0^2-k_y^2}$ and using (B.11), we obtain

$$\frac{1}{\omega^2\varepsilon_0}\frac{\omega}{c}\cos(\theta_i)=\frac{1}{\omega c\varepsilon_0}\cos(\theta_i)=\frac{1}{\omega}\sqrt{\frac{\mu_0}{\varepsilon_0}}\cos(\theta_i)=\frac{Z_0}{\omega}\cos(\theta_i), \quad \text{(B.16)}$$

or

$$\frac{1}{4L}\frac{1}{(\omega\varepsilon)^2}\frac{\partial\varepsilon\omega}{\partial\omega}\ H^*\frac{\partial H}{\partial z}\bigg|_0^L=\frac{1}{2\omega L}Z_0\cos(\theta_i)\Im(R). \quad \text{(B.17)}$$

As can be seen the first term in (B.11) reduces in vacuum or for constant non dispersive ε to

$$\frac{1}{4L}\int_0^L\left(\frac{1}{(\omega\varepsilon)^2}\frac{\partial\varepsilon\omega}{\partial\omega}\kappa^2+\mu\right)HH^*dz=\frac{1}{2L}\int_0^L\mu HH^*dz. \quad \text{(B.18)}$$

This last result can be interpreted taking into account the following

$$\langle U\rangle=\langle U_e\rangle+\langle U_m\rangle=2\langle U_m\rangle+(\langle U_e\rangle-\langle U_m\rangle). \quad \text{(B.19)}$$

So the last term in (B.11) can be interpreted as a difference between the electric and magnetic energy densities.

For the numerator of (B.1) we have that if there are no Joule losses, Poynting theorem states that [17]

$$\frac{\partial \langle U \rangle}{\partial t} = \nabla \cdot \mathbf{S},$$

and in steady state

$$\mathbf{S} = \text{constant}.$$

Given this we obtain

$$\Re\left[-\frac{i}{\omega\varepsilon}H^*\frac{\partial H}{\partial z}\bigg|_L\right] = \frac{k_v}{\omega\varepsilon_0}|\,T|^2, \tag{B.20}$$

$$\Re\left[-\frac{i}{\omega\varepsilon}H^*\frac{\partial H}{\partial z}\bigg|_0\right] = \Re\frac{k_v}{\omega\varepsilon_0}\left(1 - R^* + R - |R|^2\right) = \frac{k_v}{\omega\varepsilon_0}|\,T|^2, \tag{B.21}$$

with $k_v = (\omega/c)\cos(\theta_i)$ the following is obtained

$$\frac{k_v}{\omega\varepsilon_0}|\,T|^2 = \frac{\omega}{c}\frac{1}{\omega\varepsilon_0}\cos(\theta_i)|\,T|^2 = \sqrt{\frac{\mu_0}{\varepsilon_0}}\cos(\theta_i)|\,T|^2 = Z_0\cos(\theta_i)|\,T|^2, \tag{B.22}$$

and

$$\frac{1}{2L}\Re\int_0^L \mathbf{E}\times\mathbf{H}^* dz = \frac{Z_0}{2L}\cos(\theta_i)L|\,T|^2 = \frac{Z_0}{2}\cos(\theta_i)|\,T|^2. \tag{B.23}$$

The general expression for the energy velocity can be given as

$$V_E = \frac{LZ_0\cos(\theta_i)|\,T|^2}{\frac{1}{2}\int_0^L\left(\frac{1}{\omega^2\varepsilon^2}\frac{\partial\omega\varepsilon}{\partial\omega}\kappa^2 + \mu\right)H^*H dz + \frac{Z_0\cos\theta_i}{\omega}\Im(R)}. \tag{B.24}$$

Appendix C

Integral Approach for the calculation of the forces

C.1 Force on a slab

The time average of equation (4.52) reads

$$\langle \mathbf{f}_L \rangle = -\left\langle \frac{\partial \mathbf{g}^A}{\partial t} \right\rangle - \nabla \cdot \langle \bar{\mathcal{T}}^A \rangle \tag{C.1}$$

$$= -\nabla \cdot \langle \bar{\mathcal{T}}^A \rangle . \tag{C.2}$$

To obtain the Lorentz force this last expression has to be integrated over the whole medium

$$\int_V \langle \mathbf{f}_L \rangle \, dV = -\int_V \nabla \cdot \langle \bar{\mathcal{T}}^A \rangle \, dV \tag{C.3}$$

$$= -\oint_S \langle \bar{\mathcal{T}}^A \rangle \cdot \hat{\mathbf{n}} \, dS. \tag{C.4}$$

The normal vector is on the negative $\hat{\mathbf{z}}$ direction at the entrance and on the positive at the exit, thus

$$\int_V \langle \mathbf{f}_L \rangle \, dV = -A \left(-\left\langle \bar{\mathcal{T}}_{zz}{}^A \right\rangle \cdot \hat{z}|_{z=0} + \left\langle \bar{\mathcal{T}}_{zz}{}^A \right\rangle \cdot \hat{z}|_{z=d\to\infty} \right)$$

$$= A \left(\left\langle \bar{\mathcal{T}}_{zz}{}^A \right\rangle \cdot \hat{z}|_{z=0} - \left\langle \bar{\mathcal{T}}_{zz}{}^A \right\rangle \cdot \hat{z}|_{z=d\to\infty} \right) . \tag{C.5}$$

For the elements of the tensor we have the following

- At the entrance $z = 0$:

$$\left\langle \bar{\mathcal{T}}_{zz}{}^A \right\rangle \cdot \hat{z}|_{z=0} = \frac{|E_0|^2}{4} \varepsilon_0 \left(|1+R|^2 + |1-R|^2 \right)$$

$$= \frac{|E_0|^2}{2} \varepsilon_0 \left(1 + |R|^2 \right) . \tag{C.6}$$

- At $z = d$:

$$\left\langle \bar{\mathcal{T}}_{zz}{}^A \right\rangle \cdot \hat{z}|_{z=d} = \frac{|E_0|^2}{4} \left(\varepsilon_0 |T|^2 + \mu_0 \frac{\varepsilon_0}{\mu_0} |T|^2 \right) .$$

$$= \frac{|E_0|^2}{2} \varepsilon_0 |T|^2 \tag{C.7}$$

Thus the force is given by

$$\begin{aligned}\langle F_{Lz}\rangle &= A\frac{|E_0|^2}{2}\varepsilon_0\left(1+|R|^2-|T|^2\right)\\ &= A\frac{|E_0|^2}{2}\varepsilon_0\left(|R|^2+|T|^2+|R|^2-|T|^2\right)\\ &= A\varepsilon_0|E_0|^2|R|^2. \end{aligned} \tag{C.8}$$

As can be seen, the force given by (5.10) is equal to the expression given by equation (C.8).

C.2 Force on a semi-infinite slab

For the elements of the tensor we have the following

- At the entrance $z = 0$:

$$\begin{aligned}\left\langle \bar{\mathcal{T}}_{zz}{}^{A}\right\rangle \cdot \hat{z}|_{z=0} &= \frac{|E_0|^2}{4}\,\varepsilon_0\,\left(|1+R|^2+|1-R|^2\right)\\ &= \frac{|E_0|^2}{2}\,\varepsilon_0\,\left(1+|R|^2\right). \end{aligned} \tag{C.9}$$

- At $z = d \to \infty$:

$$\begin{aligned}\left\langle \bar{\mathcal{T}}_{zz}{}^{A}\right\rangle \cdot \hat{z}|_{z=d\to\infty} &= \frac{|E_0|^2}{4}\left(\varepsilon_0|T|^2\,e^{-2k_iz}|_{z=d\to\infty}+\mu_0\frac{\varepsilon_0}{\mu_0}\,|\varepsilon|\,|T|^2\,e^{-2k_iz}|_{z=d\to\infty}\right)\\ &= \frac{|E_0|^2}{4}\varepsilon_0\left(|T|^2\,e^{-2k_iz}|_{z=d\to\infty}+|\varepsilon|\,|T|^2\,e^{-2k_iz}|_{z=d\to\infty}\right). \end{aligned} \tag{C.10}$$

As can be seen from this last equation, the contribution to the force is only from the fields at the entrance, thus the force is given by

$$\begin{aligned}\langle F_{Lz}\rangle &= A\frac{|E_0|^2}{4}\varepsilon_0\left(2+2\,|R|^2-|T|^2\,e^{-2k_iz}|_{z=d\to\infty}-|\varepsilon|\,|T|^2\,e^{-2k_iz}|_{z=d\to\infty}\right)\\ &= A\frac{|E_0|^2}{2}\varepsilon_0\,(1+|R|^2). \end{aligned} \tag{C.11}$$

As can be seen, the force given by (C.11) is equal to the expression given by equation (5.21). In order to calculate the Helmholtz force for the semi-infinite slab, the momentum equation (4.61) will be used. The divergence of a tensor is defined as

$$\nabla\cdot(\mathbf{DE}) = \begin{pmatrix}\frac{\partial}{\partial x} & \frac{\partial}{\partial y} & \frac{\partial}{\partial z}\end{pmatrix}\cdot\begin{pmatrix}D_xE_x & D_xE_y & D_xE_z\\ D_yE_x & D_yE_y & D_yE_z\\ D_zE_x & D_zE_y & D_zE_z\end{pmatrix}. \tag{C.12}$$

Since the transversal component of the field $\mathbf{D}$ is not continuous, the divergence in (C.12) is not continuous either. The integral in (4.61) reduces under normal incidence to

$$\int_V \nabla\cdot\bar{\mathcal{T}}^M\,dV = A\int_0^\infty \frac{\partial\bar{\mathcal{T}}_{zz}^M}{\partial z}\,dz. \tag{C.13}$$

The integrand in the right hand side of (C.13) is given by

$$\frac{\partial \bar{\mathcal{T}}_{zz}^{M}}{\partial z} = (\bar{\mathcal{T}}_{zz}^{M}(z=0^{+}) - \bar{\mathcal{T}}_{zz}^{M}(z=0^{-}))\,\delta(z) \qquad z=0, \tag{C.14}$$

$$\frac{\partial \bar{\mathcal{T}}_{zz}^{M}}{\partial z} = \frac{\partial \bar{\mathcal{T}}_{zz}^{M}}{\partial z} \qquad z>0. \tag{C.15}$$

With this derivative taken into account the integral in (C.13) reduces to

$$\begin{aligned} A\int_{0}^{\infty} \frac{\partial \bar{\mathcal{T}}_{zz}^{M}}{\partial z}\,dz &= A\,(\bar{\mathcal{T}}_{zz}^{M}(z\to\infty) - \bar{\mathcal{T}}_{zz}^{M}(z=0^{-})), \\ \left\langle \mathbf{F}^{H} \right\rangle &= A\,(\left\langle \bar{\mathcal{T}}_{zz}^{M}(z=0^{-}) \right\rangle - \left\langle \bar{\mathcal{T}}_{zz}^{M}(z\to\infty) \right\rangle) \\ &= A\frac{|E_0|^2}{2}\varepsilon_0\,(1+|R|^2). \end{aligned} \tag{C.16}$$

The conclusion is then that the force given by (C.16) is equal to the expressions given by equations (C.11), (5.21) and (5.23).

C.3 Force on a Quarter-wavelength Coating

For the elements of the tensor we have the following

- At the entrance $z=0$:

$$\begin{aligned} \left\langle \bar{\mathcal{T}}_{zz}{}^{A} \right\rangle \cdot \hat{z}|_{z=0} &= \frac{|E_0|^2}{4}\,\varepsilon_0\,\left(|1+R|^2 + |1-R|^2\right) \\ &= \frac{|E_0|^2}{2}\,\varepsilon_0\,\left(1+|R|^2\right). \end{aligned} \tag{C.17}$$

- At $z=d$:

$$\begin{aligned} \left\langle \bar{\mathcal{T}}_{zz}{}^{A} \right\rangle \cdot \hat{z}|_{z=d} &= \frac{|E_0|^2}{4}\left(\varepsilon_0|T|^2 + \varepsilon_0\,\frac{c^2k_2^2}{\omega^2}\,|T|^2\right) \\ &= \frac{|E_0|^2}{4}\varepsilon_0\,(1+n_2^2)\,|T|^2 \end{aligned} \tag{C.18}$$

The force is thus given by

$$\langle \mathbf{f}_L \rangle_z = \frac{1}{4}\left\{2+2|R|^2-|T|^2-n_2^2|T|^2\right\}\,\varepsilon_0 A|E_0|^2. \tag{C.19}$$

Taking into account that

$$\begin{aligned} |R|^2 &= 0, \\ |T|^2 &= \frac{1}{n_2}, \end{aligned}$$

the total force reduces to

$$\begin{aligned}
\langle \mathbf{F}_L \rangle_z &= \frac{1}{4}\left\{2 - \frac{1}{n_2} - n_2^2\frac{1}{n_2}\right\}\varepsilon_0 A|E_0|^2 \\
&= \frac{1}{4}\left\{2 - \frac{1}{n_2} - n_2\right\}\varepsilon_0 A|E_0|^2 \\
&= -\frac{1}{4}\left\{n_2 - 2 + \frac{1}{n_2}\right\}\varepsilon_0 A|E_0|^2 \\
&= -\frac{1}{4}\left\{\frac{n_2^2 - 2n_2 + 1}{n_2}\right\}\varepsilon_0 A|E_0|^2 \\
&= -\frac{1}{4}\,\varepsilon_0\, A\,\frac{(n_2-1)^2}{n_2}\,|E_0|^2. \qquad \text{(C.20)}
\end{aligned}$$

As can be seen, the force given by (C.20) is equal to the expression given by equation (5.36).

Appendix D

Macroscopic conservation of linear momentum

To fully obtain the conservation of linear momentum, the first thing to see is that the Lorentz force is an exchange of momentum between the electromagnetic field and the particles in the body [28, 46]. The momentum exchange equation for the particles can be written as [46]

$$-\frac{\partial}{\partial t}\left(\sum_j m_j n_j \mathbf{v}_j\right) - \nabla\cdot\left(\sum_j n_j m_j \mathbf{v}_j \mathbf{v}_j + p_j \delta_{ij}\right) = -\rho\mathbf{E} - \mathbf{J}\times\mathbf{B}. \tag{D.1}$$

Adding together (4.52) and (D.1), the conservation law for the momentum of the total systems is given by

$$\frac{\partial}{\partial t}\left(\varepsilon_0\,\mathbf{E}\times\mathbf{B} + \sum_j m_j n_j \mathbf{v}_j\right) +$$

$$\nabla\cdot\left\{\frac{1}{2}\left(\varepsilon_0\mathbf{E}\cdot\mathbf{E} + \frac{1}{\mu_0}\mathbf{B}\cdot\mathbf{B}\right)\delta_{ij} - \varepsilon_0\mathbf{E}\mathbf{E} - \frac{1}{\mu_0}\mathbf{B}\mathbf{B} + \sum_j n_j m_j \mathbf{v}_j \mathbf{v}_j + p_j\delta_{ij}\right\} = 0, \tag{D.2}$$

where

- $n_j \rightarrow$ concentration of $j-th$ species.
- $\mathbf{v}_j \rightarrow$ velocity of $j-th$ species.
- $p_j \rightarrow$ pressure of the $j-th$ species.